Zeitschrift: Eclogae Geologicae Helvetiae
Herausgeber: Schweizerische Geologische Gesellschaft
Band: 77 (1984)
Heft: 3

Artikel: A Middle Jurassic-Early Cretaceous low-latitude radiolarian zonation based on unitary sssociations and age of Tethyan radiolarites
Autor: Baumgartner, Peter O.
DOI: https://doi.org/10.5169/seals-165530

Eclogae geol. Helv.	Vol. 77	Nr. 3	Pages 729–837	Basel, December 1984

A Middle Jurassic–Early Cretaceous low-latitude radiolarian zonation based on Unitary Associations and age of Tethyan radiolarites

By PETER O. BAUMGARTNER[1])

ABSTRACT

A new Bathonian to Hauterivian radiolarian zonation defined by means of Unitary Associations (U.A., GUEX 1977) is proposed. A database consisting of first and final appearances of 110 species in 43 localities (mainly from Central Atlantic and Tethys, 226 samples) was used (BAUMGARTNER 1984) to establish a system of 15 successive U.A. (grouped in 9 biochronozones) each of which is defined by a number of characteristic species or species pairs (like concurrent range zones). The radiolarian biochronozones are tied to chronostratigraphy by means of coexisting other fossil groups.

Radiolarian faunal correlation of Atlantic DSDP Site 534 (Blake-Bahama Basin) with sections of Mediterranean Tethyan ancient continental margins reveal similar Callovian–early Oxfordian poorly oxygenated conditions in deep, isolated basins in both realms but a much more siliceous record in Tethys. Radiolarian dating of the Tethyan sections documents a systematic diachronism of the basal onset of radiolarites spanning at least the Bathonian to Oxfordian. The age of the oldest radiolarites relates to the age of initial foundering of each paleogeographic realm: Triassic basins show a Bathonian, Early Jurassic basins show an early–middle Callovian and Early–Middle Jurassic plateaus and seamounts show a late Oxfordian start of radiolarite sedimentation. Basal radiolarites on oceanic crust are dated as middle–late Callovian (eastern Greece and Liguria) to late Oxfordian (Elba).

These data imply a small-scale bathymetric control of radiolarite deposition in a region of high overall silica (radiolarian) productivity. The early Callovian onset of radiolarite deposition in Jurassic basins and the latest Jurassic spread of calcareous nannofossil sedimentation coincide with drastic radiolarian faunal changes related to major paleooceanographic events, which affected at least Tethys and early Central Atlantic.

Radiolarian systematics are presented as an alphabetic listing with complete synonymies of genera and of the 110 species used in the zonation, including 5 new genera, 16 new species and 2 new subspecies. 12 new and 38 referenced radiolarian localities are included with data on access, lithology and sample location, biostratigraphy, radiolarian occurrence data and zonal assignments.

RÉSUMÉ

Une nouvelle zonation à radiolaires de l'intervalle Bathonien–Hauterivien, basée sur les Associations Unitaires (A.U., GUEX 1977) est proposée. Une base de données, constituée par les premières apparitions et par les disparitions de 110 espèces dans 43 localités (principalement situées dans l'Atlantique Central et la Téthys, 226 échantillons) a été utilisée (BAUMGARTNER 1984) dans l'élaboration d'un système de 15 U.A. successives (regroupées en 9 biochronozones) dont chacune est définie par plusieurs espèces ou paires d'espèces caractéristiques

[1]) Escuela Centroamericana de Geología, Apt. 35, Universidad de Costa Rica, America Central.
Present address: Institut de Géologie, Palais de Rumine, CH–1005 Lausanne, Switzerland.

(comparables aux «concurrent range zones»). Les biochronozones de radiolaires sont reliées aux étages standards à l'aide des autres fossiles associés aux radiolaires.

Les corrélations faunistiques à radiolaires entre le Site DSDP 534 (Basin de Blake-Bahama, Atlantique) et des coupes associées aux marges anciennes de la Téthys méditerranéenne permettent de reconnaître: a) des conditions locales d'oxygénation pauvre simultanées dans les deux bassins, pendant le Callovien–Oxfordien inférieur; b) un enregistrement plus fortement siliceux dans la Téthys. Les datations à radiolaires dans des coupes téthysiennes montrent un diachronisme systématique de la base des radiolarites recouvrant au moins l'intervalle Bathonien–Oxfordien. L'âge de la base des radiolarites est en relation directe avec l'âge de l'effondrement initial des zones paléogéographiques: L'âge des radiolarites est Bathonien dans les bassins triasiques, Callovien inférieur/moyen dans les bassins liasiques et Oxfordien supérieur sur les haut-fonds du Lias–Dogger. Les radiolarites basales qui reposent sur la croûte océanique sont datées du Callovien moyen/supérieur (Grèce Orientale, Ligurie) à l'Oxfordien supérieur (île d'Elbe).

Ces données impliquent un contrôle bathymétrique à petite échelle de la sédimentation des radiolarites, se produisant dans une région à haute productivité générale de silice (radiolaires). Le début de la sédimentation radiolaritique dans les bassins liasiques au Callovien inférieur/moyen et le passage à une sédimentation calcaire à nannofossiles au Jurassique terminal coincident avec des changements drastiques dans la faune à radiolaires qui semblent être en relation avec des événements paléoocéanographiques qui ont affecté au moins la Téthys et l'Atlantique Central.

La systématique est présentée sous forme d'une liste alphabétique avec synonymie complète des genres et des 110 espèces utilisées pour établir la zonation. Cinq genres, 16 espèces et 2 sous-espèces sont nouveaux. Douze nouvelles localités à radiolaires sont décrites et 38 localités classiques sont prises en considération dans la présente synthèse.

RESUMEN

Se propone una nueva zonación en base a radiolarios del intervalo Bathoniense–Hauteriviense, utilizando Asociaciones Unitarias (A.U., Guex 1977). Un banco de datos que consiste en la primera y última aparición de 110 especies en 43 localidades (principalmente situadas en el Atlántico Central y el Tethys, totalizando 226 muestras) ha sido utilizado (Baumgartner 1984) en la elaboración de un sistema de 15 A.U. sucesivas (agrupadas en 9 biocronozonas). Cada A.U. es definida en base a varias especies o pares de especies caractéristicas (similares a acrozonas concurrentes). Las biocronozonas de radiolarios definidas se correlacionan con la cronoestratigrafía en base a otros fósiles que coexisten con los radiolarios.

La correlación faunística entre el Sitio DSDP-534 (Blake-Bahama Basin, Atlántico) y secuencias de los márgenes continentales antiguos del Tethys mediterráneo, permite reconocer: a) condiciones locales de oxigenación pobre simultaneamente en ambas cuencas; b) una depositación mucho más silícea en el Tethys. Las dataciones efectuadas en base a radiolarios en las secuencias del Tethys documentan un diacronismo sistemático de la base de las radiolaritas, que al menos cruza el Bathoniense–Oxfordiense. La edad de la base radiolarítica esta directamente relacionada con la edad del hundimiento inicial de las areas paleogeográficas respectivas: La edad de la base radiolarítica es del Bathoniense en las cuencas Triásicas; Calloviense temprano/medio en cuencas Liásicas y Oxfordiense tardío en áreas de fondos altos del Lias–Dogger. Dataciones efectuadas en radiolaritas basales, que sobreyacen a la corteza oceánica, proporcionan una edad Calloviense media/tardía (Grecia Oriental, Liguria) a Oxfordiense tardía (isla del Elba).

Estos datos implican un control batimétrico a pequeña escala para la sedimentación de las radiolaritas, la que se produjo en una situación regional de alta productividad silícea (radiolarios). El inicio de la sedimentación radiolarítica en las cuencas Liásicas durante el Calloviense inferior y el cambio a una sedimentación calcárea con nannofósiles a finales del Jurásico, coinciden con cambios drásticos en las faunas de los radiolarios, que se relacionan con eventos paleooceanográficos que afectaron, al menos, al Tethys y al Atlántico Central.

La sistemática de los radiolarios se presenta en forma de lista alfabética incluyendo sinonimias completas de los géneros y de las 110 especies utilizadas en la zonación. Se describen 5 géneros, 16 especies y 2 subespecies nuevas. Se presentan 12 nuevas localidades con radiolarios y se analizan otras 38, con referencias sobre el acceso, las litologías y ubicación de muestras, bioestratigrafía, distribución local y zonación de los radiolarios.

CONTENTS

1. Introduction

Much of the present state of Mesozoic radiolarian paleontology and biostratigraphy is the result of the past ten years. After a period of active study of Mesozoic radiolarians in Europe at the turn of the century (RÜST 1885, 1898, PARONA 1890, SQUINABOL 1914, etc.) the interest declined and the biostratigraphic usefulness of radiolarians was questioned.

A number of favorable circumstances revitalized the field in the early seventies: The Deep-Sea Drilling Project was coring Cenozoic and Mesozoic sediments in the oceans which furnished well preserved radiolarian assemblages greatly stimulating biostratigraphic work on this group, as it did for other fossil groups. Radiolarian biostratigraphy, first worked out for the Cenozoic (summary in RIEDEL & SANFILIPPO 1978), rapidly was extended to the Cretaceous (FOREMAN 1971, 1973, 1975, 1978; MOORE 1973, RIEDEL & SANFILIPPO 1974, SCHAAF 1981). The use of hydrofluoric acid to extract fossils from siliceous rocks, known for a long time to palynologists (LEJEUNE 1936) was successfully applied to radiolarians (DUMITRICA 1970, PESSAGNO & NEWPORT 1972) and allowed the observation of isolated forms also from highly lithified siliceous limestones and cherts, leading to systematic work and first Late Jurassic–Cretaceous zonations mainly derived from land-based samples from California (PESSAGNO 1971, 1972, 1973, 1976, 1977a, b). Meanwhile, the Scanning Electron Microscope (SEM) began to be regularly used by micropaleontologists. It produced accurate illustrations even of internally recrystallized or opaque fossil material, inapropriate for transmitted light microscopy.

Only recently, Mesozoic radiolarian biostratigraphy became revitalized in the European area (see DE WEVER et al. 1979) and resulted in first zonations for Tethyan radio-

larites (BAUMGARTNER et al. 1980, KOCHER 1981). In the mean time, Japanese workers, based on the results of the late seventies, began to multiply their efforts and presented a wealth of new information on Mesozoic radiolarian biostratigraphy (e.g. volume edited by NAKASEKO 1982).

Radiolarian dating of siliceous oceanic sediments has since greatly increased the understanding of tectonically complex areas like the Californian Coast Ranges, the Alpine–Mediterranean and the Japanese orogens.

Mesozoic radiolarian biostratigraphy was aproached under the aspect of different philosophies: 1. The assemblage concept in which the presence of several characteristic species and/or the co-occurrence of species is used as criterion for the definition of a biostratigraphic interval. 2. The "datum" concept, in which biostratigraphic units are defined by the first or final appearance of "marker" species.

Early workers (e.g. FOREMAN 1973, 1975) recognized, that the advantage of the assemblage concept is its wide applicability also to poorly preserved samples, where some of the defining species may be absent. The recent Japanese radiolarian biostratigraphic work (summary in YAO 1983) is largely based on the concept of the assemblage zone.

As pointed out in several earlier papers (BAUMGARTNER 1980, 1984, BAUMGARTNER et al. 1980, 1981) radiolarian abundance and preservation is extremely dependent on lithology reflecting sedimentary environment and diagenetic history. Especially in land based Mesozoic radiolarian-bearing rocks, which underwent deep burial diagenesis, the number of identifiable morphotypes may vary form a few to over 100 within a few centimeters of the sequence. This is simply to demonstrate that the *absence* of a species from a certain part of a sequence does not necessarily have a chronologic significance. The result of these documentary gaps is obvious: In general, the sequence of first and final appearances greatly differs from section to section; therefore, these events are not useful for establishing biochronologic limits.

The basic problem is to know whether an absence from a certain interval is consistent or not. The only way to find out is to systematically analyze the mutual co-occurrences of species in all available sections, in order to find out which species do co-occur and which are mutually exclusive and thus represent consistent absences from certain stratigraphic intervals. GUEX (1977) coined the term *Unitary Associations* (U.A.) for maximal sets of mutually coexisting species and has since elaborated the logics and mathematics to calculate U.A. from the locality data (GUEX & DAVAUD 1982, 1984). The concept of U.A. has been successfully applied to radiolarians (BAUMGARTNER et al. 1980, KOCHER 1981) and the zonation presented in this paper is based on a recent computation of U.A. as discussed in BAUMGARTNER (1984).

This paper represents a synthesis of the majority of the presently available radiolarian samples from the Central Atlantic and Western Tethys and some other samples all around the world. The presented database (appendix) is founded on earlier work by BAUMGARTNER et al. (1980) and KOCHER (1981). However, much of the sample material has been revised under the aspect of sharper defined and more numerous morphotypes included. Very well preserved late Middle and Late Jurassic samples from DSDP Site 534 (Leg 76) have greatly facilitated the definition of species used in the zonation, and at this site a good part of the zonation can be tied to chronostratigraphy (see chapter 3).

Principal objectives

The main focus of this paper is to document as complete as possible the data used for the elaboration and calibration of the presented zonation.

In chapter 2 the procedures which led to the present zonation by means of U.A. are summarized from BAUMGARTNER (1984) and modifications are explained.

In chapter 3 the established zonation is compared to earlier radiolarian biostratigraphic work and to chronostratigraphy.

Chapter 4 draws the consequences resulting from the radiolarian dating of the studied sequences: A chronostratigraphic correlation between Atlantic and Western Tethys and the timing of Middle–Late Jurassic siliceous sedimentation in Tethys and its paleooceanographic significance. Radiolarian faunal changes are related to paleooceanography.

Chapter 5 gives an alphabetic listing of genera and the 110 species used in the zonation, including 5 new genera, 16 new species and 2 new subspecies.

Chapter 6 gives the data pertaining to the studied localities: Access, lithology, location of samples and radiolarian and other biostratigraphic data for those sections not illustrated in Plate 12. Detailed objectives and procedures are given in the introduction to each chapter.

2. Radiolarian biochronology

2.1 Introduction

In a recent paper (BAUMGARTNER 1984) the Middle Jurassic–Early Cretaceous database (as included herein except minor revisions) was used to compute Unitary Associations (U.A.) and probabilistic ranking and scaling (RASC, AGTERBERG & NEL 1982a, b), in order to test "deterministic" versus probabilistic quantitative biostratigraphic methods applied to radiolarians. Since the Mesozoic radiolarian fossil record is largely dissolution-controlled, the sequence of first and final appearances of taxa differs greatly from section to section and the scatter of these events along a relative time scale is large compared to the range of the taxa. Thus, these data do not satisfy the statistical assumptions made in probabilistic methods. U.A. produce maximum ranges of the taxa relative to each other by stacking cooccurrence data from all sections and therefore compensate for local dissolution effects (poor preservation). Ranking and scaling, assuming a symmetrical, random scatter of the events narrowly clustered around the endpoints of a species range, produces "average" ranges which are for most species much shorter than the maximum U.A. ranges and can easily be contradicted by any well preserved sample. It is therefore clearly indicated to use U.A. for the elaboration of a radiolarian biochronology which should account for the nature of the data and produce a zonation of wide, non-contradictory applicability.

The procedures which led to the presented zonation by means of Unitary Associations (U.A.), computed by a program by DAVAUD (in GUEX & DAVAUD 1982, 1984) is explained in detail in BAUMGARTNER 1984 and will not be repeated here.

2.2 Recent modification of the zonation

GUEX (in press) has since proposed an additional test which constructs a second graph "Gk 2" in which the vertical sequencing of A.U. is based on the observed stratigraphic relationships of all species, rather than only the characteristic species (or species pairs) of single U.A., as in the graph "Gk 1" of the program in GUEX & DAVAUD (1984). The longest path in this additional solution should generally result longer than the one of the standard program, which may in some cases produce a desirable increase of vertical resolution, at the cost of good lateral reproducibility and superpositional control. The slightly updated database was run with this new option and the results are found to confirm the earlier version of the zonation. In addition, they allow for a better resolution in Zone A0.

Instead of 13 U.A. resulting from the coalescence of 28 initial U.A. as given in Gk 1 (see BAUMGARTNER 1984, Fig. 2) the new option resulted in 26 U.A. with only one case of gathering (of 27 initial U.A.). However, the superpositional control and the lateral reproducibility of these alternative U.A. is very poor. It results that the gathering as calculated in Gk 1 is an optimal way of grouping the initial U.A. for most of the studied interval. In Gk 1 three initial U.A. were gathered into U.A. 1 of BAUMGARTNER (1984), whereas in Gk 2 these appear to be superposed based on their specific content. Indeed, there is now also physical superpositional control in locality 26 (see Pl. 12) which allows to divide U.A. 1 into "U.A. 0" which results from a coalescence of the two lowest initial U.A. (I.U.A. 10 and 1 of BAUMGARTNER 1984) and "U.A. 1" which is initial U.A. 17 (ibid.). This new subdivision increases the resolution at the lower end of the zonation in that many species that reached the base of the zonation now are excluded from U.A. 0 and therefore receive a defined base.

The Cretaceous portion of the zonation continues to be a problem in the calculated versions. Although the physical superpositional control of samples is good, it seems that very incomplete superpositional relationships between the included species result in unrealistic virtual associations. The present solution is taken from BAUMGARTNER (1984) without changes. Of the four proposed U.A. only U.A. 11 and U.A. 14 have a good reproducibility (see Fig. 1). U.A. 12 and 13 remain to be confirmed by further locality data of Neocomian sections. It is hoped that the Neocomian part of the zonation can be refined by the inclusion of more localities and more species.

2.3 Procedure of data acquisition

Step 1: Definition of morphotypes. – The definition of morphotypes is based without exception on an SEM study of well preserved material prior to the actual search for stratigraphic data: For the lowest levels (Zone A0) the sample IN 7, provided by A. Yao (loc. 40, see locality descriptions) and samples from Lombardy basin were used. For the Callovian–Oxfordian interval (Zones A1–A2) very well preserved material of DSDP Site 534 (loc. 30) substantially increased the understanding and selection of morphotypes used in this zonation. For the Oxfordian–Tithonian interval (Zones B–C) samples from the Argolis Peninsula, Greece, northern and central Italy and Sicily were used. For the Neocomian interval (Zones D–E) well preserved samples from the Maiolica in Lombardy and excellent samples from the Murcugeva Formation, Romania (loc. 16), provided by P. Dumitrica were studied.

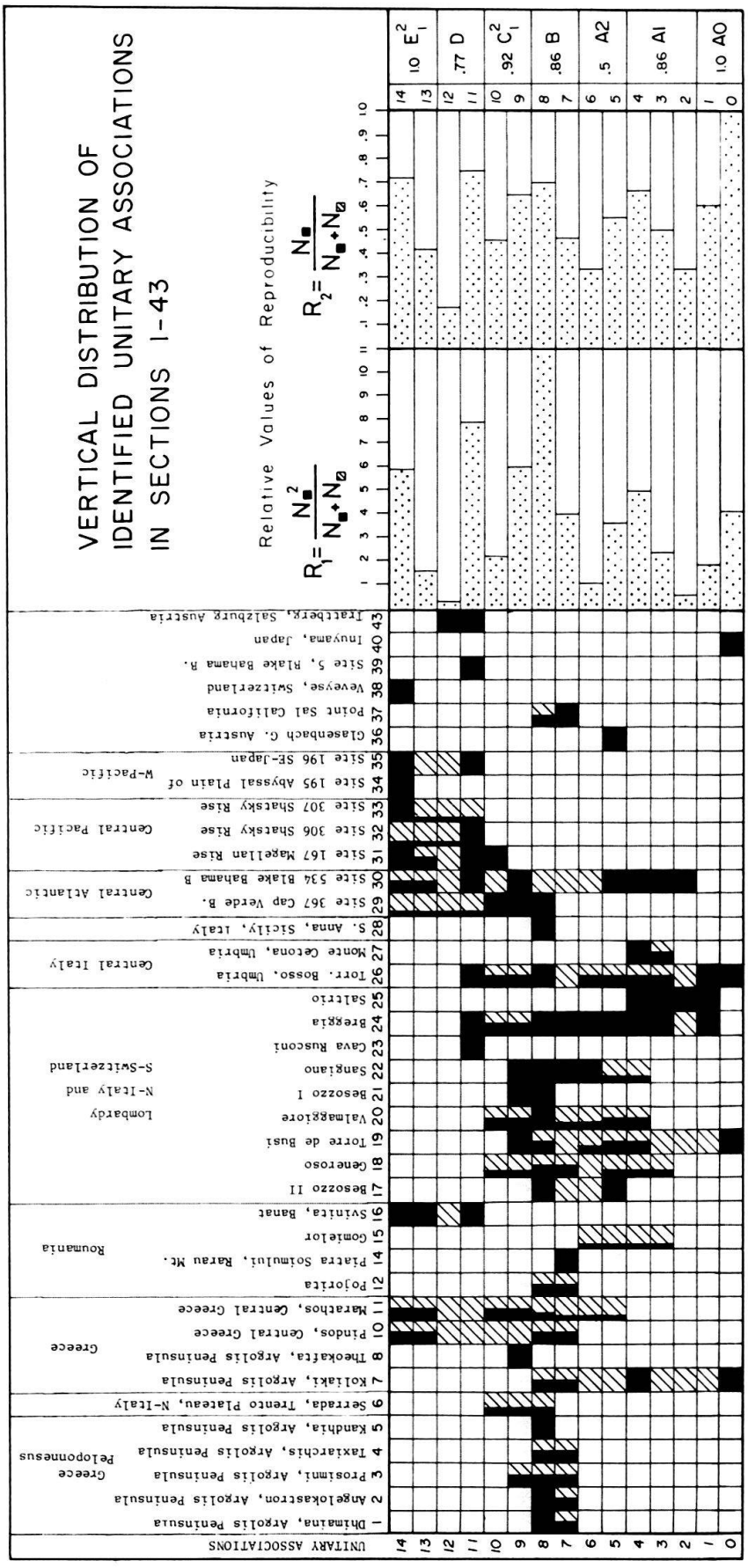

Fig. 1. Distribution of identified (black) and potentially identifiable (hachured) Unitary Associations in studied localities 1–43. Samples assignable to 2, 3 or 4 U.A. receive 2 superposed half, 3 third or 4 fourth squares respectively. R1 and R2 are relative values of reproducibility. A0 to E2 are proposed biochronozones with R2 indicated, taking the identification of the zone as a whole. Modified after BAUMGARTNER (1984).

To avoid any bias towards preselected morphologic units all encountered morphotypes were included without any attempt to group them. Morphotypes appearing during the stratigraphic search were examined by means of the SEM and included, which often required reexamination of a number of samples.

Step 2: Stratigraphic search. – For the stratigraphic search at least two densily strewn Plummer cells (2 × 4.5 cm, subdivided into 5 × 12 squares) were searched systematically through (2–5 hours) by means of a stereomicroscope at 100× magnification. Encountered morphotypes were always compared to posted SEM reference pictures to avoid a subjective shift of morphologic concepts. The nearly 300 morphotypes initially included (pob 1–300) represent an estimate of 80–90% of the total assemblages for the Callovian–Tithonian interval (Zones A1–C) but only a small percentage of the earliest (Zone A0) and the Neocomian assemblages. A presence is defined as the occurrence of at least one securely identified specimen. Doubted identifications are treated as absences.

Step 3: Compilation for U.A. treatment. – A selection of 110 morphotypes was prepared for computer treatment owing to the limitations of the U.A. program. Excluded were: very rare, very long ranging and morphologically poorly defined morphotypes. In some cases, the data for two morphotypes were merged for treatment as one species. The data included in the database as presented herein (and as used by U.A. treatment) were compiled from the original sample data and consist in the lowest and highest occurrence of each morphotype at each locality, hence do not reflect the consistency of occurrence within the local range.

2.4 Definition of zones

The biochronologic interpretation of the U.A. resulting in the definition of biochronozones is based on the principle of lateral reproducibility (GUEX 1979). The values of reproducibility given in Figure 1 are, of course, only guidelines for establishing biochronozones. The criteria for the proposed zonal limits are discussed in BAUMGARTNER (1984) and will not be repeated here.

It should be noted that each zone is defined by one or more U.A. each of which is defined by the totality of its characteristic species or species pairs. Hence a given sample can be assigned to a zone if one or more of its U.A. can be identified by means of one or more characteristic species or species pairs. In practice, U.A. and the defined zones work exactly like concurrent range zones.

The advantage of this type of zonation is obvious: The more species included in the zonation the better is the definition of each zone. A zonal unit defined by many species pairs has more chances to be recognized in a poorly preserved sample than a zone based on the presence of one or two "marker" species.

3. Comparison to other zonations and chronostratigraphic calibration

3.1 Comparison to earlier zonations

3.1.1 Introduction

The comparison of the present zonation with earlier ones depends on a number of factors that need to be mentioned.

1. The correlation is strictly based on species that are represented in the range charts of both zonations.

2. The specific concept (morphologic delimitations) of these species has to be the same in both zonations, as far as this is defined in illustrations, synonymy and descriptions.

3. A zonation based on maximum ranges compiled from cooccurrences in a large number of samples is likely to demonstrate partial or total overlap of earlier zones established on the basis of local or incomplete ranges. It should be noted that this is not the effect of virtual associations produced by the computer program. For most of the cooccurrences which result in overlap of earlier zones there is direct sample evidence documented in the database (appendix). The correlations discussed below are graphically presented in Figure 2.

3.1.2 Correlation with BAUMGARTNER et al. (1980)

The zonation presented in BAUMGARTNER et al. (1980) was based on a limited database, a small number of species and some rather lumping specific concepts. The data for the present zonation are completely revised on the basis of more accurately defined specific delimitations and both the number of samples and included species have increased by a factor of about three. As a consequence, some earlier ranges prove to be incomplete, others tend to be shorter owing to narrower specific definitions. A number of new U.A. arise from the inclusion of much more species.

A chronostratigraphic comparison of the two zonations was given in BAUMGARTNER (1983, Fig. 1). However, the mentioned figure does not give the actual correlation of old and new U.A. Instead, it compares the tentative time range of the old U.A. (as suggested in BAUMGARTNER et al. 1980, Table 3a) with the time range of the present U.A. For instance that new U.A. 9 (Zone C1) covers part of old Zone B and part of old Zone C is a result of a new calibration of the limit B/C and does not represent the correlation of the faunal content of the U.A. (it is theoretically impossible that a new U.A. recovers parts of old U.A.).

The fact that old Zone A is now part of new Zone B, etc. may equally be misleading. However, since Figure 2 illustrates that overlaps are inevitable it is hoped that the present definitions only will be used for subsequent radiolarian work.

— *Old A1* is correlated to new U.A. 3–5 on the basis of the present range of *Stylocapsa oblongula.*

— *Old A2* is correlative of new U.A. 4–6, based on the cooccurrence of *Mirifusus mediodilatatus* with *Guexella nudata* and *Napora pyramidalis.* The partial overlap of old A1 and A2 is the result of the now established cooccurrence of *M. mediodilatatus* s.l. and *Stylocapsa oblongula* in new U.A. 4–5 (see also KOCHER 1981).

— *Old A3* can be correlated with new U.A. 6–8, if the cooccurrence of *Emiluvia pessagnoi* with *Ristola procera* is considered, it is new U.A. 7–8, if it is with *Emiluvia orea.*

— *Old B4–5* is correlative with new U.A. 8 or 7–8 on the basis of *Podocapsa amphitreptera,* defining the base of old B4 now in new U.A. 8, *Formanella hipposidericus,* defining the base of old B5, now in new U.A. 7, and all tops of old B4 and B5 now in new U.A. 8.

— *Old B6*, defined by the cooccurrence of *Sethocapsa cetia* with *Triactoma cornuta* coincides with new U.A. 9. Owing to a more restricted definition of *S. cetia* it is no longer cooccurring with *Mirifusus guadalupensis*.
— *Old C7–9* can be correlated with new U.A. 9–10, since the base of old C7, *Acaeniotyle umbilicata* and the base of old C8, *Acanthocircus dicranacanthos* are both in new U.A. 9 and all tops of old C7–9 are in new U.A. 10. The base of old C9 was defined by *Obesacapsula rotunda* which now first appears in new U.A. 11 (owing to narrower specific definition), thus old C9 = old C8.
— *Old D10*, defined by the cooccurrence of *Napora lospensis, Emiluvia pessagnoi* and *Podocapsa amphitreptera* with *Ristola cretacea, Ditrabs sansalvatorensis* and *Parvicingula cosmoconica* equals new U.A. 11.
— *Old D11*, defined by the cooccurrence of *Alievum helenae* with *Ristola cretacea* is correlative of new U.A. 11–13, as *A. helenae* is now known to cooccur also with *P. amphitreptera* (e.g. loc. 24 sample 24: POB 1330, see database, appendix).
— *Old D12* equals new U.A. 14, defined by the base of *Cecrops septemporatus*.

3.1.3 Correlation with Kocher (1981)

The zonation presented by Kocher (1981) is based on Unitary Associations which were calculated by means of a first program by Davaud (in Davaud & Guex 1978) which had the principal drawback of eliminating all those species which left indetermi-

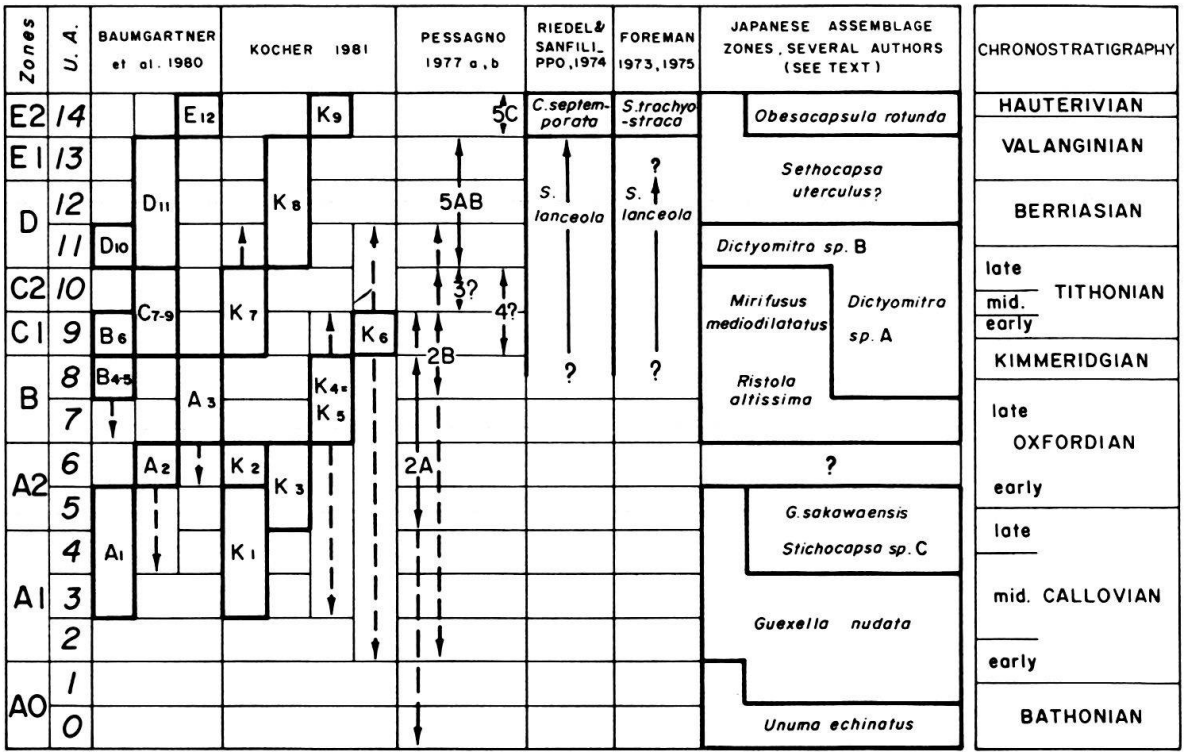

Fig. 2. Comparison of the Unitary Associations 0–14 with earlier zonations, based on species occurring in both zonations. The thick-lined squares and continuous arrows represent a minimal correlation based on defining species with a minimal range in terms of U.A. Dashed arrows gives the maximal correlation based on species which have a maximal coverage of U.A. For details see text.

nate stratigraphic relationships in the species/species matrix. In the case of KOCHER's data this was about a third of all species, which were manually reintroduced by KOCHER based on observed cooccurrences. Despite the problems arising from this procedure, KOCHER's zonation easily compares with the succession of the present U.A., if only the bulk of the defining species pairs is considered (heavy lined rectangles in figure 2). Nevertheless, there are "extreme" species pairs which produce much overlap (arrows in Figure 2, see below). In the following KOCHER's U.A. are designated with the letter "K".

— *K1*, defined by the cooccurrence of *Stylocapsa oblongula* with many other species corresponds to U.A. 3–5. Some species zoned by KOCHER as K1 are now zoned as U.A. 1–2, based on the presence of other species not included with KOCHER's zonation.

— *K2*, defined by the cooccurrence of Hagiastrid sp. A with *Mirifusus chenodes* equals U.A. 6.

— *K3*, defined by the cooccurrence of *Napora pyramidalis, Gorgansium pulchrum* and *Guexella nudata* with *Tritrabs exotica*, corresponds to U.A. 5–6.

— *K4* is the same U.A. as *K5*, since no cooccurrences other than those in K5 are present. The bulk of defining species pairs have their cooccurrence in U.A. 7–8 of the present zonation. Some of the pairs defining K4–5 are no longer cooccurring in the present zonation: *Higumastra imbricata, Monotrabs plenoides* and *Theocapsomma cordis* are not cooccurring with *Sethocapsa cetia* and *Podocapsa amphitreptera*. Extreme pairs of K4–5 include *Triactoma blakei* cooccuring with *Paronaella mulleri* and *Tritrabs hayi* which span U.A. 2–9 of the present zonation.

— *K6* is defined by cooccurrences of *Acanthocircus* with many species, the bulk of which occur in U.A. 9 of the present zonation. However, the occurrence of *Spongocapsula palmerae* with *Triactoma tithonianum* spans U.A. 2–11! And on the other hand, *Tritrabs casmaliaensis* and *Bernoullius dicera* do not cooccur with *A. dicranacanthos*.

— *K7* is defined by cooccurrences of *Acaeniotyle umbilicata* and *Triactoma echiodes* with many other species, the bulk of these cooccurrences are found in U.A. 9–10 of the present zonation. The extreme correlation extends to U.A. 11 because of *Emiluvia sedecimporata salensis* which has its top in K7.
It should be noted that *Mirifusus guadalupensis* which reaches up to K7, in the present zonation only reaches up to U.A. 8 and thus does not cooccur with the young species of K6–7.

— *K8* is equal to D10–11 and *K9* is equal to E12 of BAUMGARTNER et al. (1980), they thus correlate to U.A. 11–13 and U.A. 14 respectively (see Fig. 2).

3.1.3 Correlation with PESSAGNO (1977a, b)

The correlation of this type of biostratigraphy with the range charts presented by PESSAGNO (1977a, b) is very difficult owing to extreme discrepancies in first and final appearances of the species used for definition, as discussed in BAUMGARTNER et al. (1980, p. 44). The purpose of the few following remarks is to explain the ranges given in Figure 2. Only species which occur in both zonations with a similar delimitation are mentioned.

PESSAGNO's Zones 0 and 1 do not appear in Figure 2, since they are based on absences only (further detail given in BAUMGARTNER et al. 1980). The base of PESSAGNO's Zone 2 (and Subzone 2A) is defined by the first occurrence of *Emiluvia hopsoni, Paronaella bandyi, Perispyridium ordinarium, Ristola procera, Mirifusus guadalupensis* and other species which have their base in the present zonation in U.A. 0–5. The top of Subzone 2A is defined by the final appearance of *M.guadalupensis* and *Angulobracchia purisimaensis* which have their top in U.A. 8–9 of the present zonation.

The base of Subzone 2B is defined by the first appearance of *Ristola altissima* which has its base in U.A. 2 and *Mirifusus mediodilatatus baileyi* (not included in database) which may have its base in U.A. 8. The top of Subzone 2B (and Zone 2) is defined by the final appearance of *Emiluvia hopsoni, Perispyridium ordinarium* and *Hsuum maxwelli* and other species which have their highest appearance in U.A. 9–11.

Zone 3 of PESSAGNO (1977a) is an interval zone which is defined as between the final appearances of the species which mark the top of Zone 2 and the final appearances of *Triactoma blakei* and *Eucyrtidiellum ptyctum* which both terminate in U.A. 10. Thus Zone 3 may either not exist or be at best located in U.A. 10.

The base of Zone 4 of PESSAGNO (1977a) is defined by the first appearance of *Sethocapsa cetia* based in U.A. 9, though with a different specific delimitation. The top is given as the final occurrence of *Ristola altissima* which has its top in U.A. 10 and *R.procera* which has its top in U.A. 8. Thus Zone 4 certainly overlaps with Zone 3 and part of Subzone 2B. It should be noted that Zones 3 and 4 are superposed on the basis of cooccurring *Buchia* only. There is no lithostratigraphic control of this superposition.

Zone 5A–B of PESSAGNO (1977b) can be reasonably well correlated to U.A. 11–13 on the basis of the lowest occurrence of *Obesacapsula rotunda* and the base of *Cecrops septemporatus* which forms the base of Zone 5C, which equals U.A. 14.

3.1.4. Correlation with RIEDEL & SANFILIPPO (1974) and FOREMAN (1973, 1975)

The correlation with these earlier zonations was discussed in BAUMGARTNER et al. 1980 and is given in Figure 2.

3.1.5 Correlation with the Japanese assemblage zones

Numerous Japanese workers have made a fantastic effort in the last few years to unravel the complex Japanese geology by means of radiolarian biostratigraphy (summary e.g. in YAO 1983). The volume edited by NAKASEKO (1982) gives part of the wealth of new data and at the same time documents the striking similarity of Tethyan and Japanese radiolarian morphotypes. A framework of assemblage-zones has been developed, in which rather coarse biostratigraphic units, each defined by a number of characteristic species, are superposed on the basis of stratigraphic sequences and radiolarian faunal content. This concept lends itself for comparison with the present zonation based on U.A.

It appears, however, that the studied sequences often have a complex anatomy due to resedimentation (olistostromes) and tectonism (YAO 1984). Hence, it cannot be excluded that the present scheme of assemblage-zones includes some gaps which could reflect times of nondeposition and/or tectonism. Further work, especially a U.A. treatment

of Japanese data together with the present database is required to elucidate this problem.

The *Unuma echinatus* Assemblage-zone (YAO et al. 1980) has been amply described by several Japanese authors: YAO (1972, 1979, 1983, 1984), ICHIKAWA & YAO (1976), YAO & MATSUOKA (1981), YAO et al. (1982). It is characterized by *Unuma echinatus* and several other species not included in the present zonation. This assemblage is clearly represented by U.A. 0 but may also (at least in part) be represented by U.A.1, and thus partly overlap with the *Guexella nudata* Assemblage-zone since *Unuma echinatus* and *Guexella nudata* are cooccurring in U.A. 1.

The *Guexella nudata* Assemblage-zone was described by MATSUOKA (1981), YAO & MATSUOKA (1981), MATSUOKA (1982), YAO et al. (1982), and YAO (1983, 1984). A characteristic species is *Stylocapsa oblongula* and some other species included in the present zonation have their base in this assemblage-zone: *Guexella nudata, Ristola altissima* and *Eucyrtidiellum ptyctum*. Based on these species, this assemblage-zone may be correlated with U.A. 1–5 and thus, in the present zonation seems to overlap with the *Gongylothorax sakawaensis–Stichocapsa* sp. C Assemblage-zone.

The *Gongylothorax sakawaensis–Stichocapsa* sp. C Assemblage-zone as defined by YAO et al. (1982) can be correlated on the basis of the top of *Tricolocapsa plicarum* and *Mirifusus fragilis* and of the base of *Mirifusus mediodilatatus* s.l. in that zone to U.A. 4–5 of the present zonation. However, more species have to be examined to firmly establish this correlation. The *Tricolocapsa* sp. 0 Assemblage-zone cannot be recognized on the basis of the presently included species.

The *Mirifusus mediodilatata–Ristola altissima* Assemblage-zone as introduced by NAKASEKO et al. (1979) and redefined by NAKASEKO & NISHIMURA (1981) includes, besides the defining species which in the present zonation range farther down, *Archaeodictyomitra apiara,* which allows a correlation to U.A. 7–10. The *Mirifusus baileyi* Assemblage-zone introduced by MIZUTANI (1981) and described also by ADACHI (1982) probably corresponds also to this interval.

The *Dictyomitra* sp. B–*Dictyomitra* sp. A Assemblage-zone as defined in YAO et al. (1982) and YAO (1983, 1984) includes *Podocapsa amphitreptera* and thus may be correlated with U.A. 8–11. However it would be desirable to have more common species for comparison.

The *Obesacapsula rotunda* Assemblage-zone was introduced by NAKASEKO et al. (1979) and redefined by NAKASEKO & NISHIMURA (1981). It includes *Cecrops septemporatus* and is thus correlative with U.A. 14. The *Sethocapsa uterculus* Assemblage-zone as defined by YAO (1984) is probably also correlative with U.A. 14 as it includes *Sethocapsa uterculus*. However, many species defining this latter assemblage zone range from U.A. 11–14 in the present zonation: *Obesacapsula rotunda, Alievum helenae, Pseudodictyomita carpatica* and *Xitus* sp. (cf. *X. spicularius*). It may thus be possible that *Sethocapsa uterculus* has a lower range in Japanese localities and hence the *S. uterculus* Assemblage-zone would be an equivalent of U.A. 11–14.

3.2 Chronostratigraphic calibration and distribution of Unitary Associations

Introduction

It is well true that the first step in working out a fossil zonation is to obtain the relative succession of the used taxa and we have followed this rule. However, in order

to date rocks a chronostratigraphic calibration is essential. While it is believed that the present zonation has reached a certain degree of stability not affected by future inclusion of more localities and more species, it is obvious that the correlation to other fossil zonations, magnetostratigraphy and ultimately to chronostratigraphy needs much further work and the solution presented here is preliminary (Fig. 2, 3, Pl. 12).

A primary problem with radiolarians is their general occurrence in siliceous lithologies usually devoid of ammonites which would allow to tie radiolarian zones directly to Jurassic ammonite zones and thus to stages. It is well known and logic, considering dissolution facies and diagenesis, that radiolarians and aragonitic macrofossils like ammonites are hard to be found together. Radiolarians tend to calcify in the presence of abundant lime and thus lose much of their specific characters, whereas ammonites almost never are found in silica-rich sediments, because these are, as we believe, certainly deposited below the ACD and probably near or below the CCD. Rare and invaluable exceptions have been found in the Subbetic and in the Lombardy Basin, where single ammonites or masses of ammonite-bearing limestones were gravitationally displaced into deeper basins hosting silica-rich lithologies (see below). An other possible solution is to search for basinal sequences including very detrital calcareous and partly organic-rich lithologies in which both ammonites and radiolarians have a preservation potential (Lower–Middle Jurassic of Oregon see PESSAGNO & BLOME 1980 and PESSAGNO & WHALEN 1982, and loc. 38 herein). The third and much less reliable way is to tie radiolarian zones to zonations of other microfossils coexisting with radiolarians: calpionellids, calcareous nannofossils, dinoflagellates. Owing to lack of better criteria much of the present calibration is based on this indirect correlation.

U.A. 0–1 (Zone A0) have been found in Tethyan and Japanese basinal sequences but have not been directly dated. At DSDP Site 534A (loc. 30) it becomes clear that they must be of pre-middle Callovian age. In the Sierra de Ricote (Subbetic, loc. 45) U.A. 2 was found less than 20 m above *Cadomites* sp. (cf. *C. daubenyi*) (Bathonian, see SEYFRIED 1978) in a basinal cherty limestone sequence. More samples from this section are in preparation. On the other hand in BAUMGARTNER et al. (1980) we have, following KÄLIN et al. (1979), used the argument that the uppermost Marne a Posidonia (which in basinal sections show U.A. 0–1) are of Callovian age, to date the earliest radiolarite deposition as late Callovian. It is now evident that the onset of radiolarite deposition is very diachronous and essentially dependent of the local subsidence history (see Fig. 3 and conclusions). Southeastern Tuscany, where KÄLIN et al. (1979) suggested much of the Callovian to be represented by the Marne a Posidonia facies may be an area where radiolarite deposition started slightly later than in the surrounding deeper basins (e.g. Fiume Bosso, Umbria, loc. 26), a hypothesis which needs to be tested by radiolarian faunas from these localities. Thus it is believed that U.A. 0–1 (Zone A0) may correspond to much (if not all) of the Bathonian and probably the basal part of the Callovian.

U.A. 2–4 (Zone A1) have been found in various Tethyan sections and at DSDP Site 534A (loc. 30) from Core 126-4, 14 cm to Core 124-1, 52 cm. This interval is assigned to the middle Callovian by HABIB & DRUGG (1983) based on dinoflagellates, and by ROTH (1983, p. 603) based on calcareous nannofossils (*Stephalolithion hexum* Subzone). In Sierra de Ricote (Subbetic, Spain, loc. 45) two samples assignable to U.A. 4–5 are found directly above displaced limestones containing middle to late Callovian ammoni-

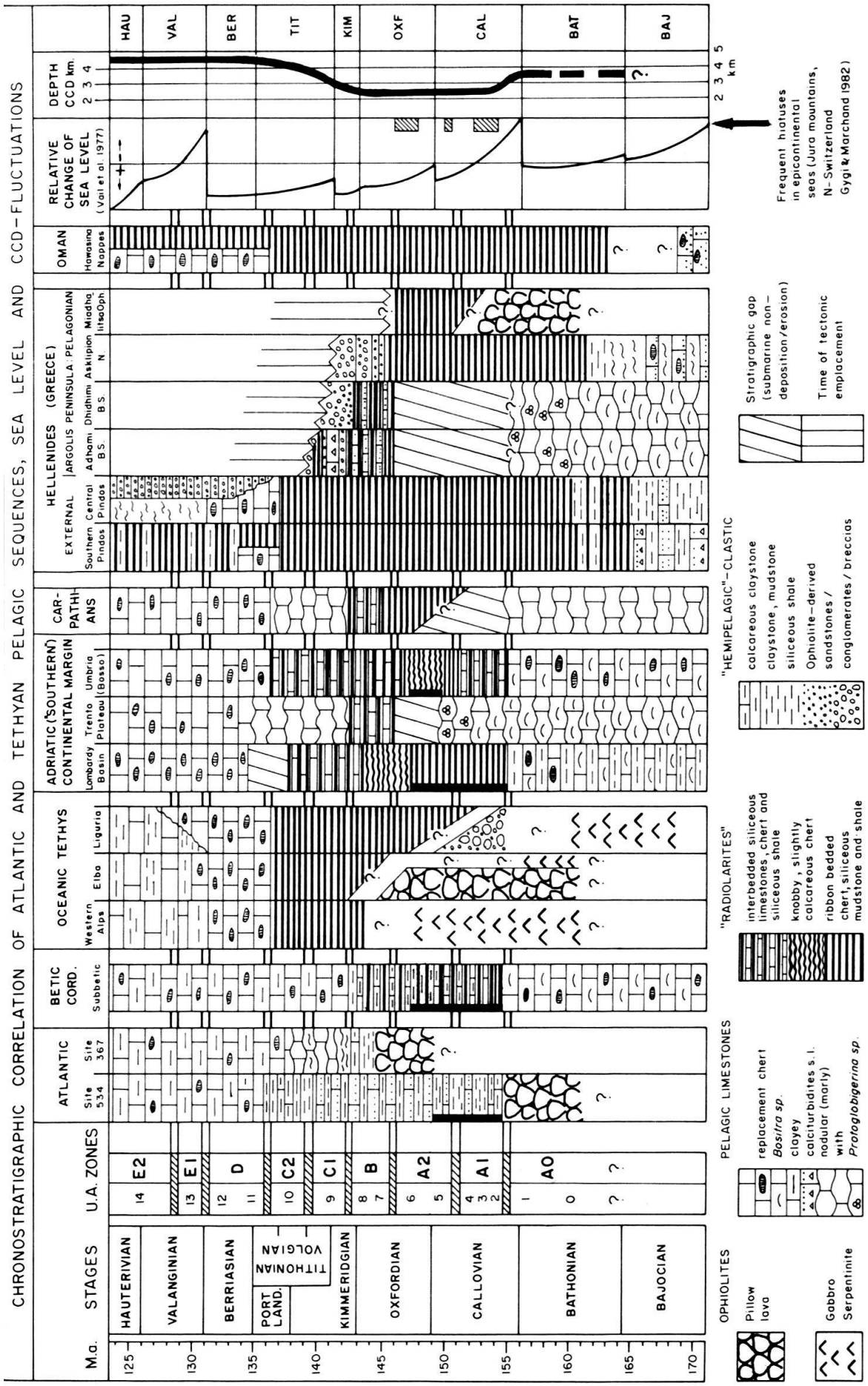

Fig. 3. Chronostratigraphic correlation of Atlantic and Tethyan pelagic sequences for the Bajocian–Hauterivian time interval, principally based on radiolarian data presented in this paper. Note the Bathonian onset of radiolarite deposition in basins existing since the Triassic, early Callovian onset in basins individualized since the Early Liassic and late Oxfordian onset on seamounts and plateaus. The early Callovian onset seems to express a rise of the calcite compensation depth in concert with a rapidly rising sea level. Note also a minimum late Middle Jurassic age for oceanic crust in Greece (Pelagonian s.l.), Liguria and western Alps and Late Jurassic nappe emplacement in eastern Greece (Pelagonian s.l.).

Apart from radiolarian data and own field observations the following sources were consulted for lithology and age information: Site 534: SHERIDAN, GRADSTEIN et al. 1983. Site 367: LANCELOT, SEIBOLD et al. 1978. Subbetic SEYFRIED 1978. Western Alps (Schistes lustrés): DE WEVER & CABY 1981, Trento Plateau: STURANI 1964, FÖGELGESANG 1975. Carpathians: AVRAM 1976 and references summarized in BAUMGARTNER et al. 1980. Southern Pindos: THÉBAULT et al. 1980, DE WEVER & THÉBAULT 1981. Central Pindos: FLEURY 1974, 1975. Argolis Peninsula: BAUMGARTNER 1980, 1981, BAUMGARTNER et al. 1980. Oman: GLENNIE et al. 1974, BERNOULLI & WEISSERT (pers. comm.). Sea level fluctuations: VAIL et al. 1977. CCD: BOSELLINI & WINTERER 1975, LAUBSCHER & BERNOULLI 1977, WINTERER & BOSELLINI 1981, JENKYNS & WINTERER 1982 and own interpretations.

tes (see Pl. 12 and SEYFRIED 1978). U.A. 2–4 (Zone A1) thus certainly represent the middle Callovian and probably parts of the early and the late Callovian.

U.A. 5 (Zone A2) has been found in several Tethyan sections and at DSDP Site 534A (loc. 30) from Core 122-1, 131 cm to Core 111-1, 12 cm. This interval includes the upper Callovian and the entire Oxfordian according to HABIB & DRUGG (1983) based on dinoflagellates. According to ROTH (1983, p. 603) this interval includes the *Cyclagelosphaera margarelii* nannofossil Subzone which spans the late Callovian and the early Oxfordian and the lower part of the *Vagalapilla stradneri* Zone (starting in Core 113-1, 47 cm) which would represent at least part of the middle Oxfordian.

U.A. 6 (Zone A2) has thus far only been positively identified in the Lombardy basin without coexisting other fossils. It has a very low value of reproducibility (see Fig. 1) and may or may not have a biochronologic significance.

The level of the Callovian/Oxfordian boundary at Site 534A was a matter of considerable debate amongst the various nannofossil and dinoflagellate specialists involved. This is reflected by some discrepancies between the Site Report (SHERIDAN, GRADSTEIN et al. 1983) and the papers by ROTH et al. (1983), ROTH (1983) and HABIB & DRUGG (1983) in the same volume. The calibration presented in BAUMGARTNER (1983) was based on preliminary dinoflagellate data giving the Callovian/Oxfordian boundary above Core 124 (and thus coinciding with the limit of Zones A1/A2). The present solution follows the consensus ROTH (1983)–HABIB & DRUGG (1983). Further work is needed to substantiate the age assignment of the limit of Zones A1/A2.

U.A. 7–8 (Zone B) is widely distributed in Tethys, Atlantic and California (Point Sal). It marks the time of onset of radiolarite deposition on most deeper submerged submarine highs in Tethys (see conclusions and Fig. 3). Considerable uncertainty still exists concerning the chronostratigraphic range of this zone, which partly results from a scarcity of coexisting fossils throughout the studied localities and partly from fundamental problems concerning the Tethyan Late Jurassic biochronostratigraphy. U.A. 8 was determined at DSDP Site 367 (loc. 29) in Core 37-1, 147 cm to Core 36-3, 49 cm, an interval which was assigned to the Oxfordian and possibly the lower Kimmeridgian based on foraminifers, aptychi and calcareous nannofossils (see LANCELOT, SEIBOLD et al. 1978). In Santa Anna (Sicily, loc. 28) Oxfordian to earliest Kimmeridgian ammonites were found above U.A. 8 (BAUMGARTNER et al. 1980, p. 31). In the Ceniga section (Trento, northern Italy, loc. 44) U.A. 8 is included in late Oxfordian to earliest Kimmeridgian siliceous limestones (FOGELGESANG 1975). Thus it is concluded that U.A. 7 represents part of the middle and part of the late Oxfordian and U.A. 8 part of the entire late Oxfordian and part of the early Kimmeridgian.

U.A. 9 (Zone C1) has been found in the Atlantic, Lombardy and Greece. At DSDP Site 534A (loc. 30) it was found in sample 106-1, 29 cm which is located near the top of the *Valagapilla stradneri* Nannofossil-Zone which is given as latest Kimmeridgian (ROTH 1983, p. 603). HABIB & DRUGG (1983), based on dinoflagellates locate the Kimmeridgian/Tithonian boundary just above this sample in Cores 105-1 to 104-2. At DSDP Site 367 (loc. 29) U.A. 9 was found in Cores 35-2, 42 cm to 34-4, 104 cm, which is immediately below a sample (34-4, 44 cm) containing the latest Kimmeridgian/earliest Tithonian aptychus *Granulaptychus planulati* (QUENSTEDT) (RENZ 1978, see remarks in BAUMGARTNER et al. 1980, p. 32). In Lombardy, Tuscany and Umbria U.A. 9 is found in the middle and upper parts of the Rosso ad Aptici, which are dated by aptychi and rare ammonites as Tithonian (summary of biostratigraphic data in

BAUMGARTNER et al. 1980). It is concluded that U.A. 9 (Zone C1) represents the late Kimmeridgian (sensu gallico) and the early Tithonian (Volgian).

U.A. 10 (Zone C2) has been recorded in the Atlantic, Tethys and Pacific. At DSDP Site 367 it is present in the sample 32-4, 9 cm just above samples (up to 32-4, 136 cm) assigned to the *Parhabdolithus embergeri* Nannofossil-Zone, but below samples assigned to the *Nannoconus colomi* Zone, which has its base in sample 32-3, 59 cm. Thus the sample is certainly of middle–late Tithonian age. In Tethyan sections U.A. 10 is found in strata immediately below the basal Maiolica limestone which in some places reach the late Tithonian dated by the first calpionellids corresponding to the *Crassicollaria* Zone A of REMANE. Thus U.A. 10 (Zone C2) may represent the middle and part of the late Tithonian.

U.A. 11 (Zone D) is widely distributed in Atlantic, Tethyan and Pacific localities. Its lowest occurrence coincides with the onset of nannofossil limestone sedimentation of the basal Maiolica Limestone in Tethys and the Blake Bahama Formation in the Atlantic. In the Fiume Bosso section (Umbria, loc. 26) U.A. 11 has been found a few meters above the base of the Maiolica Limestone where it is associated with *Crassicollaria intermedia, C. brevis* and *Calpionella alpina* (MICARELLI et al. 1977) indicating a latest Tithonian age. At DSDP Site 534A, sample 89-2, 47 cm contains U.A. 11, immediately above samples assigned to *Calpionella* Zone B, earliest Berriasian. In the Svinita section (Romania, loc. 9.) U.A. 11 is dated as late Berriasian by ammonites and calpionellids (AVRAM 1976, summary in BAUMGARTNER et al. 1980). Thus U.A. 11 (Zone D) spans the latest Tithonian to late Berriasian.

U.A. 12 (Zone D) has only been found in one section: Trattberg (Austria, loc. 43), its biochronologic significance is thus not yet established.

U.A. 13 (Zone E1) has been positively identified in the Svinita section, where it occurs at the top of the *Calpionellopsis* Zone and in the *Calpionellites* Zone. It does not reach the top of this zone, hence, represents the early Valanginian. At DSDP Site 534A, three samples in Core 81-2 are assignable to U.A. 13–14 and occur immediately below dinoflagellate samples indicating the basal Valanginian.

U.A. 14 (Zone E2) is widely distributed in Tethyan, Pacific, Japanese and possibly also Atlantic sections. In the Svinita section (Romania, loc. 16) it occurs first at the very top of the *Calpionellites* Zone and starts thus in the late early Valanginian. In the Veveyse section (Switzerland, loc. 38) U.A. 14 coexists with the *Callidiscus* Ammonite-zone of the terminal Valanginian. At DSDP Site 167 (Central Pacific, loc. 31) it occurs in samples from core 76-2, 67 cm upwards which according to nannofossils are of Late Valanginian age and younger. The upper limit of this U.A. has not been established.

4. Significance of dating radiolarites and conclusions

4.1 Chronostratigraphy: Correlation of Atlantic and Tethys and timing of Middle–Late Jurassic siliceous sedimentation

4.1.1 Correlation of Atlantic and Tethyan pelagic sequences

The occurrence of the same succession of U.A. at DSDP Site 534 and in various Tethyan basinal sections allows for a detailed correlation of the middle Callovian to

Neocomian pelagic facies (cf. BAUMGARTNER 1983). The middle to late Callovian–early Oxfordian dark-colored, partly organic-rich claystones and calcareous claystones drilled at Site 534 contrast with the coeval very siliceous basal radiolarites (BOSELLINI & WINTERER 1975, Diaspri facies A and B of KÄLIN et al. 1979) of many Tethyan basinal sequences (Fig. 3). The common features of these lithologies and of the cored rocks in the Atlantic are the scarcity or absence of carbonate indicating sedimentation in proximity or below the CCD and the possibly poorly oxygenated sedimentary and/or early diagenetic environment resulting in dark colored, pyrite-rich beds which sometimes preserve a very fine lamination. However, poorly oxygenated conditions must have prevailed in rather small, deeply submerged basins, since coeval sections on adjacent submarine highs (e.g. Trento Plateau cf. WINTERER & BOSELLINI 1981) show well-oxygenated nodular limestones and still other basinal radiolarite sections (Asklipion Nappe, Greece; Oman) show no sign of poor oxygenation. Otherwise, the sedimentation at Site 534 was much more clay-rich and in addition received abundant turbiditic carbonate input from shallower pelagic areas and from carbonate platforms (SHERIDAN, GRADSTEIN et al. 1983). The radiolarian silt layers constitute generally less than 2% and no more than 5.2% of the total sediment in Cores 127–122 (SHERIDAN, GRADSTEIN et al. 1983). Thus, even considering the effects of deep burial diagenesis the sediments in the two realms are not comparable in their silica content.

During the Oxfordian, deposition at Site 534 was predominantly turbiditic and does not compare to the peculiar facies of knobby radiolarites (BOSELLINI & WINTERER 1975, Diaspri facies C of KÄLIN et al. 1979) deposited in a well oxygenated environment at that time in Tethyan basins.

During the Kimmeridgian and most of the Tithonian reddish calcareous claystones and marly chalks assigned to the Cat Gap Formation were deposited both at Site 534 and 367 (Cap Verde Basin). They resemble the Ammonitico Rosso Superiore of Tethyan submarine swells both in faunal content *(Saccocoma)* and dissolution facies (deposited near or above the aragonite compensation depth, SHERIDAN, GRADSTEIN et al. 1983), but are far less siliceous than the coeval Rosso ad Aptici of Tethyan basinal sections, a fact which indicates deeper carbonate dissolution surfaces and/or a shallower seafloor in the Atlantic at that time.

Close to the Jurassic/Cretaceous boundary, in the late Tithonian, sedimentation became more similar in Central Atlantic and Western Tethys with the onset of lightcolored nannofossil chalk or limestone deposition of the Blake-Bahama Formation and the Tethyan Maiolica Formation. On a general scale, Tethyan deposition was still more siliceous. This type of deposition remained remarkably constant and widespread through the entire Neocomian.

4.1.2 Temporal distribution of radiolarite deposition related to subsidence history of Tethyan continental margins and ocean basins

A number of recent papers have dealt with Tethyan Jurassic radiolarite deposition (BOSELLINI & WINTERER 1975, FOLK & MCBRIDE 1978, MCBRIDE & FOLK 1979, KÄLIN et al. 1979, WINTERER & BOSELLINI 1981, BARRETT 1979, 1982, JENKYNS & WINTERER 1982). Much of the interpretations and models in these papers are based on insufficient age control, which led to assumptions like general contemporaneity of radiolarite de-

position across oceans and margins. The biochronologic evidence presented in this paper proves a systematic diachronism of the onset of radiolarite deposition and intends to relate this to the subsidence history of the studied paleogeographic realms. As a consequence, some models become very likely and others can clearly be ruled out.

a) Triassic basins – Bathonian onset of radiolarite deposition. – There are a number of basins usually associated with the "Alpine" Triassic that existed prior to the opening of the central Tethys (LAUBSCHER & BERNOULLI 1977) and were the site of deep-water sedimentation at least since the middle Triassic through the entire Mesozoic. Some examples are (Fig. 3): Pindos (FLEURY 1974, 1975, THIÉBAULT et al. 1981, DE WEVER & THIÉBAULT 1981), Asklipion Nappe, Central Argolis Peninsula (BAUMGARTNER 1981) and Hawasina Nappes, Oman (GLENNIE et al. 1974, BERNOULLI & WEISSERT unpubl. mscr.). The Triassic deep-water facies have been dated classically with *Halobia* and more recently by means of conodonts. The Jurassic facies, being very siliceous, have only recently been dated more precisely. At least in the southern Pindos (THIÉBAULT et al. 1980) it appears that carbonate-free radiolarite deposition began in the Bathonian, although this age is based on displaced shallow water foraminifers. The radiolarian data presented herein confirm this early age of onset of radiolarite deposition: U.A. 0 (lower part of Zone A0, Bathonian, see chapter 3) is present in lime-free cherts in the Asklipion Nappe and the Hawasina Nappes.

b) Jurassic basins – early–middle Callovian onset of radiolarite deposition. – Many areas of the Tethyan continental margins are characterized by Early–Middle Liassic tensional tectonics accompanied by rapid subsidence reflected by aprupt changes from shallow water to pelagic facies (e.g. BERNOULLI 1972). The relative basins studied for radiolarians are: The internal Subbetic (AZÉMA 1977, SEYFRIED 1978), Lombardy Basin (BERNOULLI 1964, KÄLIN & TRÜMPY 1977, WINTERER & BOSELLINI 1981) and Umbria (CENTAMORE et al. 1971, BERNOULLI et al. 1979). Subsidence was differential: troughs coexisted with submarine highs on which shallow carbonate sedimentation persisted up to the Pliensbachian (Umbria, etc.) or Aalenian (Trento Plateau) (see below). In the troughs Middle–Late Liassic sediments typically include cherty limestones with abundant redeposited carbonates, ammonite-bearing marls and marly limestones which grade up-section into marls and slightly cherty limestones rich in "pelagic" bivalves *(Bositra)* which were deposited during the Toarcian–Callovian p.p. (KÄLIN et al. 1979) or Aalenian–Bajocian–early Callovian (Umbria: BERNOULLI et al. 1979) below the aragonite solution surface (ibid.). These *Bositra*-rich cherty limestones have furnished radiolarian assemblages assignable to U.A. 0 and to U.A. 1 in their uppermost part. A sudden change to very siliceous or even lime-free radiolarite sedimentation can be observed in all these basins. Since the lowest radiolarites contain usually U.A. 2, this change occurs in all studied sections at the limit between Zone A0 and Zone A1 (a major faunal break, see below), which has been placed within the early Callovian (see chapter 3).

c) Early–Middle Jurassic plateaus and seamounts – late Oxfordian onset of radiolarite deposition. – In many areas affected by the Liassic tensional tectonics, local seamounts or extended plateaus, documented by a remarkably different depositional history, coexisted with adjacent troughs. The examples studied for radiolarians are: Trento Plateau (STURANI 1964, WINTERER & BOSELLINI 1981) and Argolis Peninsula Basal Sequences (BAUMGARTNER 1980, 1981) (seamount sequences from Umbria are in

preparation). On these highs shallow water sedimentation persisted up to the Middle Liassic (Argolis Peninsula) or up to the Aalenian (Trento Plateau) and was succeeded, with intervening times of nondeposition/erosion documented by hardgrounds, by condensed pelagic sedimentation. Nodular, marly pelagic limestones typically include Toarcian to Callovian ammonite faunas and *Protoglobigerina*. The first radiolarites generally rest on an important hardground which documents nondeposition during possibly the entire Callovian and early Oxfordian in the Argolis Peninsula and during at least the early Oxfordian on the Trento Plateau. The seamount radiolarites are generally siliceous limestones with chert nodules and stringers interbedded with thin marls or clays (in the Argolis Peninsula calcareous radiolarites [Angelokastron and Ayos Nikolaos Cherts] are overlain by lime-free siliceous mudstones and ophiolitic clastics [Dhimaina Formation] reflecting rapid subsidence related with the Late Jurassic obduction of the Vardar and equivalent ophiolites in eastern Greece, cf. BAUMGARTNER 1981). The lowest seamount radiolarites have furnished radiolarian assemblages assignable to U.A. 7 (Argolis Peninsula) or U.A. 7–8 (Trento Plateau), which would correspond to a Late Oxfordian age.

d) Examples of oceanic crust – middle Callovian–Oxfordian onset of radiolarite deposition. – Dating basal radiolarites resting on pillow lavas, gabbro and serpentinite commonly interpreted as allochthonous remnants of oceanic crust has proven to be delicate owing to the advanced diagenetic or anchimetamorphic stage of these rocks. Nevertheless a few dates are presented here and more are in preparation.

DE WEVER & CABY (1981) determined a late Oxfordian/early Kimmeridgian (U.A. 8) age in metaradiolarites overlying serpentinites and ophiolite breccias in the Chabrières series – the base of postophiolitic schistes lustrés of the western Alps.

On Elba island, the base of the radiolarites resting on what has been interpreted as Ligurian oceanic crust has been dated in two places (cf. locality descriptions loc. 46, 47 and Pl. 12). Surprisingly enough both the base of the probably thickest known radiolarite sequence around Monte Campannello (see also BARRETT 1979, 1982) and the most reduced sequence in the area San Felo–Namia (see also BERNOULLI et al. 1979) show the same age: U.A. 7–8 = Zone B which means a Late Oxfordian to possibly early Kimmeridgian age.

In Liguria the base of anchimetamorphic radiolarites resting on a gabbro boulder conglomerate near Rocchetta di Vara (loc. 48) is dated as U.A. 3–5 (Zones A1/A2) which corresponds to a middle/late Callovian or possibly early Oxfordian age.

In the ophiolites overlying the Pelagonian s.l. units of the internal Hellenides two ages are available at the moment: In the Migdhalitsa Ophiolite Unit of the Argolis Peninsula (loc. 9) a radiolarian sample some m above pillow lavas is assignable to U.A. 3–8, possibly restricted to 3–5, which would correspond to a middle/late Callovian–early Oxfordian age. A well preserved sample from interpillow sediment (J. Simantov, personal communication), of northern Evvoia (loc. 49) is assignable to U.A. 4–5 (Zones A1/A2) which corresponds to a middle/late Callovian possibly early Oxfordian age.

These ages are of prime importance for the paleotectonic reconstruction of the Tethys ocean, which will be discussed elsewhere (WINTERER & BAUMGARTNER, in preparation).

4.2 Paleooceanographic conclusions

The presented radiolarian ages demonstrate fundamental chronostratigraphic relationships which are no longer left to the imagination of the geologist. The proposed age relationships and the following immediate interpretations should be the basis of any paleooceanographic model of the Western Tethys ocean:

1. The contemporaneous deposition of limestone on seamounts/plateaus and of lime-poor to lime-free sediments in immediately adjacent troughs is now firmly established. This clearly implies a bathymetric control of radiolarite deposition (cf. BOSELLINI & WINTERER 1975, etc.).

2. The progressive extension of siliceous radiolarite deposition from older to younger basins and finally onto submarine plateaus shows that the diachronism of the radiolarites is not basin-to-basin as it may appear as for instance in JENKYNS & WINTERER 1982 (Fig. 2) but basin-to-swell, i.e. it is controlled by the subsidence history, reflected by the time of onset of pelagic deposition, of each depositional realm. This implies again a primarily bathymetric control of radiolarite deposition.

3. If it is bathymetry that primarily controlled the sites of radiolarite *deposition,* other factors must have controlled abundant radiolarian *production.* In comparing coeval Atlantic and Tethyan sequences it results that even admitting 6 times higher accumulation rates for the Atlantic to account for detrital and carbonate dilution, radiolarian production/preservation must have been on the order of 5–10 times higher in Tethys to result in the observed silica accumulation rates. Similar conditions may have led to the accumulation of thick Jurassic-Cretaceous chert sequences in western North America (typical example: Marine Headlands, north of San Francisco), southern Central America (Nicoya Ophiolite Complex), Japan and other circumpacific ophiolite-related terranes. The "small-basin" hypothesis, as portrayed by JENKYNS & WINTERER (1982) seems the most plausible way to explain these occurrences.

4. Basins individualized since at least the Middle Triassic had subsided by the end of the Bajocian to depths below the (CCD at that time possibly at 3–4 km) to receive radiolarite deposition.

5. The synchronous early Callovian onset of radiolarite sedimentation in basins created in the early Liassic implies a basinwide paleooceanographic event, related to the paleotectonic evolution of the western Tethys and possibly reflecting also a "worldwide" sealevel rise (see Fig. 3). A rapid rise of the carbonate dissolution surfaces (CCD from 3–4 to 2–3 km) is the most plausible explanation of the observed abrupt change from cherty limestones to chert in many sections (BOSELLINI & WINTERER 1975).

6. The late Oxfordian onset of calcareous radiolarite deposition on seamounts/plateaus may be an indication of a further shallowing of the CCD and/or a relative culmination of radiolarian production or, alternatively, the effect of rapid (rejuvenated) subsidence of these areas to depths close to the CCD.

7. As stressed by many authors, a first-order paleooceanographic change related with an evolutionary bloom of calcareous nannoplankton near the end of the Late Jurassic caused a synchronous change from siliceous or clay-rich to coccolith sedimentation in Atlantic and Tethys and is confirmed by a drastic radiolarian faunal change at this boundary. A drop of the CCD by the order of 2 km (to come to 4–5 km) is reasonable (cf. BOSELLINI & WINTERER 1975). Basins lacking Neocomian limestones

(e.g. southern Pindos, THIÉBAULT et al. 1981) must have subsided to depths below the Neocomian CCD (approx 4.5 km, cf. LAUBSCHER & BERNOULLI 1977).

8. The surprisingly young ages of basal radiolarites on presumable oceanic crust in various ophiolite units contrast with the radiometric ages of the underlying igeous rocks (BIGAZZI et al. 1973). However, age and siliceous facies of the basal sediments on oceanic crust are in agreement with a very shallow (2–3 km) CCD at that time. Likewise, early Middle Jurassic sediments on oceanic crust would have to be calcareous.

These few conclusions refer to the temporal/spatial distribution of radiolarites only. Other aspects like sedimentation processes, duration and intensity of synsedimentary faulting and the subsidence history of the various types of basins and swells need to be reevaluated in view of the new chronologic constraints.

4.3 Radiolarian faunal changes and provincialism related to paleooceanography

As more and more well preserved sample material becomes available, successions of closely related morphotypes can be recognized, which may be interpreted as evolutionary lineages on an intraspecific or intrageneric level (see systematic part of this paper). Several authors have documented the evolutionary nature of vertical faunal change in Mesozoic radiolarians: BAUMGARTNER (1980), PESSAGNO & BLOME (1980, 1982), PESSAGNO & WHALEN (1982), MATSUOKA (1983), etc. However, at most half of the first and final appearances of species included in this study can be related to evolutionary processes, for the other half of the species we do not know possible ancestors nor descendants. Certainly, this can be blaimed to a still fragmentary knowledge of Mesozoic radiolarians owing to a limited amount of samples (the number of studied well preserved samples does, at present, not exceed a few hundreds) and to preservational problems mentioned in the introduction and emphasized in several earlier papers (BAUMGARTNER 1980, 1984, BAUMGARTNER et al. 1980, 1981).

On the other hand, we must be aware of the fact that the presently studied samples are strongly biased towards low and middle paleolatitudes and perhaps towards other paleoecologic niches like small, highly fertile basins with predominantly siliceous biogenic deposition. This would allow for a mecanism of time-related faunal change as suggested in BAUMGARTNER et al. (1980, p. 46): Regional paleooceanographic changes (e.g. changes of water circulation patterns, temperature, salinity and availability of nutrients) would cause a high mortality rate amongst the preexisting radiolarian fauna and subsequent immigration of other species adapted to the new paleooceanographic conditions, rather than evolutionary adaptation of stationary lineages. The ancestors of the newly immigrated and the descendants of the extinct species were to be found in sequences deposited in different paleolatitudinal and/or paleooceanographic settings.

The data presented in this paper do support this hypothesis at least for two events:

1. The early Callovian onset of radiolarite deposition in Jurassic basins of Tethyan continental margins (interpreted as a rise of the CCD in concert with a sea-level rise).

2. The establishment of calcareous nannofossil sedimentation near the end of the Jurassic throughout Atlantic and Tethys (interpreted as a substantial drop of the CCD). Both events coincide with a drastic change in radiolarian faunal composition, which is only partially acknowledged in the present zonation, since a small portion only of the Middle Jurassic and the Early Cretaceous assemblages are included. Of

course, these "faunal changes" were at first hand suspected to be preservational (cf. DE WEVER in BAUMGARTNER et al. 1980, p. 47), related to changing seafloor and diagenetic environments. However, the same faunal breaks seem to be recorded in sequences which maintain a siliceous record across the mentioned events (e.g. Southern Pindos, Argolis Peninsula, Oman), a fact which would support faunal changes induced by paleooceanographic events.

Further work is needed to establish whether these faunal breaks are limited to Mediterranean Tethys and Atlantic or whether they are found "worldwide" in low latitudes. The published Japanese assemblage-zones compare favorably to the zonation presented herein and suggest similar faunal breaks in Japanese sequences.

There is now definite evidence for Jurassic radiolarian provincialism, which may be either of paleolatitudinal or of paleoecological origin or both. Callovian radiolarian faunas from southern Alaska and eastern Oregon studied by BLOME (in press), have virtually nothing in common with Callovian assemblages presented herein and in many Japanese papers (summary in YAO 1983). BLOME's (in press) material as well as other Early and Middle Jurassic material presented by PESSAGNO & BLOME (1980) and PESSAGNO & WHALEN (1982) comes from western North American sequences which are predominantly detrital (partly organic-rich sand-, silt- and claystones intermixed with carbonate). These sequences were certainly deposited in a different paleotectonic/paleo-oceanographic setting than was the detritally starved early Central Atlantic–Tethyan seaway, a circumstance which should at least in part account for the different radiolarian faunas.

Alternatively, it may turn out, that the forementioned radiolarian assemblages reflect also a middle to higher latitude influence, although many terranes of western North America are now believed to be of low-latitude origin (e.g. JONES et al. 1982). Much further work of comparing assemblages of known zonal assignment or age is required to substantiate Jurassic faunal provinces. At present it is certainly an oversimplification to distinguish only "Tethyan" (= low latitude) and "Boreal" (= higher latitude) faunal provinces.

4.4 Final conclusions and perspectives

4.4.1 Radiolarian biochronology

Establishing Unitary Associations has proved to be a very effective (if not the only possible) way to integrate a large amount of highly dissolution controlled radiolarian data into a biochronologic framework. The cooccurrence chart of species, formed by vertically ordered U.A., represents maximum ranges of each species with respect to all other species. This is the only type of range which can be accurately defined for radiolarians, based on a given set of data (average ranges are poorly defined and directly contradicted by well preserved samples, see BAUMGARTNER 1984). It is believed that the presented zonation has reached a certain stability in that it should not be altered, but refined by the inclusion of data from further localities and more species in the database.

The geographic reproducibility of many of the proposed zones is still low (see

Fig. 1), owing to the fact that only a few sections cover each time interval. More work is required to test reproducibility within and beyond the studied realms.

The process of further refinement of radiolarian biochronology is twofold:

1. The morphologic units ("morphotypes", "species" or "subspecies") used to establish a range need to be redefined as accurately as possible in terms of vertical morphologic successions (i.e. vertical character change) interpreted as evolutionary lineages. The presented coarse biochronologic framework is the necessary base for this process to ascertain regional correlation and to eliminate local effects of dissolution.

2. More species (drawn from an already existing database of approx. 300 morphotypes) need to be included in order to refine the zonation and to allow better correlation with other zonations.

4.4.2 Extension through the Middle and Early Jurassic

Extending radiolarian biostratigraphy further down into the lower Middle and Early Jurassic in the Tethyan area is mainly a preservational problem. Pelagic limestones in a "starved" continental margin environment have thus far shown a low preservation potential for radiolarians. Much of the replacement chert present in these sequences seems to originate from displaced sponge spicules rather than from radiolarians, but more work is required. Key sections for an Early–Middle Jurassic radiolarian record may be found in basins which inherited pelagic conditions from Triassic times (Lagonegro, Pindos, Asklipion/Othris [internal Hellenides], Antalya, Oman, etc.). These basins were already in the Early Jurassic deep enough to preserve a moderately siliceous sedimentary record, which became entirely siliceous in the Middle Jurassic.

4.4.3 Diachronism of onset of Tethyan radiolarite deposition

A systematic diachronism of the onset of radiolarite deposition, which spans at least the Bathonian to Oxfordian, is documented. The age of the oldest radiolarite clearly relates to the subsidence and bathymetric history of its depositional site expressed by the age of the first pelagic sediment (limestone) underlying the radiolarites. More data, especially from the Umbrian realm, are in preparation to substantiate this relationship. A further step will be the modelling of the Jurassic CCD by means of subsidence curves of individual blocks. However, more direct information on the timing and intensity of synsedimentary block faulting is required to determine the times of rejuvenation of subsidence.

5. Systematic Paleontology

Explanatory remarks

Purpose. – The purpose of the following alphabetic listing of genera and species is twofold:

a) To define as clearly and concisely as possible the morphologic limits of each taxon as they were used in establishing the database and the resulting zonation. Where it seemed practical for routine determination, these morphologic limits were set rather large to deliberately include two or more morphotypes. In other cases, where an increase of vertical stratigraphic resolution was expected, the morphologic limits are defined by differential

diagnostic criteria as narrow as possible. A near-to-complete but critical synonymy should provide reference to morphologic variability (illustrations) and stratigraphic occurrences other than the ones included in the database.

b) To describe new taxa and redefine some of the described ones under the light of supposed evolutionary relationships on a generic level. Suprageneric relationships and classification will be discussed in a later stage of work.

Criteria for introducing new taxa and for taxonomic ranking. – a) Subspecies: A subspecies level is assigned to some taxa hitherto treated as species and to some newly introduced ones in the following cases: If two or more taxa merely represent the end members of a highly variable group of morphotypes, these end members are treated as subspecies and the group is treated as species (e.g. *Emiluvia sedecimporata*). If two or more morphotypes constitute an apparent evolutionary lineage expressed as gradual or small successive morphologic changes in vertical sequences, morphotypic limits have to be set rather arbitrarily and the used rank is subspecific (e.g. subspecies of *Mirifusus mediodilatatus*). Much of the future increase of vertical resolution may be achieved by quantifying this type of "intraspecific" or "character" evolution (cf. SACHS & FAIRBANKS 1979).

b) Species: New species are introduced where morphotypes or groups of morphotypes are clearly definable, have a proven wide geographic distribution (hence are useful for correlation) and where sufficient well preserved type material is available.

c) Genera: New genera are introduced if the following criteria coincide: 1. The species obviously bear no resemblance to the type species of the genus to which they are presently assigned. 2. Two or several described or yet undescribed species form a morphologic entity or vertical succession strongly suggesting an evolutionary relationship. The criteria for the emendation of existing genera are analogous.

Species numbers. – Owing to data processing several numbering systems had to be used for the studied species: The *data* numbers refer to the species numbers used in the database (appendix and BAUMGARTNER 1984). The *range* numbers are sequential numbers in Plate 11 which enable to quickly locate a species in the range chart. The *pob* numbers are the original numbers assigned to 300 morphotypes in the database of the author (cited here for future reference). The *rk* numbers are the species numbers of KOCHER (1981).

Definition and repository of types. – Holotypes and paratypes are defined in the plates (see plate explanations). Type material, measured type series and all other illustrated material will be deposited under the indicated C-numbers at the *Naturhistorisches Museum, Basel, Switzerland.* Type localities and type levels are described in chapter 6: locality descriptions and indicated on Plate 12.

Alphabetic listing of genera and species

Genus *Acaeniotyle* FOREMAN

Acaeniotyle FOREMAN 1973, p. 258.
Type species: Xiphosphaera umbilicata RÜST 1898.

Acaeniotyle diaphorogona FOREMAN, s.l.

Data 59, range 77, pob 90, rk –, Pl. 1, Fig. 1–2

Acaeniotyle diaphorogona FOREMAN 1973, p. 258, Pl. 2, Fig. 2–5. FOREMAN 1975, Pl. 2F, Fig. 1–3 (not 4, 5), Pl. 3, Fig. 1–2.
Acaeniotyle sp. aff. *A. diaphorogona* FOREMAN 1973, Pl. 2, Fig. 6, 7, Pl. 16, Fig. 16. FOREMAN 1975, p. 607, Pl. 1F, Fig. 1. YAO 1984, Pl. 3, Fig. 24.
Tripocyclia sp. aff. *T. trigonum* RÜST, PESSAGNO 1977a, p. 80, Pl. 7, Fig. 8–9.
Acaeniotyle diaphorogona FOREMAN, MUZAVOR 1977, p. 34, Pl. 1, Fig. 1. MIZUTANI 1981, p. 175, Pl. 61, Fig. 1–2. DE WEVER & THIÉBAULT 1981, p. 582, Pl. 2, Fig. 7. KANIE et al. 1981, Pl. 1, Fig. 1. AOKI 1982, Pl. 1, Fig. 1.

Remarks. – Included are all forms having 3 primary spines and a central spherical nodose shell with fine pores, typical for *Acaeniotyle*. Jurassic forms may have spines shorter than the diameter of the shell.

Acaeniotyle diaphorogona dentata BAUMGARTNER n. subsp.

Data 94, range 99, pob 281, rk –, Pl. 1, Fig. 3–4

Acaeniotyle diaphorogona FOREMAN 1975, p. 607, Pl. 2F, Fig. 5 (only). SCHAAF 1981, p. 431, Pl. 15, Fig. 2. ?NAKASEKO et al. 1979, Pl. 4, Fig. 9. ?NAKASEKO & NISHIMURA 1981, Pl. 1, Fig. 12.

Description. – Central spherical nodose shell as with species, spines generally equal or longer than diameter of shell, bearing 3 broad blades with one to several teeth on distal half of spines.

Remarks. – This form is separated from the bulk of *A. diaphorogona* on the basis of the teeth present on the spines, a character which occurs in the Cretaceous only.

Etymology. – *dentatus, -a, -um* (Latin): equipped with teeth.

Measurements (in μ)

	Holotype	Average of 12 spec.	min.	max.
Diameter of central shell:	187	188	149	238
Average length of 3 spines:	195	188	153	213
Number of teeth on spines:	5–6	4.2	3	6

Type locality. – Locality no. 23 of locality descriptions.

Acaeniotyle umbilicata (RÜST)

Data 80, range 88, pob 92, rk 18, Pl. 1, Fig. 5

Xiphosphaera umbilicata RÜST 1898, p. 7, Pl. 1, Fig. 9. RENZ 1974, p. 799, Pl. 2, Fig. 9–12, Fig. 21.
Acaeniotyle umbilicata (RÜST), FOREMAN 1973, p. 258, Pl. 1, Fig. 12–14, 16. FOREMAN 1975, p. 607, Pl. 2E, Fig. 14–17, Pl. 3, Fig. 3. MUZAVOR 1977, p. 26, Pl. 1, Fig. 3. BAUMGARTNER et al. 1980, Pl. 2, Fig. 8. SCHAAF 1981, p. 431, Pl. 6, Fig. 11, Pl. 15, Fig. 2. NAKASEKO & NISHIMURA 1981, p. 141, Pl. 1, Fig. 7, Pl. 14, Fig. 2. KANIE et al. 1981, Pl. 1, Fig. 2.

Genus *Acanthocircus* SQUINABOL, emend. DONOFRIO & MOSTLER

Acanthocircus SQUINABOL, 1903, p. 124, emend. DONOFRIO & MOSTLER 1978, p. 22.
Type species: Acanthocircus irregularis SQUINABOL 1903.

Acanthocircus dicranacanthos (SQUINABOL)

Data 82, range 86, pob 87, rk 17, Pl. 1, Fig. 7.

Saturnalis dicranacanthos SQUINABOL 1914 (pars), p. 289, Pl. 20, Fig. 1, Pl. 22, Fig. 1, Pl. 22, Fig. 4, 6 (not 5, 7), Pl. 23, Fig. 7.
Acanthocircus dizonius(?) (RÜST) FOREMAN 1973, p. 260, Pl. 4, Fig. 4, 5. RIEDEL & SANFILIPPO 1974, p. 775, Pl. 2, Fig. 4, 5 (not 3).
Acanthocircus dicranacanthos (SQUINABOL) emend. FOREMAN, 1975, p. 610, Pl. 2D, Fig. 5–6. Emend. PESSAGNO 1977a, p. 73, Pl. 3, Fig. 5. MUZAVOR 1977, p. 37, Pl. 4, Fig. 4. Emend. DONOFRIO & MOSTLER 1978, p. 28, Pl. 2, Fig. 3, Pl. 4, Fig. 4, 7–9, Pl. 5, Fig. 10–11. NAKASEKO et al. 1979, Pl. 2, Fig. 7. BAUMGARTNER et al. 1980, p. 49, Pl. 1, Fig. 11. OKAMURA 1980, Pl. 19, Fig. 8. SCHAAF 1981, p. 431, Pl. 7, Fig. 1, Pl. 16, Fig. 3. KOCHER 1981, p. 51, Pl. 12, Fig. 3. NAKASEKO & NISHIMURA 1981, p. 141, Pl. 1, Fig. 6. KANIE et al. 1981, Pl. 1, Fig. 3. AOKI 1982, Pl. 1, Fig. 3. OKAMURA & UTO 1982, Pl. 4, Fig. 12–14, Pl. 5, Fig. 17.

Acanthocircus suboblongus (YAO)

Data 24, range 30, pob 85, rk 41, Pl. 1, Fig. 6

Spongosaturnalis (?) *suboblongus* YAO, 1972, p. 29, Pl. 3, Fig. 1–6, Pl. 10, Fig. 3a–c.
Acanthocircus variabilis (SQUINABOL), PESSAGNO 1977a, p. 74, Pl. 3, Fig. 6.
Acanthocircus sp. cf. *S.* (?) *suboblongus* YAO, FOREMAN 1978, p. 744, Pl. 1, Fig. 8. KOCHER 1981, p. 52, Pl. 12, Fig. 4–5.

Genus *Alievum* PESSAGNO

Alievum PESSAGNO 1972, p. 297. FOREMAN 1973, p. 262.
Type species: Theodiscus superbus SQUINABOL 1914.

Alievum helenae SCHAAF

Data 104, range 103, pob 228, rk 20, Pl. 1, Fig. 8–10.

Alievum sp. FOREMAN 1973, p. 262, Pl. 9, Fig. 1–2. NAKASEKO et al. 1979, Pl. 2, Fig. 4. MATSUYAMA et al. 1982, Pl. 1, Fig. 8. OKAMURA & UTO 1982, Pl. 6, Fig. 13, 16.
Alievum spp. FOREMAN 1975, p. 613, Pl. 2D, Fig. 7–8, Pl. 5, Fig. 14.
Alievum sp. A PESSAGNO 1977b, p. 29, Pl. 3, Fig. 10, 18.
Alievum helenae SCHAAF in BAUMGARTNER et al. 1980, p. 49, Pl. 1, Fig. 8. SCHAAF 1981, p. 431, Pl. 7, Fig. 9, Pl. 10, Fig. 2a, b. KANIE et al. 1981, Pl. 1, Fig. 4, AOKI 1982, Pl. 2, Fig. 3. OKAMURA & UTO 1982, Pl. 4, Fig. 7, Pl. 5, Fig. 20.
Alievum sp. cf. *A. helenae* FOREMAN, NAKASEKO & NISHIMURA 1981, Pl. 2, Fig. 1.
Praeconocaryomma regularis WU HAO-RUO & LI HONG-SHENG 1982, Pl. 1, Fig. 2–3.
Praeconocaryomma regularis spinosa WU HAO-RUO & LI HONG-SHENG 1982, Pl. 1, Fig. 4.
Actinommid, gen. et sp. indet. AOKI 1982, Pl. 1, Fig. 2.
Pseudoaulophacidae gen. et sp. indet. AOKI 1982, Pl. 1, Fig. 4.

Genus *Andromeda* BAUMGARTNER

Andromeda BAUMGARTNER in BAUMGARTNER et al. 1980.
Type species: Andromeda crassa BAUMGARTNER in BAUMGARTNER et al. 1980.

Andromeda podbielensis (OZVOLDOVA)

Data 16, range 43, pob 8, rk 87, Pl. 1, Fig. 11–12.

Anthocorys podbielensis OZVOLDOVA, 1979, p. 257, Pl. 4, Fig. 1–3.
Andromeda violae BAUMGARTNER in BAUMGARTNER et al. 1980, p. 50, Pl. 4, Fig. 10–14 Pl. 6, Fig. 11. SATO et al. 1982, Pl. 4, Fig. 9. NISHIZONO et al. 1982, Pl. 2, Fig. 15.
Acanthocorys podbiliensis OZVOLDOVA, STEIGER 1981, Pl. 14, Fig. 9 (incorrect secondary spelling IRZN Art. 33b.).

Andromeda praecrassa BAUMGARTNER n. sp.

Data 10, range 5, pob 7, rk –, Pl. 1. Fig. 16–18.

Description. – Inflated conical form of 7 segments. Cephalis with short slender horn. Cephalis and thorax together conical, externally smooth, thorax with a single row of pores distally. Abdomen cylindrical with small pores in irregular vertical rows. Postabdominal segments rapidly growing in width and height, inflated cylindrical, tyre-

shaped. Last segment only slightly higher than second last, tyre-shaped, with few, slender outwards directed spines on basal edge. Basal surface concave, with large aperture.

Remarks. – This species differs from *A. crassa,* which may be its decendant, in including only thorax and abdomen in the proximal smooth portion of the test. It furthermore differs in having a last segment which is only slightly larger than the second last.

Etymology. – *prae-* (Latin): before, to indicate the probable phyletic relationship to *A. crassa.*

Measurements (in μ)

	Holotype	Average of 5 spec.	min.	max.
Height of cephalis, thorax and abdomen:	–	72	64	87
Width of abdomen:	60	70	56	99
Height/width of 4th segment:	32/102	35/122	32/102	38/150
Height/width of 5th segment:	34/150	47/196	34/150	57/246
Height/width of 6th segment:	52/192	63/263	52/192	78/320
Height/width of 7th segment:	86/330	90/330	85/305	100/355
Width of basal aperture:	–	180	–	–

Type locality. – Locality no. 19 of locality descriptions.

Andromeda praepodbielensis BAUMGARTNER n. sp.

Data 3, range 2, pob 6, rk –, Pl. 1, Fig. 13–15

Description. – Test composed of 7 or 8 segments forming a regular stepped cone. Cephalis, thorax and abdomen very similar to *A. podbielensis* with sparse, irregular pores. Postabdominal segments gradually growing in width and height, with vertical rows of pores. Last segment nearly two times as high as second last, bell-shaped, wedging outwards to basal edge which is fringed with numerous spines or teeth. Basal surface planar or concave.

Remarks. – This species differs from *A. podbielensis,* which may be its decendant, by having one or two more segments and by having a planar to concave, rather than convex basal surface. It seems as if the last and second last segment would become the last segment of *A. podbielensis.*

Etymology. – *prae-* (Latin): before, to indicate the probable phyletic relationship to *A. podbielensis.*

Measurements (in μ)

	Holotype	Average of 5 spec.	min.	max.
Height of cephalis, thorax and abdomen:	72	70	52	85
Width of abdomen:	66	60	49	69
Height/width of 4th segment:	36/96	24/87	20/70	36/96
Height/width of 5th segment:	39/123	31/117	25/94	39/146
Height/width of 6th segment:	39/168	40/173	31/146	45/209
Height/width of 7th segment:	48/240	49/246	42/209	60/267
Height/width of 8th segment:	90/387	88/348	63/313	104/387
Width of basal aperture:	–	237	198	288

Type locality. – Locality no. 19 of locality descriptions.

Genus *Angulobracchia* BAUMGARTNER

Angulobracchia BAUMGARTNER 1980, p. 310.
Type species: Paronaella (?) *purisimaensis* PESSAGNO 1977a.

Angulobracchia (?) *portmanni* BAUMGARTNER n. sp.

Data 98, range 97, pob 285, rk –, Pl. 2, Fig. 1–3

Hagiastrids gen. et sp. indet. FOREMAN 1973, Pl. 7, Fig. 1, 3, 5, not: 2, 4, 6, 7.
Paronaella sp. SCHAAF 1981, p. 436, Pl. 8, Fig. 7.

Description. – Three-rayed patulibracchiid with an axially raised central area. Central area in lateral view almost spherical, with roughly horizontal rows of small pores (corresponding to layers of internal spongy meshwork), in vertical view with convex outlines between rays, equipped with coarse irregular nodes and small pores. Rays in lateral view rapidly wedging out from central area to tip, in vertical view proximally constricted, with club-shaped ray tip. Ray tip may bear cylindrical extensions and some short lateral spines. Nodes on rays sometimes finer than on central area, in roughly parallel rows which lead to beams of the cylindrical extensions. These may be as broad as ray tip or thinner, more fragile.

Remarks. – This species differs from *A. digitata* BAUMGARTNER which has similar cylindrical extensions, by a highly raised central area and flattened, club-shaped ray tips. It is questionably assigned to *Angulobracchia* because of the thickened central area and the lack of distinct lateral external beams.

Etymology. – Named in honour of Adolf Portmann (1897–1982), biologist and philosopher from Basel, Switzerland, for his support during my first scientific essays.

Measurements (in μ)

	Holotype	Average of 8 spec.	min.	max.
Length of rays:	AX: 169 BX: 135 CX: 185	190	135	284
Width of rays:	41	42	35	49
Width of ray tip:	63	78	60	92
Width of extensions:	36	69	36	121
Max. length of extension:	65	121	65	177

Type locality. – Locality no. 24 of locality descriptions.

Angulobracchia purisimaensis (PESSAGNO)

Data 67, range 57, pob 144, rk 42, Pl. 2, Fig. 4

Paronaella (?) *purisimaensis* PESSAGNO 1977a, p. 71, Pl. 2, Fig. 4–6.
Angulobracchia purisimanensis (PESSAGNO) BAUMGARTNER 1980, p. 312, Pl. 1, Fig. 14, Pl. 10, Fig. 11–14, Pl. 12, Fig. 9–10. KOCHER 1981, p. 55, Pl. 12, Fig. 12.
Angulobracchia sp. C. BAUMGARTNER 1980, p. 314, Pl. 10, Fig. 16–17. ISHIDA 1983, Pl. 10, Fig. 11.
Angulobracchia sp. SATO et al. 1982, Pl. 3, Fig. 9.

Genus *Archaeodictyomitra* PESSAGNO

Archaeodictyomitra PESSAGNO 1976, p. 49, emend. PESSAGNO 1977b, p. 41.
Type species: Archaeodictyomitra squinaboli PESSAGNO 1976.

Archaeodictyomitra apiaria (RÜST)

Data 75, range 82, pob 263, rk 14, Pl. 2, Fig. 5–6

Lithocampe apiarium RÜST 1885, p. 314, Pl. 39 (14), Fig. 8.
Dictyomitra apiarium (RÜST), RÜST 1898, p. 58. FOREMAN 1975, p. 613, Pl. 2G, Fig. 7–8.
Dictyomitra excellens (TAN SIN HOK), BAUMGARTNER & BERNOULLI 1976, p. 615, Fig. 12k.
Archaeodictyomitra apiara (RÜST), PESSAGNO 1977b, p. 41, Pl. 6, Fig. 6, 14.
Dictyomitra apiarum (RÜST), NAKASEKO et al. 1979, Pl. 3, Fig. 4, not 3.
Archaeodictyomitra apiarium (RÜST), KOCHER 1981, p. 56, Pl. 12, Fig. 13.
Archaeodictyomitra apiara (RÜST), NAKASEKO & NISHIMURA 1981, p. 145, Pl. 6, Fig. 2–4, not 1, Pl. 15, Fig. 2, 6. WU HAO-RUO & LI HONG-SHENG 1982, Pl. 1, Fig. 15–16. MATSUYAMA et al. 1982, Pl. 1, Fig. 1. OKAMURA & UTO 1982, Pl. 5, Fig. 2.
not: *Lithomitra excellens* TAN SIN HOK 1927, p. 56, Pl. 11, Fig. 85.
Archaeodictyomitra sp. E. NISHIZONO & MURATA 1983, Pl. 3, Fig. 17.

Remarks. – Included are only the short forms with a proximal dome-shaped part, a short distal cylindrical part and a final segment which is less wide than the second last.

Archaeodictyomitra excellens (TAN SIN HOK)

Data 100, range 102, pob 287, rk –, Pl. 2, Fig. 7–8

Lithomitra excellens TAN SIN HOK 1927, p. 56, Pl. 11, Fig. 85. MOORE 1973, p. 827, Pl. 4, Fig. 3–4.
Dictyomitra excellens (TAN SIN HOK), RENZ 1974, Pl. 8, Fig. 8 (not 7), Pl. 11, Fig. 35.
Dictyomitra apiarum (RÜST), NAKASEKO et al. 1979, Pl. 3, Fig. 3, not 4.
Archaeodictyomitra apiara (RÜST), SCHAAF 1981, p. 432, Pl. 18, Fig. 2a, b. NAKASEKO & NISHIMURA 1981, p. 145, Pl. 6, Fig. 1, not 3–4. KANIE et al. 1981, Pl. 1, Fig. 8. OKAMURA & UTO 1982, Pl. 2, Fig. 1–2.

Remarks. – Included under this name are forms with a dome-shaped proximal portion followed by a slender, often slightly constricted, cylindrical central portion and terminating in a stout second last and a less wide last segment. The separation of this form from *A. apiaria* (see above) seems useful, as *A. excellens* is restricted to Berriasian and younger strata.

Genus *Archaeohagiastrum* BAUMGARTNER n. gen.

Type species: Archaeohagiastrum munitum BAUMGARTNER n. sp.

Description. – Test composed of four rays, placed at right angles and of about equal length. The rays are formed of a primary beam, three primary canals and six external beams.

Remarks. – The rays of *Archaeohagiastrum* correspond to the medullary rays of the more evolved hagiastrins and represent the simplest possible hagiastrid structure. It was referred to as ancestor of *Hagiastrum* in BAUMGARTNER (1980, Textfig. 7 and p. 284). *Tetraporobracchia* KOZUR & MOSTLER 1979 has the same ray structure but rays are arranged along tetraedric or cubic axes. *Archaeotriastrum* DE WEVER 1981 has a similar ray structure but has three rays.

Because of its simple ray structure this genus is tentatively included with the hagiastrins. It should, together with *Archaeotriastrum,* be assigned to a new subfamily ancestral to the Hagiastrinae.

Etymology. – *achaeo-:* ancient (Greek), ancestral form to *Hagiastrum.*

Range. – Sinemurian or older to Callovian.

Archaeohagiastrum munitum BAUMGARTNER n. sp.

Data 92, range 40, pob 271, rk –, Pl. 2, Fig. 9–13

Crucella sp. A. SASHIDA et al. 1982, Pl. 1, Fig. 9.
Tetratrabs sp. B. WAKITA 1982, Pl. 5, Fig. 4.

Description. – Small form with four smooth to nodose rays of about equal length constructed as with genus. Central area small, occupied by four to five broad, highly raised, connected nodes, which alternate with four pores placed at the proximal termination of the median beams. The fifth node is central or slightly excentric and fused to one of the corner nodes. A nearly centrally placed pore often occurs. Lateral beams are continuous around the central area.

The external beams of rays are slightly to strongly nodose, nodes increase in size towards central area and are sometimes connected by a blade-like ridge. Ray tip blunt or with short central spine of round cross section.

Remarks. – *A. munitum* differs from other yet undescribed species of this genus by being distinctly smaller and by having a strongly nodose test.

Etymology. – *munitum:* fortified, protected (Latin), referring to the nodose surface of test and central area.

Measurements (in μ)

	Holotype	Average of 7 spec.	min.	max.
Length of rays:	AX: 114			
	BX: 120			
	CX: 108			
	DX: 111	95	87	120
Width of rays:	51	42	35	51
Max. length of spines:	66	48	28	66
Width of central nodose area:	65	60	47	76

Type locality. – Locality no. 30 of locality descriptions.

Genus *Bernoullius* BAUMGARTNER n. gen.

Type species: Eucyrtis (?) *dicera* BAUMGARTNER 1980.

Description. – Spongodiscid spumellarian with distinct bilateral symmetry: A delicate, finely spongy main body of flattened egg-shape carries on the narrow end two symmetric, strongly developed, usually triradiate lateral spines and sometimes one central spine.

Remarks. – Because of the clear bilateral symmetry, the spines were interpreted as cephalic horns of a nassellarian by BAUMGARTNER in BAUMGARTNER et al. (1980). Well preserved specimens from DSDP Site 534A show that the spines are attached to a

finely spongy body lacking any resemblance to nassellarian morphology. For most specimens, the spongy body is not or poorly preserved as spongy round mass at the base of the spines.

KOZUR & MOSTLER (1979, Pl. 21, Fig. 2) illustrated a Triassic form which possibly belongs to this genus.

Etymology. – Dedicated to Daniel Bernoulli, Basel, Switzerland, in honour of his contribution to the understanding of ancient passive continental margins in the Alpine–Mediterranean realm.

Range. – ?Triassic to Late Jurassic.

Bernoullius cristatus BAUMGARTNER n. sp.

Data 39, range 39, pob 221, rk 109, Pl. 2, Fig. 14–15

Eucyrtis (?) *dicera* BAUMGARTNER in BAUMGARTNER et al. 1980, Pl. 6, Fig. 6.
Eucyrtis (?) sp. A, KOCHER 1981, p. 68, Pl. 13, Fig. 19–20.

Description. – Form with two stout triradiate spines, which touch each other at the base and stand at an angle of 90 to 120 degrees. Proximal portion of spines straight or slightly outwardly curved, short distal portion kinked to a horizontal or downward position. The upwards directed ridge of the spines becomes bladelike near the kink and forms one or two characteristic teeth pointing upwards. Sometimes additional small teeth arise from the lateral ridges of the spines.

Remarks. – This form differs from *B. dicera* by the presence of teeth and a kinked distal portion of the two spines. Stratigraphic data suggest that this form is ancestral to *B. dicera*.

Etymology. – *cristatus:* equipped with teeth (Latin).

Measurements (in μ)

	Holotype	Average of 8 spec.	min.	max.
Width between ends of two spines:	315	318	250	405
Width of spines at base:	50	42	33	67
Observed length of spongy portion:	135	106	56	158

Type locality. – Locality no. 30 of locality descriptions.

Bernoullius dicera (BAUMGARTNER)

Data 35, range 56, pob 223, rk 69, Pl. 2, Fig. 16

Lophophaena sp., OZVOLDOVA 1979, p. 259, Pl. 4, Fig. 4–5.
Eucyrtis (?) *dicera* BAUMGARTNER in BAUMGARTNER et al. 1980, p. 54, Pl. 3, Fig. 16, Pl. 6, Fig. 10, not Fig. 6. KOCHER 1981, p. 68, Pl. 13, Fig. 17–18. DE WEVER & CABY 1981, Pl. 2, Fig. 2I.

Genus *Cecrops* PESSAGNO

Cecrops PESSAGNO 1977b, p. 32.
Type species: Staurosphaera septemporata PARONA 1890.

Cecrops septemporatus (PARONA)

Data 110, range 108, pob 229, rk 24, Pl. 2, Fig. 17–18

Staurosphaera septemporata PARONA, p. 151, Pl. 2, Fig. 4–5. CITA & PASQUARE 1959, p. 398, Fig. 3, no. 7. MOORE 1973, p. 824, Pl. 2, Fig. 2. FOREMAN 1973, p. 259, Pl. 3, Fig. 4. RIEDEL & SANFILIPPO 1974, p. 780, Pl. 1, Fig. 6–8. FOREMAN 1975, p. 609, Pl. 2E, Fig. 7, Pl. 3, Fig. 6. MUZAVOR 1977, p. 53, Pl. 1, Fig. 9–10. SCHAAF 1981, p. 439, Pl. 7, Fig. 8a, b, Pl. 16, Fig. 10a, b. NAKASEKO et al. 1979, Pl. 2, Fig. 5–6. NAKASEKO & NISHIMURA 1981, p. 161, Pl. 1, Fig. 2. KANIE et al. 1981, Pl. 1, Fig. 5.
Cecrops septemporatus (PARONA), PESSAGNO 1977b, p. 33, Pl. 3, Fig. 11. BAUMGARTNER et al. 1980, p. 51, Pl. 2, Fig. 7. OKAMURA & UTO 1982, Pl. 7, Fig. 19.

Genus *Diacanthocapsa* SQUINABOL, emend. DUMITRICA

Diacanthocapsa SQUINABOL, emend. DUMITRICA 1970.
Type species: Dicolocapsa euganea SQUINABOL 1903.

Diacanthocapsa normalis YAO

Data 34, range 10, pob 54, rk –, Pl. 2, Fig. 20

Diacanthocapsa normalis YAO 1979, p. 28, Pl. 2, Fig. 1–15. YAO et al. 1982, Pl. 3, Fig. 9.

Genus *Diboloachras* FOREMAN

Diboloachras FOREMAN 1973, p. 265.
Type species: Diboloachras tytthopora FOREMAN 1973.

Diboloachras chandrika KOCHER

Data 55, range 75, pob 265, rk 43, Pl. 2, Fig. 19

Diboloachras chandrika KOCHER 1981, p. 61, Pl. 13, Fig. 1–2.

Genus *Ditrabs* BAUMGARTNER

Ditrabs BAUMGARTNER 1980, p. 293.
Type species: Amphibracchium sansalvadorensis PESSAGNO 1971.

Ditrabs sansalvadorensis (PESSAGNO)

Data 103, range 96, pob 227, rk 21, Pl. 2, Fig. 21

Amphibracchium sansalvadorensis PESSAGNO 1971, p. 21, Pl. 19, Fig. 9–10.
Amphibracchium ossiforme MUZAVOR 1977, p. 59, Pl. 2, Fig. 6.
Ditrabs sansalvadorensis (PESSAGNO), BAUMGARTNER et al. 1980, p. 52, Pl. 2, Fig. 9.

Genus *Emiluvia* FOREMAN

Emiluvia FOREMAN 1973, p. 262, emend. 1975, p. 612.
Type species: Emiluvia chica FOREMAN 1973.

Emiluvia hopsoni PESSAGNO

Data 74, range 69, pob 225, rk 29, Pl. 3, Fig. 1

Emiluvia hopsoni PESSAGNO 1977a, p. 76, Pl. 4, Fig. 14–16, Pl. 5, Fig. 1–7, Pl. 12, Fig. 15–16. BAUMGARTNER et al. 1980, Pl. 1, Fig. 9. KOCHER 1981, p. 64, Pl. 13, Fig. 6–7.

Emiluvia orea BAUMGARTNER

Data 60, range 81, pob 224, rk 63, Pl. 3, Fig. 5.

Emiluvia orea BAUMGARTNER in BAUMGARTNER et al. 1980, p. 52, Pl. 1, Fig. 1–7. KOCHER 1981, p. 64, Pl. 13, Fig. 6–7.

Emiluvia (?) sp. P.

Data 41, range 59, pob 219, rk 90, Pl. 3, Fig. 10
Gen. et sp. indet. KOCHER 1981, p. 69, Pl. 14, Fig. 2.

Remarks. – This form is doubtfully assigned to *Emiluvia* because of the presence of a patagium-like spongy meshwork extended between the four spines in the equatorial plane.

Emiluvia pessagnoi FOREMAN s.l.

Data 71, range 71, pob 226, rk 36, Pl. 3, Fig. 3

Emiluvia pessagnoi FOREMAN 1973, p. 262, Pl. 8, Fig. 6. FOREMAN 1975, p. 612. PESSAGNO 1977a, p. 76, Pl. 5, Fig. 8. FOREMAN 1978, p. 744, Pl. 1, Fig. 1–2. BAUMGARTNER et al. 1980, p. 53, Pl. 1, Fig. 10.

Remarks. – Included under this name are all forms with a fine regular meshwork and variably developed nodes. The Early Cretaceous forms included herein have very small nodes and thus differ from the original species definition.

Emiluvia premyogii BAUMGARTNER n. sp.

Data 19, range 14, pob 210, rk 88, Pl. 3, Fig. 6, 8–9, 11–12

Emiluvia (?) sp. B. KOCHER 1981, p. 66, Pl. 13, Fig. 12.
?*Emiluvia salensis* PESSAGNO, ISHIDA 1983, Pl. 11, Fig. 5–6.
?*Emiluvia chica* FOREMAN, SATO et al. 1982, Pl. 3, Fig. 14.

Description. – Small *Emiluvia* with the 4 spines at right or slightly oblique angle (X-shaped). Opposed spines generally of unequal, adjacent spines of similar length. Nodes of central body placed on bars distinctly aligned with spines, forming 2 rows that meet in the center to form a cross. About 6 pairs of nodes between opposed spines. Center of cross forms a raised polygonal structure often with a central node. 4 large pores are placed around center, between the branches of cross. Additional lateral meshwork without significant nodes.

Remarks. – This species differs from other *Emiluvia* by having nodes distinctly aligned in the shape of a cross. *Emiluvia* sp. A of KOCHER 1981 (p. 65, Pl. 13, Fig. 11) is not included, as it lacks the regular cross-shape of the central area.

Etymology. – Named in honour of Swami Prem Yogi alias Rudolph Kocher, for his contribution to Jurassic radiolarian stratigraphy.

Measurements (in μ)

	Holotype	Average of 8 spec.	min.	max.
Length of long spines:	AX: 130 BX: 127	148	95	218
Length of short spines:	CX: 120 DX: –	129	92	165
Width of central area:				
Between base of spines:	95	114	95	139
Between concave sides:	77	83	71	111
Width of base of spines:	36	36	30	47

Type locality. – Locality no. 30 of locality descriptions.

Emiluvia sedecimporata salensis PESSAGNO

Data 33, range 50, pob 215, rk 44 & 45, Pl. 3, Fig. 4, 7

Emiluvia salensis PESSAGNO 1977a, p. 76, Pl. 5, Fig. 9–11. KOCHER 1981, p. 65, Pl. 13, Fig. 10.
?*Staurosphaera antiqua* PARONA, MUZAVOR 1979, p. 52, Pl. 1, Fig. 8.
Emiluvia sp. A. KOCHER 1981, p. 65, Pl. 13, Fig. 11.

Remarks. – The group of *Emiluvias* with slender central bodies with concave sides between adjacent spines include various morphotypes and intermediate forms which are included here under the species *E. sedecimporata* (RÜST) 1885. *E. salensis* is considered to be one of these morphotypes and thus adquires a subspecific level.

Emiluvia sedecimporata elegans (WISNIOWSKI).

Data 40, range 18, pob 216, rk –, Pl. 3, Fig. 2

Staurosphaera sedecimporata RÜST var. *elegans* WISNIOWSKI 1889, p. 683, Pl. 13, Fig. 48. Not KOCHER 1981, p. 65, rk 68.

Remarks. – This name is used to denominate forms with a clearly square pore pattern of 16 similar pores as illustrated by RÜST (1885) and WISNIOWSKI (1889). Nodes on quadruple junctions are moderately developed, a pair of nodes sits at the base of each spine.

Eucyrtid gen. et sp. indet.

Data 63, range 7, pob 74, rk –, Pl. 3, Fig. 13–16

Description. – Large, spindle-shaped multicyrtid nassellarian. Proximal portion long, slender conical, including cephalis, thorax, abdomen and several (6–10?) postabdominal segments. Segmentation externally not or very poorly visible. Cephalis seems to bear a horn, internal structure unknown. Closely spaced costae, separated by one row of pores, originate on proximal portion. Pore frames roughly rectangular, sometimes marked by faint horizontal ridges. Distal portion inflated spindle-shaped, consisting of numerous (at least 10) segments. The costae which are continuous from proximal portion are more widely spaced and seem to be an outer layer placed over a system of transverse ridges delimitating a rectangular pore pattern with two, sometimes three

rows of pores between adjacent costae. Additional costae may originate on spindle-shaped portion and others may merge on its distal constricted end.

Remarks. – Shape and wall structure of this form are very distinct and even fragments of the spindle-shaped part can be identified.

Genus *Eucyrtidiellum* BAUMGARTNER n. gen.

Type species: Eucyrtidium (?) *unumaensis* YAO 1979.

Description. – Test composed of four segments. Cephalis small, spherical, poreless with variably developed straight or slightly oblique apical horn, rare forms with apical and vertical horn. A sutural pore is present at collar stricture or on proximal portion of thorax. Thorax dome-shaped, poreless, with irregular ornamentation consisting of ridges and nodes leaving depressions ("closed pores" of some authors) or with plicae. One or two rows of pores may occur at stricture between thorax and abdomen. Abdomen inflated annular to hemispherical, poreless, except for the distal quarter, where one or two irregular rows of pores may occur. Ornamentation of abdomen varying with species. One row of large pores marks the joint with fourth segment. Fourth segment delicate, mostly cylindrical, covered with circular pores in loose diagonal rows, with a distal poreless constriction.

Remarks. – The Mesozoic species hitherto questionably assigned to *Eucyrtidium* are assigned to this new genus, because they bear no resemblance to the type species *E. acuminatum* (EHRENBERG).

Range. – Late Triassic to Late Jurassic (Tithonian).

Eucyrtidiellum ptyctum (RIEDEL & SANFILIPPO)

Data 56, range 66, pob 17, rk 46 (pars), Pl. 4, Fig. 1–3

Eucyrtidium (?) *ptyctum* RIEDEL & SANFILIPPO 1974, p. 778, Pl. 5, Fig. 7, Pl. 12, Fig. 14, not Fig. 15. BAUMGARTNER & BERNOULLI 1976, p. 617, Fig. 11e, g not f. PESSAGNO 1977a, p. 94, Pl. 12, Fig. 7. BAUMGARTNER et al. 1980, p. 53, Pl. 3, Fig. 13. OKAMURA 1980, Pl. 20, Fig. 10. MIZUTANI 1981, p. 182, Pl. 64, Fig. 1a–b, 2. AOKI & TASHIRO 1982, Pl. 3, Fig. 1–3, Pl. 4, Fig. 10. OKAMURA & UTO 1982, Pl. 6, Fig. 18. ADACHI 1982, Pl. 3, Fig. 7–8. AITA 1982, Pl. 2, Fig. 8, 9a–b, not 10. NISHIZONO et al. 1982, Pl. 2, Fig. 12, not 11. MIZUTANI et al. 1982, p. 57, Pl. 4, Fig. 5. ISHIDA 1983, Pl. 9, Fig. 4. YAO 1984, Pl. 2, Fig. 30.

Remarks. – Under this name are included only forms with tiny, short horn (if preserved) and abdomen with regular, well developed broad vertical plicae (about 7 to 12 visible per half circumference), which tend to terminate near the irregular row of pores at the base of abdomen. KOCHER (1981), instead, included also forms with less distinct plicae (transitional forms to *E. unumaensis*) and forms with plicae originating on thorax possibly belonging to another genus (undescribed species pob 238).

This narrower definition explains the later first occurrence of *E. ptyctum* in this paper, compared to KOCHER's (1981) data.

Eucyrtidiellum pustulatum BAUMGARTNER n. sp.

Data 91, range 44, pob 13, rk –, Plate 4, Fig. 4–5

?SHASHIDA et al. 1982, Pl. 1, Fig. 3.

Description. – Cephalis covered with small nodes and variably developed horn. Thorax distinctly nodose and proximal portion of abdomen with irregular coalescent nodes (short ridges) and pustules. Distal portion of abdomen smooth, with few very small pores placed in an irregular row.

Remarks. – This species differs from *E. unumaensis* by having an irregularly nodose abdomen.

Etymology. – *pustulatum:* pustulate (Latin).

Measurements (in μ)

	Holotype	Average of 7 spec.	min.	max.
Height/width of cephalis:	18/24	18/23	16/21	21/25
Height/width of thorax:	25/44	25/45	25/43	26/48
Height/width of abdomen:	54/80	63/86	54/80	68/92
Height of 4th segment:	63	61	58	63
Length of apical horn:	16	18	12	27

Type locality. – Locality no. 30 of locality descriptions.

Eucyrtidiellum unumaensis (YAO)

Data 17, range 12, pob 12, rk 89, Pl. 4, Fig. 6

Eucyrtidium (?) *ptyctum* RIEDEL & SANFILIPPO 1974, p. 778, Pl. 12, Fig. 15. BAUMGARTNER & BERNOULLI 1976, Fig. 11f.
Eucyrtidium (?) *unumaensis* YAO 1979, p. 39, Pl. 9, Fig. 1–11. KOCHER 1981, p. 67, Pl. 13, Fig. 15. YAO et al. 1982, Pl. 3, Fig. 7. SASHIDA et al. 1982, Pl. 2, Fig. 3. KOJIMA 1982, Pl. 1, Fig. 11. WAKITA 1982, Pl. 3, Fig. 1. MATSUOKA 1982, Pl. 1, Fig. 15. WAKITA & OKAMURA 1982, Pl. 8, Fig. 7. SAKA 1983, Pl. 5, Fig. 6–7.

Genus *Foremanella* MUZAVOR

Foremanella MUZAVOR 1977, p. 67.
Type species: Foremanella alpina MUZAVOR 1977.

Foremanella diamphidia (FOREMAN)

Data 79, range 85, pob 112, rk 13, Pl. 6, Fig. 18

Paronaella (?) *diamphidia* FOREMAN 1973, p. 262, Pl. 8, Fig. 3–4. FOREMAN 1975, p. 612, Pl. 5, Fig. 4–5. RIEDEL & SANFILIPPO 1974, Pl. 12, Fig. 4. FOREMAN 1978, p. 744, Pl. 1, Fig. 5–6. BAUMGARTNER 1980, p. 302, Pl. 4, Fig. 4.
Foremanella alpina MUZAVOR 1977, p. 67, Pl. 3, Fig. 8.
Paronaella (?) sp. YAO 1984, Pl. 3, Fig. 25.

Foremanella hipposidericus (FOREMAN)

Data 78, range 83, pob 111, rk 12, Pl. 6, Fig. 19

Paronaella (?) *hipposidericus* FOREMAN 1975, p. 612, Pl. 2E, Fig. 1–2, Pl. 5, Fig. 3, 7, 10. BAUMGARTNER 1980, p. 302, Pl. 4, Fig. 1–3. BAUMGARTNER et al. 1980, p. 57, Pl. 2, Fig. 4.

Genus *Gorgansium* PESSAGNO & BLOME

Gorgansium PESSAGNO & BLOME 1980, p. 234.
Type species: Gorgansium silviesense PESSAGNO & BLOME 1980.

Gorgansium pulchrum (KOCHER)

Data 11, range 28, pob 76, rk 105, Pl. 4, Fig. 7

Trilonche pulchra KOCHER 1981, p. 104, Pl. 17, Fig. 16–17.
Gorgansium sp. A, AITA 1982, Pl. 3, Fig. 20–21.

Remarks. – This species differs from other species of this genus illustrated by PESSAGNO & BLOME (1980) in having pore frames with broad ridges and knobs at their junctions. Instead of 4-bladed, as indicated by KOCHER (1981), the spines rather seem to be 3-bladed.

Genus *Guexella* BAUMGARTNER n. gen.

Type species: Lithocampe nudata KOCHER 1980.

Description. – Test ellipsoidal or spindle-shaped, composed of 2 or more (usually 4) segments. Cephalis hemispherical, poreless or with few basal pores, internally smooth with wide, undivided basal aperture to thorax. No cephalic spines have been observed. Thorax and postthoracic segments form together a thinwalled body without external strictures, covered with small circular pores. Thorax at least 2 times as wide as cephalis, trapezoidal, with a sharp proximal edge. Variable ornamentation (spines, ridges) may cover the planiform top of thorax and completely obscure the cephalis. The last segment (usually 4th) delicate, cup-shaped or constricted, with small basal aperture without tubular extension.

Remarks. – This genus differs from *Theocapsomma* HAECKEL, emend. FOREMAN 1968, from *Novodiacanthocapsa* EMPSON-MORIN 1981 and from *Gongylothorax* FOREMAN 1968, emend. DUMITRICA 1970, by a cephalis which is not partly immersed in the thorax and by the peculiar sharp-edged thorax. This genus is erected to include several forms related to *G. nudata* now used in biostratigraphy of the Jurassic (e.g. *Lithocampe* (?) sp. aff., *L. nudata* KOCHER, MATSUOKA 1983, p. 27, Pl. 4, Fig. 12–13, Pl. 9, Fig. 15.).

Etymology. – Dedicated to Jean Guex, Lausanne, in honour of his contribution to the fundamentals of biostratigraphy.

Range. – Middle Jurassic or older to Late Jurassic.

Guexella nudata KOCHER

Data 7, range 27, pob 61, rk 106, Pl. 5, Fig. 5–7

Lithocampe nudata KOCHER in BAUMGARTNER et al. 1980, p. 55, Pl. 6, Fig. 3. KOCHER 1981, p. 75, Pl. 14, Fig. 18–19.
Lithocampe (?) *nudata* KOCHER, YAO et al. 1982, Pl. 4, Fig. 1–2. MATSUOKA 1982, Pl. 2, Fig. 1–2. AITA 1982, Pl. 1, Fig. 19a–c. MATSUOKA 1983, p. 27, Pl. 9, Fig. 12–14. YAO 1984, Pl. 2, Fig. 1.

Remarks. – Well preserved material shows a complex spiny ornamentation placed on the hemispherical cephalis. Characteristic is the dense, regular arrangement of small circular pores.

Hagiastrid sp. A.

Data 8, range 41, pob 153, rk 107 & 108, Pl. 4, Fig. 8–9

Hagiastrid sp. cf. *Tetratrabs bulbosa* BAUMGARTNER, KOCHER 1981, p. 69, Pl. 14, Fig. 3.
Hagiastrid sp. cf. *Tetratrabs zealis* (OZVOLDOVA), KOCHER 1981, p. 70, Pl. 14, Fig. 5–6.

Remarks. – Only fragments of this form are preserved. It consists of a very long (more than 650–700 microns), thin (35–40 microns) hollow tube (?) made of 6 external beams with a single row of pores between each adjacent beam. One end of the tube has a bulbous tip, the other bears a short, blunt triradiate spine. KOCHER (1981) assigned the two ends to different taxa.

Genus *Haliodictya* HOJNOS

Haliodictya HOJNOS 1916, p. 349.
Type species: Haliodictya loerentheyi HOJNOS 1916.

Haliodictya (?) *hojnosi* RIEDEL & SANFILIPPO

Data 86, range –, pob 254, rk 3, Pl. 4, Fig. 10–11

Haliodictya hojnosi RIEDEL & SANFILIPPO 1974, p. 779, Pl. 2, Fig. 6, Pl. 12, Fig. 2, not 3. KOCHER 1981, p. 70, Pl. 14, Fig. 7. AITA 1982, Pl. 3, Fig. 13.

Remarks. – RIEDEL & SANFILIPPO (1974) illustrated several morphotypes under this name. The forms included herein lack a preserved spongy meshwork and have, like the holotype, well-defined, solid spines at the corners of the square central body. These forms have been recorded throughout the studied interval, thus the name does not appear in the range chart.

Genus *Higumastra* BAUMGARTNER

Higumastra BAUMGARTNER 1980, p. 290.
Type species: Higumastra inflata BAUMGARTNER 1980.

Higumastra imbricata (OZVOLDOVA)

Data 13, range 29, pob 110, rk 92, Pl. 4, Fig. 13

Crucella (?) imbricata OZVOLDOVA 1979, p. 254, Pl. 3 Fig. 1, 4. KOCHER 1981, p. 71, Pl. 14, Fig. 8.
Higumastra sp., SATO et al. 1982, Pl. 3, Fig. 11.

Remarks. – Relatively large form with broadly based, porous, spined lateral protrusions at ray tips which often leave a semicircular space between adjacent rays.

Higumastra sp. aff. *H. inflata* BAUMGARTNER

Data 66, range 15, pob 107, rk 47, Pl. 4, Fig. 12

Higumastra sp. aff. *H. inflata* BAUMGARTNER 1980, p. 290, Pl. 3, Fig. 4. KOCHER 1981, p. 71, Pl. 14, Fig. 9.

Remarks. – Small form often with preserved spongy meshwork between rays.

Genus *Holocryptocanium* DUMITRICA

Holocryptocanium DUMITRICA 1970, p. 31, 75.
Type species: Holocryptocanium tuberculatum DUMITRICA 1970.

Holocryptocanium barbui DUMITRICA

Data 108, range 106, pob 292, rk –, Pl. 4, Fig. 14

Holocryptocanium barbui DUMITRICA 1970, p. 76, Pl. 17, Fig. 105–108a, b, Pl. 21, Fig. 136. SCHAAF 1981, p. 435, Pl. 2, Fig. 1a, b, Pl. 10, Fig. 6a, b. YAO 1984, Pl. 5, Fig. 1.
Holocryptocanium japonicum NAKASEKO et al. 1979, Pl. 5, Fig. 8, 10. OKAMURA 1980, Pl. 21, Fig. 5.
Holocryptocanium barbui japonicum NAKASEKO & NISHIMURA 1981, p. 154, Pl. 3, Fig. 5a–b, 6, 7a–b, Pl. 14, Fig. 8.

Remarks. – The forms with smooth abdominal surface lacking pore frames assigned to *Holocryptocanium barbui barbui* by NAKASEKO & NISHIMUARA (1981, p. 152, Pl. 3, Fig. 1–4) should be assigned to another name, since the holotype of *H. barbui* has pore frames. The smooth morphotype has not been observed in the Neocomian.

Genus *Homoeoparonaella* BAUMGARTNER

Homoeoparonaella BAUMGARTNER 1980, p. 288.
Type species: Paronaella elegans PESSAGNO 1977a.

Homoeoparonaella argolidensis BAUMGARTNER

Data 43, range 37, pob 103, rk 30, Pl. 4, Fig. 15

Hagiastrid cf. *Amphibracchium* sp. BAUMGARTNER & BERNOULLI 1976, Fig. 10h.
Homoeoparonaella argolidensis BAUMGARTNER 1980, p. 288, Pl. 2, Fig. 1, 8–12, Pl. 11, Fig. 4. KOCHER 1981, p. 71, Pl. 14, Fig. 10.

Homoeoparonaella elegans (PESSAGNO)

Data 65, range 63, pob 104, rk 48, Pl. 4, Fig. 16

Paronaella elegans PESSAGNO 1977a, p. 70, Pl. 1, Fig. 10–11.
Homoeoparonaella elegans (PESSAGNO), BAUMGARTNER 1980, p. 289, Pl. 2, Fig. 2–6, Pl. 11, Fig. 6. KOCHER 1981, p. 72, Pl. 14, Fig. 11.

Homoeoparonaella giganthea BAUMGARTNER

Data 70, range 68, pob 105, rk 37, Pl. 4, Fig. 17

Homoeoparonaella giganthea BAUMGARTNER 1980, p. 289, Pl. 2, Fig. 13–16, Pl. 11, Fig. 5. KOCHER 1981, p. 72, Pl. 14, Fig. 12.

Genus *Hsuum* PESSAGNO

Hsuum PESSAGNO 1977a, p. 81.
Type species: Hsuum cuestaensis PESSAGNO 1977a.

Hsuum brevicostatum (OZVOLDOVA)

Data 23, range 23, pob 181, rk 49, Pl. 5, Fig. 1–2

Dictyomitra sp. D. BAUMGARTNER & BERNOULLI 1976, p. 617, Fig. 12j.
Lithostrobus brevicostatus Ozvoldova 1975, p. 84, Pl. 102, Fig. 1. OZVOLDOVA 1979, p. 259, Pl. 5, Fig. 2.
Hsuum brevicostatum (OZVOLDOVA), KOCHER 1981, p. 73, Pl. 14, Fig. 13.
Hsuum maxwelli PESSAGNO, MIZUTANI 1981, p. 176, Pl. 59, Fig. 5.
?*Hsuum* cfr. *maxwelli* PESSAGNO, SASHIDA et al. 1982, Pl. 2, Fig. 7.

Remarks. – Under this name are included forms with slender conical, lobate outline (well visible segmental divisions) with discontinuous costae limited to one segment and irregular horizontal bars connecting costae at their highest bulge. Two vertical rows of pores between costae.

Hsuum maxwelli PESSAGNO group

Data 47, range 42, pob 180, rk 93, Pl. 5, Fig. 3–4

Hsuum maxwelli PESSAGNO 1977a, p. 81, Pl. 7, Fig. 14–16. KOCHER 1981, p. 73, Pl. 14, Fig. 14. AOKI & TASHIRO 1982, Pl. 1, Fig. 14–17. SAKA 1983, Pl. 4, Fig. 10.
Hsuum sp. aff. *H. maxwelli* PESSAGNO 1977a, p. 82, Pl. 8, Fig. 1–2.

Remarks. – The studied material contains a number of morphotypes which come close to the cited forms in having a bluntly conical, smooth outline, often with a moderate distal constriction and poorly or undefined segmental divisions. Costae are discontinuous, merging, reach over 1–3 segments. One or two irregular rows of pores between costae.

Genus *Mirifusus* PESSAGNO, emend.

Mirifusus PESSAGNO 1977a, p. 83.
Type species: Mirifusus guadalupensis PESSAGNO 1977a.

Emended definition. – General shape of test as given by PESSAGNO (1977a). Proportions and shape of conical proximal and inflated median portion of test may vary intraspecifically and are often distorted by diagenetic flattening of the large test. Test wall consisting of two layers: Inner layer formed by regular circular to triangular pore frames with two to five transverse rows of pores per segment. Outer layer consisting of regular to irregular diagonal or vertical bars extending over each segment and joining at nodes on circumferential ridges. Outer layer may be variably developed: Early forms may have a poorly developed outer layer on the median portion, whereas later forms tend to have a strongly developed outer layer which may coalesce on the conical proximal portion of test. Late species may show spines extending from nodes and cephalis.

Remarks. – The genus is emended to include *Lithocampe chenodes* RENZ and early forms like *M. fragilis* n.sp.

Mirifusus chenodes (RENZ)

Data 77, range 80, pob 162, rk –, Pl. 5, Fig. 9, 15

Lithocampe chenodes RENZ 1974, p. 793, Pl. 7. Fig. 30, Pl. 12, Fig. 14a–d. RIEDEL & SANFILIPPO 1974, p. 779, Pl. 6, Fig. 5–7, Pl. 13, Fig. 1. SCHAAF 1981, p. 435, Pl. 5, Fig. 2, Pl. 25, Fig. 5a–b, 7. KOCHER 1981, p. 74, Pl. 14, Fig. 17.

Remarks. – The entire test of this species is generally smaller compared to other species of *Mirifusus*. The inner layer has 3–5 rows of pores per segment. The outer layer is constructed of very irregular, branched diagonal bars that join at moderate circumferential ridges. Stout spines may arise from nodes on inflated median portion. The crown-like spine on the cephalis of some specimens may also originate from the outer layer.

Mirifusus fragilis BAUMGARTNER n. sp.

Data 14, range 9, pob 159, rk –, Pl. 5, Fig. 12, 16–17, 20–21

?Mirifusus (?) sp. aff. *M.* (?) *mediodilatata* RÜST, PESSAGNO 1977a, p. 84, Pl. 11, Fig. 3.
Mirifusus aff. *guadalupensis* PESSAGNO, YAO et al. 1982, Pl. 4, Fig. 24. YAO 1983, Fig. 3, 8.
?Mirifusus sp. A, KIDO et al. 1982, Pl. 3, Fig. 1–2, 4. AITA 1982, Pl. 2, 13.

Description. – Test fragile, fusiform as with genus, composed of 20 or more segments. Cephalis hemispherical, poreless or sparsely porous (ditrema and apical pore), often covered with small spinelets. Thorax inflated trapezoidal poreless or with sparse, irregular pores, covered with spinelets. Abdomen and following 7 to 9 postabdominal segments form together a slender conical portion of the test with an inner layer of 3 rows of pores per segment in hexagonal arrangement and a weakly developed outer layer of diagonal bars forming triangular frames in which the inner layer is usually exposed, except for the abdomen and the first postabdominal chambers, where the outer layer may form irregular nodes which obscure the regular pore structure of the inner layer. The following about 10 segments form a variably inflated median portion of the test with the same pore structure as the proximal conical part of the test. The outer layer is weakly developed or may be almost absent. Circumferential ridges of outer layer are narrow, of round cross section and bear small vertically elongated nodes at junctions with diagonal bars.

Remarks. – Successions of well-preserved samples in the Blake-Bahama Basin (DSDP Site 534), Lombardy (Breggia) as well as the published Japanese material (edited by NAKASEKO 1982) show that this species is the immediate ancestor of *M. guadalupensis* and is partly coexisting with it. *M. fragilis* differs from *M. guadalupensis* by being generally smaller, more fragile and having a weakly developed (late forms) to almost lacking (early forms) outer layer of mostly triangular pore frames which always allow to see the hexagonal pore arrangement of the inner layer, whereas with *M. guadalupensis* it tends to be obscured by the thick, more irregular outer layer. *M. fragilis* has thin, round circumferential ridges, whereas *M. guadalupensis* has broad circumferential ridges with flat outer surface. There are transitional forms.

Etymology. – *fragilis,* fragile (Latin), referring to te thin fragile test wall.

Measurements (in μ)

	Holotype	Average of 8 spec.	min.	max.
Proximal conical portion				
Width:	126	134	114	156
Height:	192	209	192	227
Number of segments:	9–11	9.5	9	11
Inflated median portion				
Width:	249	277	249	312
Height:	279	311	279	334
Width between circumferential ridges:	21	27	21	32

Type Locality. – Locality no. 40 of locality descriptions.

Mirifusus guadalupensis PESSAGNO

Data 37, range 55, pob 160, rk 50, Pl. 5, Fig. 8, 22

Mirifusus guadalupensis PESSAGNO 1977a, p. 83, Pl. 10, Fig. 9–14. BAUMGARTNER et al. 1980, p. 55, Pl. 5, Fig. 12–14. ISHIDA 1983, Pl. 5, Fig. 6a–b. YAO 1984, Pl. 2, Fig. 29.
Lithocampe mediodilatata RÜST, OZVOLDOVA 1979, p. 258, Pl. 5, Fig. 3.

Remarks. – This species seems to evolve from *M. fragilis* n. sp. The two species are compared under the latter.

Mirifusus mediodilatatus (RÜST) s.l.

Data 76, range 67, pob 161, rk 4 (pars)

Remarks. – Under this name are included all synonymies listed under the two subspecies *M. mediodilatatus baileyi* and *M. mediodilatatus mediodilatatus.*

In BAUMGARTNER et al. (1980) we synonymized *M. baileyi* with *M. mediodilatatus* based on the fact, that both show two staggered rows of pores per segment and that in poorly preserved material it is impossible to decide, whether the pore frames are triangular or circular. We do, however, agree that there are two distinct Late Jurassic morphotypes and that *M. baileyi* may have a later first appearance than *M. mediodilatatus.* It seems more practical to deal with these two morphotypes as subspecies, since an assignation to either one is impossible for transitional forms as well as for poorly preserved material.

During the Tithonian *M. baileyi* seems to gradually reduce the number of segments included in the conical proximal portion, to become *M. mediodilatatus minor* n. subsp. (see below).

The database has been established based on the concept of BAUMGARTNER et al. (1980) excluding *M. m. minor* n. subsp.

Mirifusus mediodilatatus baileyi PESSAGNO

Pl. 5, Fig. 10, 18

Lithocampe mediodilatata RÜST, RIEDEL & SANFILIPPO 1974, p. 779, Pl. 7, Fig. 3, not Fig. 1–2, 4.
Mirifusus baileyi PESSAGNO 1977a, p. 83, Pl. 10, Fig. 6–8, Pl. 11, Fig. 9–11. PESSAGNO 1977b, p. 48, Pl. 8, Fig. 1, 26, not 8–9. MIZUTANI 1981, p. 177, Pl. 60, Fig. 1. ADACHI 1982, Pl. 1, Fig. 1.4. OKAMURA & UTO 1982, Pl. 7, Fig. 3. ?ISHIDA 1983, Pl. 5. Fig. 7.

Mirifusus mediodilatatus (RÜST), BAUMGARTNER et al. 1980, p. 56, Pl. 5, Fig. 9–10, not 11. NAKASEKO & NISHIMURA 1981, p. 155, Pl. 8, Fig. 15. YAO et al. 1982, Pl. 4, Fig. 30. MURATA et al. 1982, Pl. 1, Fig. 11, 14. AOKI & TASHIRO 1982, Pl. 4, Fig. 8. YAO 1984, Pl. 3, Fig. 22.

Emended definition. – Cephalis, thorax and abdomen and sometimes first postabdominal segments externally smooth, poreless or sparsely porous. Remaining postabdominal segments (5–7) of conical proximal portion of test with well developed outer layer of irregular vertical and diagonal bars joining at circumferential ridges in broad nodes; outer layer mostly obscuring inner layer of two rows of pores. Segments of inflated median portion of test with inner layer of two rows of alternating triangular pores per segment. Outer layer becoming regular triangular and congruent with inner layer at top of or in upper part of the inflated median portion of test. Circumferential ridges of outer layer broad, with flat outer surface interrupted by flat nodes at junction of diagonal bars. Distal cylindrical portion delicate, without circumferential ridges (without segments?), with more or less regular transverse rows of pores.

Remarks. – Instead of a three-layered structure as proposed by PESSAGNO (1977a) for *M. baileyi,* we can only observe a two-layered structure, where the outer layer becomes completely congruent with the inner layer on the median part of the test.

Mirifusus mediodilatatus mediodilatatus (RÜST)

Pl. 5, Fig. 13, 19

Lithocampe mediodilatata RÜST 1885, p. 316, Pl. 40, Fig. 9. RIEDEL & SANFILIPPO 1974, p. 779, Pl. 7, Fig. 2, ?Fig. 4, not Fig. 1, 3.
Mirifusus (?) *mediodilatata* (RÜST), PESSAGNO 1977a, p. 84, Pl. 11, Fig. 1–2.
Mirifusus mediodilatatus (RÜST), BAUMGARTNER et al. 1980, p. 56, Pl. 5, Fig. 11. NISHIZONO et al. 1982, Pl. 3, Fig. 10.
Mirifusus baileyi PESSAGNO, ISHIDA 1983, Pl. 5, Fig. 8a–b, not 7.

Remarks. – This subspecies differs from *M. m. baileyi* in having two staggered rows of rounded triangular to circular pores per segment, relatively narrow, slightly nodose circumferential ridges and an outer layer which seems to terminate on upper median inflated portion of the test. There are intermediate forms between the two subspecies.

Mirifusus mediodilatatus minor BAUMGARTNER n. subsp.

Data 99, range 90, pob 286, rk 4 (pars), Pl. 5, Fig. 11–14

Lithocampe mediodilatata RÜST, ?PESSAGNO 1969, p. 610, Pl. 4, Fig. G, H. MOORE 1973, p. 828, Pl. 2, Fig. 5, 6.
Theoperid gen. et sp. indet. FOREMAN 1973, Pl. 12, Fig. 2.
Lithocampe mediodilatata RÜST, RIEDEL & SANFILIPPO 1974, Pl. 7, Fig. 1 only. FOREMAN 1975, p. 616, Pl. 2K, Fig. 2, ?Pl. 6, Fig. 17.
Mirifusus mediodilatatus (RÜST), FOREMAN 1978, Pl. 2, Fig. 3. STEIGER 1981, Pl. 14, Fig. 4. KANIE et al. 1981, Pl. 1, Fig. 14.
Mirifusus baileyi (PESSAGNO), OKAMURA 1980, Pl. 20, Fig. 4.

Description. – Proximal conical portion composed of spherical cephalis, inflated thorax and abdomen and one to at most three postabdominal segments. Entire conical portion externally smooth, sparsely porous, or with irregular, vertically elongated slots formed by the coalescent outer layer. Transverse rows of pores and circumferential

ridges delimiting segments appear at the base of the conical portion of test. Inflated median and conical distal portion of test identical as for *M. mediodilatatus baileyi.*

Remarks. – *M.m. minor* differs from *M.m. baileyi* as defined in this chapter by including only 4–6 segments in the proximal conical portion instead of 8–10. As a consequence, almost the entire conical portion is externally smooth. *M. m. minor* seems to evolve from *M. m. baileyi* during the Tithonian by a gradual decrease of the number of segments included in the conical portion (retardation). No forms assignable to *M.m. baileyi* have been found in the Neocomian.

Etymology. – *minor* = younger (Latin), referring to its descendance from *M.m. baileyi.*

Measurements (in μ)

	Holotype	Average of 7 spec.	min.	max.
Proximal conical portion				
Height:	138	136	106	184
Width:	123	133	89	156
Number of segments:	5?	6	4?	7?
Inflated median portion				
Height:	444	385	319	444
Width:	356	320	277	405

Type locality. – Locality no. 23 of locality descriptions.

Genus *Monotrabs* BAUMGARTNER n. gen.

Type species: Monotrabs plenoides BAUMGARTNER n. sp.

Description. – Form consisting of one hagiastrid-like (tritrabin?) ray, with two rows of alternating pores in depression between adjacent external longitudinal beams. No central area can be observed. One end tapering to a structure of triangular cross section made of three beams, the other end blunt, bearing spines.

Remarks. – Fragments of forms belonging to this genus mimick hagiastrid rays belonging to the Tritrabinae BAUMGARTNER 1980. Because of the absence of a central area and the peculiar tapering of one end, this form can only doubtfully be included with the hagiastrids.

Monotrabs plenoides BAUMGARTNER n. sp.

Data 42, range 54, pob 152, rk 91, Pl. 6, Fig. 1–2, 5

Hagiastrid sp. cf. *Tetraditryma pseudoplena* BAUMGARTNER, KOCHER 1981, p. 70, Pl. 14, Fig. 4.

Description. – Hagiastrid-like ray with two stout, triradiate lateral spines at one end, which stand at right angle to the axis of ray as with *Tetraditryma pseudoplena.* Ray structure rather tritrabin: 3–5 longitudinal, slightly nodose external beams visible per half circumference are separated by a depression with two rows of alternating pores. The opposite end tapers into an extension consisting of three beams connected by bars forming longitudinal rows of pores. The external beams may bear long secondary lateral spines.

Remarks. – Fragments of this species can be distinguished from fragments of *Tetraditryma pseudoplena* by having a tritrabin, rather than a tetraditrymin ray structure.

Etymology. – *plenoides:* In allusion to the lateral spines of *Tetraditryma pseudoplena.*

Measurements (in μ)

	Holotype	Average of 4 spec.	min.	max.
Length of ray:	216	333	216	450
Width of ray:	50	51	44	60
Length of lateral spines:	31	62	31	100
Length of extension:	77	–	–	–

Type locality. – Locality no. 30 of locality descriptions.

Genus *Napora* PESSAGNO

Napora PESSAGNO 1977a, p. 94.
Type species: Napora bukryi PESSAGNO 1977a.

Napora bukryi PESSAGNO

Data 73, range 61, pob 34, rk 31, Pl. 6, Fig. 4

Napora bukryi PESSAGNO 1977a, p. 94, Pl. 12, Fig. 8. KOCHER 1981, p. 77, Pl. 14, Fig. 31.
Napora lospensis DE WEVER & CABY 1981, Pl. 2, Fig. 2K.

Remarks. – Included are small *Napora* with a clearly visible cephalis with a short triradiate horn with a central and three lateral points. Cephalis offset from thorax by a stricture, thorax rounded, almost hemispherical and thin curved feet.

Napora deweveri BAUMGARTNER

Data 46, range 62, pob 35, rk 95, Pl. 6, Fig. 3

Napora deweveri BAUMGARTNER, BAUMGARTNER et al. 1980, p. 56, Pl. 3, Fig. 1–3, 5, Pl. 6, Fig. 9. KOCHER 1981, p. 78, Pl. 14, Fig. 24.
Not: *Napora* aff. *deweveri* BAUMGARTNER, ISHIDA 1983, Pl. 9, Fig. 5 (too small).

Napora lospensis PESSAGNO

Data 72, range 76, pob 36, rk 32, Pl. 6, Fig. 6

Napora lospensis PESSAGNO 1977a, p. 96, Pl. 12, Fig. 9–10.
?BAUMGARTNER et al. 1980, p. 57, Pl. 3, Fig. 4.
Not: DE WEVER & CABY 1981, Pl. 2, Fig. 2K.

Remarks. – Under this name we include large *Napora* with a small triradiate horn sitting on a broad cephalis, which is separated by a stricture from an inflated annular thorax. Some included forms may have a different pore structure than the holotype.

Napora pyramidalis BAUMGARTNER n. sp.

Data 12, range 11, pob 33, rk 104, Pl. 6, Fig. 11–12

Napora sp. A, BAUMGARTNER et al. 1980, p. 57, Pl. 3, Fig. 6–7. KOCHER 1981, p. 78, Pl. 15, Fig. 1–3.
Not: ISHIDA 1983, Pl. 9, Fig. 6 (too large).

Description. – Very small *Napora* with distinctly pyramidal overall shape. Cephalis completely hidden under a sharp apical horn bearing six ridges separated by six deep groves which originate on top of thorax. Three lateral points may sit on three of the ridges. Thorax pyramidal, with round pores in horizontal rows. The outer ridge of the feet originate on the edges of thorax. Basal aperture triangular, large. Feet triradiate almost in a straight line with edges of thorax, or slightly curved inward, equal or shorter than height of thorax.

Remarks. – This species differs from other *Napora* by its small size, its triangular-pyramidal shape, the sharp ridges completely hiding the cephalis and short, almost straight feet.

Etymology. – *pyramidalis* = like a pyramide (Latin).

Measurements (in μ, including data by KOCHER 1981).

	Holotype	Average of 22 spec.	min.	max.
Cephalis and horn				
Height:	52	61	41	79
Width:	29	33	28	43
Thorax				
Height:	54	66	54	78
Width between feet:	80	88	69	107
Length of feet:	38	67	38	86

Type locality. – Locality no. 30 of locality descriptions.

Genus *Obesacapsula* PESSAGNO

Obesacapsula PESSAGNO 1977a, p. 87.
Type species: Obesacapsula morroensis PESSAGNO 1977a.

Obesacapsula rotunda (HINDE)

Data 83, range 95, pob 202, rk 16, Pl. 6, Fig. 13

Stichocapsa rotunda HINDE 1900, p. 41, Pl. 3, Fig. 24. MUZAVOR 1977, p. 122, Pl. 5, Fig. 11–12. OZVOLDOVA 1979, p. 257, Pl. 5, Fig. 5–6.
Stichocapsa (?) *rotunda* HINDE, FOREMAN 1973, p. 265, Pl. 11, Fig. 2, Pl. 16, Fig. 20. FOREMAN 1975, p. 616, Pl. 2J, Fig. 6, Pl. 7, Fig. 5.
Obesacapsula rotunda (HINDE), PESSAGNO 1977b, p. 53, Pl. 9, Fig. 4, 12, 18. NAKASEKO et al. 1979, Pl. 2, Fig. 11a–b. NAKASEKO & ISHIMURA 1981, p. 156, Pl. 11, Fig. 12.
Syringocapsa rotunda (HINDE), FOREMAN 1978, p. 749, Pl. 2, Fig. 2. BAUMGARTNER et al. 1980, p. 62, Pl. 3, Fig. 12. KOCHER 1981, p. 97, Pl. 16, Fig. 30.

Obesacapsula rusconensis BAUMGARTNER n. sp.

Data 95, range 100, pob 282, rk–, Pl. 6, Fig. 7–9

Description. – Cephalis, thorax and abdomen together smooth, conical, almost without stricture to first postabdominal segment. First, second and third postabdominal segment cylindrical, growing gradually in width and little in height. Fourth postabdominal/final segment inflated annular to spherical, about half the height of entire test, with long tubular extension (where preserved as long as heigth of entire test) of about the width of third postabdominal segment. Postabdominal segments densely porous, final segment with a ornamentation of rounded irregular, sometimes spiny ridges which enclose areas of a few pores.

Remarks. – This species differs form *O. morroensis* which may be its ancestor, in having a final postabdominal segment which is less inflated and includes only about half of the test height instead of three quarters. It is further differentiated by the peculiar ornamentation on the final segment.

Etymology. – Referring to the type locality *Cava Rusconi* in Lombardy (northern Italy, see locality descriptions).

Measurements (in μ)

	Holotype	Average of 5 spec.	min.	max.
Cephalis, thorax and abdomen				
Width:	65	56	50	67
Height:	68	62	57	68
4th segment				
Width:	96	84	78	96
Height:	36	29	25	36
5th segment				
Width:	165	144	121	165
Height:	60	48	32	64
6th segment				
Width:	234	209	170	234
Height:	63	58	43	64
7th, last segment				
Width:	330	316	305	330
Height:	206	245	206	284
Tubular extension				
Width:	245	218	185	245
Length:	275	245	213	284

Type locality. – Locality no. 23. of locality descriptions.

Genus *Pantanellium* PESSAGNO

Pantanellium PESSAGNO 1977a, p. 78.
Type species: Pantanellium riedeli PESSAGNO 1977a.

Pantanellium (?) *berriasianum* BAUMGARTNER n. sp.

Data 93, range 92, pob 280, rk –, Pl. 6, Fig. 14–15

Description. – Ellipsoidal to spherical cortical shell with massive bipolar spines and one to several triradiate secondary spines placed on some nodal points of the pentago-

nal to hexagonal pore frames. The secondary spines are short, tapering into a sharp point, and seem to be randomly placed both in equatorial and peripolar position. Their number varies from one (usually in peripolar position) to six or eight. The remaining triple-junctions of the pore frames are slightly raised and bear moderate nodes.

Remarks. – This species differs from all other species included with *Pantanellium* and *Pachyoncus* PESSAGNO & BLOME 1980, in having short, sharp secondary spines placed randomly on some nodal points of the pore frames. The species is doubtfully included with *Pantanellium* as its definition (PESSAGNO 1977a) does not include such secondary spines. It is not included with *Pachyoncus* because the secondary spines of this genus are different and occur at most nodal points.

Etymology. – Referring to the first occurrence of this species in the Berriasian.

Measurements (in μ)

	Holotype	Average of 7 spec.	min.	max.
Cortical shell				
Polar diameter:	132	104	78	132
Equatorial diameter:	135	102	78	135
Polar spines				
Length, short:	78	65	51	78
Length, long:	117	89	64	117
Width at base:	52	33	23	52
Secondary spines				
Length:	36	38	23	64
Width at base:	27	23	18	27

Type locality. – Locality no. 23 of locality descriptions.

Genus *Paronaella* PESSAGNO

Paronaella PESSAGNO 1971, emend. BAUMGARTNER 1980.
Type species: Paronaella solanoensis PESSAGNO 1971.

Paronaella bandyi PESSAGNO

Data 58, range 21, pob 135, rk 51, Pl. 6, Fig. 16

Paronaella bandyi PESSAGNO 1977a, p. 69, Pl. 1, Fig. 1–3. BAUMGARTNER 1980, p. 300, Pl. 9, Fig. 4.
?*Paronaella mulleri* PESSAGNO, ISHIDA 1983, Pl. 10, Fig. 4.

Paronaella broennimanni PESSAGNO

Data 53, range 73, pob 137, rk 71, Pl. 6, Fig. 17

Paronaella broennimanni PESSAGNO 1977a, p. 69, Pl. 1, Fig. 4–5. BAUMGARTNER 1980, p. 300, Pl. 9, Fig. 6. KOCHER 1981, p. 80, Pl. 15, Fig. 5.

Paronaella kotura BAUMGARTNER

Data 48, range 64, pob 140, rk 85, Pl. 6, Fig. 20

Paronaella kotura BAUMGARTNER 1980, p. 302, Pl. 9, Fig. 15–19, Pl. 12, Fig. 8. KOCHER 1981, p. 80, Pl. 15, Fig. 7.
Paronaella sp. cf. *P. kotura* BAUMGARTNER, SATO et al. 1982, Pl. 3, Fig. 1.

Paronaella mulleri PESSAGNO

Data 38, range 32, pob 139, rk 96, Pl. 6, Fig. 21

Paronaella mulleri PESSAGNO 1977a, p. 71, Pl. 2, Fig. 2–3. BAUMGARTNER 1980, p. 304, Pl. 9, Fig. 8.

Genus *Parvicingula* PESSAGNO

Parvicingula PESSAGNO 1977a, p. 84.
Type species: Parvicingula santabarbarensis.

Remarks. – Included with this genus are also forms without or with weakly developed horn, which otherwise fit to PESSAGNO's (1977a) definition. *Ristola* PESSAGNO & WHALEN 1982, which has been erected to include these forms, is herein emended to include only the very long cylindrical parvicingulid species (see remarks under that genus).

Parvicingula cosmoconica (FOREMAN)

Data 102, range 94, pob 255, rk 22, Pl. 7, Fig. 1

Dictyomitra cosmoconica FOREMAN 1973, p. 263, Pl. 9, Fig. 11, Pl. 16, Fig. 3. FOREMAN 1975, p. 614, Pl. 1G, Fig. 5–6.
Parvicingula cosmoconica (FOREMAN), BAUMGARTNER et al. 1980, p. 58, Pl. 5, Fig. 16, Pl. 6, Fig. 7.

Parvicingula dhimenaensis BAUMGARTNER n.sp.

Data 90, range 33, pob 197, rk –, Pl. 7, Fig. 2–4

Amphipyndax sp. BAUMGARTNER & BERNOULLI 1976, p. 611, Fig. 12e, i, m.
Parvicingula boesii (PARONA) KOCHER 1981, p. 81, Pl. 15, Fig. 11, not 10. DE WEVER & CABY 1981, Pl. 2, Fig. 2C.
Parvicingula sp. C, AITA 1982, Pl. 1, Fig. 13–14.
Amphipyndax? sp. NISHIZONO et al. 1982, Pl. 3, Fig. 16.
Unnamed Nassellaria, WAKITA & OKAMURA 1982, Pl. 7, Fig. 7.

Description. – Slender conical to spindle-shaped parvicingulid. Cephalis hemispherical without or with a weakly developed horn, externally smooth, with a few small pores at base (ditrema). Thorax and abdomen trapezoidal, with irregular pores in roughly horizontal rows. All postabdominal segments with three rows of pores per segment in a uniform hexagonal arrangement. Circumferential ridges at segmental divisions bear nodes or small spines which are regularly spaced between every second adjacent pore. Diagonal bars may connect between nodes of circumferential ridges and form triangular frames which always enclose three pores. Last segment bears a tubular extension with closely spaced pores but without nodes or bars.

Remarks. – This species differs from other *Parvicingulas* in having circumferential ridges with regularly spaced nodes and diagonal bars connecting between nodes. At least two morphotypes are included with this species; they may be separated in a later stage of work. Some workers have included these forms with *Parvicingula boesii* (PARONA) 1890. This species differs from *P. dhimenaensis* by being broadly spindle-shaped, and having pronounced circumferential ridges without any nodes nor diagonal bars (see PARONA 1890, Pl. 6, Fig. 9!).

Etymology. – Named after a locality in the Argolis Peninsula (Peloponnesus, Greece), where this species abundantly occurs.

Measurements (in μ)

	Holotype	Average of 7 spec.	min.	max.
Total height of test:	270	255	230	300
Max. width of test:	113	117	105	135
Width of last segment:	80	91	80	109

Type locality. – Locality no. 5 of locality descriptions.

Genus *Perispyridium* DUMITRICA

Perispyridium DUMITRICA 1978, p. 9 35.
Type species: Trilonche (?) *ordinaria* PESSAGNO 1977a.

Perispyridium ordinarium (PESSAGNO)

Data 31, range 48, pob 100, rk 53, Pl. 7, Fig. 5–6

Trilonche (?) *ordinaria* PESSAGNO 1977a, p. 79, Pl. 6, Fig. 14.
Perispyridium ordinarium (PESSAGNO), DUMITRICA 1978, p. 9, 35, Pl. 3, Fig. 1, 2, 5, Pl. 4, Fig. 9. KOCHER 1981, p. 83, Pl. 15, Fig. 15. PESSAGNO & BLOME 1982, p. 294, Pl. 6, Fig. 4, 12, 15. NISHIZONO et al. 1982, Pl. 2, Fig. 9. AITA 1982, Pl. 3, Fig. 23.
Trigonocyclia sp. OZVOLDOVA 1979, p. 253, Pl. 3, Fig. 2.
?*Perispyridium* (?) *ordinarium* (PESSAGNO), DE WEVER & CABY 1981, Pl. 2, Fig. 2A.

Genus *Podobursa* WISNIOWSKI, emend. FOREMAN

Podobursa WISNIOWSKI 1889, p. 686, emend. FOREMAN 1973, p. 266.
Type species: Podobursa dunikowskii WISNIOWSKI 1889.

Podobursa helvetica (RÜST)

Data 18, range 13, pob 169, rk 98, Pl. 7, Fig. 7

Theosyringium helveticum RÜST 1885, p. 309, Pl. 27, Fig. 14.
Podobursa helvetica (RÜST), BAUMGARTNER et al. 1980, p. 60, Pl. 3, Fig. 11. KOCHER 1981, p. 84, Pl. 15, Fig. 17. DE WEVER & CABY 1981, Pl. 2, Fig. 20.

Podobursa spinosa (OZVOLDOVA)

Data 64, range 78, pob 230, rk 54, Pl. 7, Fig. 8

Indeterminatum in HEITZER 1930, p. 387, Pl. 27, Fig. 7.
Podobursa pantanellii (PARONA), RIEDEL & SANFILIPPO 1974, p. 779, Pl. 8, Fig. 5, Pl. 13, Fig. 6.
Heitzeria spinosa OZVOLDOVA 1975, p. 78, Pl. 101, Fig. 2.
Podobursa berggreni PESSAGNO 1977a, p. 90, Pl. 12, Fig. 1–5.

Podobursa spinosa (OZVOLDOVA), OZVOLDOVA 1979, p. 256, Pl. 2, Fig. 4, BAUMGARTNER et al. 1980, p. 60, Pl. 3, Fig. 10. KOCHER 1981, p. 85, Pl. 15, Fig. 18.
Not *Podocapsa pantanellii* PARONA 1890, p. 164, Pl. 5, Fig. 8.

Remark. – See remarks in BAUMGARTNER et al. (1980).

Genus *Podocapsa* RÜST, emend. FOREMAN

Podocapsa RÜST 1885, p. 304, emend. FOREMAN 1973, p. 267.
Type species: Podocapsa guembeli RÜST 1885.

Podocapsa amphitreptera FOREMAN

Data 69, range 84, pob 171, rk 38, Pl. 7, Fig. 9–10

Podocapsa amphitreptera FOREMAN 1973, p. 267, Pl. 13, Fig. 11. FOREMAN 1975, p. 617, Pl. 6, Fig. 15. MUZAVOR 1977, p. 112, Pl. 7, Fig. 4. FOREMAN 1978, p. 749, Pl. 1, Fig. 16. BAUMGARTNER et al. 1980, p. 61, Pl. 3, Fig. 8–9. KOCHER 1981, p. 86, Pl. 15, Fig. 20. ?DE WEVER & CABY 1981, Pl. 2, Fig. 2M. YAO et al. 1982. Pl. 4, Fig. 29. YAO 1984, Pl. 3, Fig. 14.
Nassellaria gen. et sp. indet. NAKASEKO & NISHIMURA 1981, Pl. 8, Fig. 12a–b.

Genus *Praeconocaryomma* PESSAGNO

Praeconocaryomma PESSAGNO 1976, p. 40.
Type species: Praeconocaryomma universa PESSAGNO 1976.

Praeconocaryomma (?) *hexacubica* BAUMGARTNER n. sp.

Data 87, range 31, pob 244, rk –, Pl. 7, Fig. 11–14

Description. – Cortical shell is a sphere or a rounded cube with eight stout, triradiate primary radial spines extending from the corners of the cube. These spines may be reduced or absent. Surface of cortical shell bears a meshwork of bars forming equilateral triangles which join to form regular hexagones centered around a raised knob with a central pore. Each triangle of bars encloses three pores which results in a perfectly hexagonal pore arrangement of the inner side of cortical shell, visible in fragments or broken up specimens. The central pore of the outer bar hexagones is the depressed central, seventh pore of the internal, concave pore hexagones which are delimited by moderate rounded ridges (see Pl. 7, Fig. 13). First medullary shell smooth, spherical, with circular pores in pentagonal to hexagonal arrangement, connected to cortical shell by six triradiate radial beams which reach to the center of the square sides of cortical shell. No second medullary shell has been observed.

Remarks. – This form is distinguished even in small fragments by its very characteristic wall structure of the cortical shell, which somehow resembles the mammary pore frames described for *Praeconocaryomma media* by PESSAGNO & POISSON (1981). However, this species is doubtfully included with *Praeconocaryomma* as instead of a radial spine there is a pore in the center of each bar hexagone. Besides that, this species may have stout primary radial spines which do not connect inwards to the first medullary shell, which is instead connected by beams centered between the outer spines. Only one, instead of three medullary shells has been observed.

Etymology. – *hexa:* referring to the hexagonal pore frames; *cubica:* referring to the shape of the cortical shell.

Measurements (in μ)

	Holotype	Average of 8 spec.	min.	max.
Diameter of cortical shell between sides:	195	198	172	225
Diameter of first medullary shell:	–	50	45	55
Diameter of bar hexagones:	55	58	52	65
Length of external spines.	75	60	20	76

Type locality. – Locality no. 30 of locality descriptions.

Genus *Protunuma* ICHIKAWA & YAO

Protunuma ICHIKAWA & YAO 1976, p. 114.
Type species: Protunuma fusiformis ICHIKAWA & YAO 1976.

Protunuma costata (HEITZER)

Data 21, range 35, pob 232 and 233, rk 62 and 67, Pl. 7, Fig. 15

?*Cenellepsis costata* HEITZER 1930, p. 388, Pl. 17, Fig. 12. MUZAVOR 1977, p. 71, Pl. 4, Fig. 7.
Protunuma sp. aff. *Cenellepsis costata* HEITZER, KOCHER 1981, p. 86, Pl. 15, Fig. 21.
?*Cenellepsis multicostata* HEITZER 1930, p. 388, Pl. 17, Fig. 13. MUZAVOR 1977, p. 70, Pl. 4, Fig. 8.
Protunuma sp. aff. *Cenellepsis multicostata* HEITZER, KOCHER 1981, p. 87, Pl. 15, Fig. 22.
Protunuma sp. D, YAO et al. 1982, Pl. 4, Fig. 24. YAO 1984, Pl. 3, Fig. 12, 17.

Remarks. – This name is used to include fusiform *Protunumas* without externally individualized cephalis nor with a terminal extension, with plicae that run from cephalis to base of test and two to five longitudinal rows of circular uniform pores between them. It includes two or more morphotypes which are difficult to separate in routine radiolarian work.

Genus *Pseudocrucella* BAUMGARTNER

Pseudocrucella BAUMGARTNER 1980, p. 291.
Type species: Crucella sanfilippoae PESSAGNO 1977a.

Pseudocrucella adriani BAUMGARTNER

Data 52, range 34, pob 129, rk 72, Pl. 7, Fig. 16

Pseudocrucella adriani BAUMGARTNER 1980, p. 291, Pl. 8, Fig. 4, 8, 12, 15, 16. KOCHER 1981, p. 88, Pl. 15, Fig. 23.

Pseudocrucella sanfilippoae (PESSAGNO)

Data 51, range 58, pob 126, rk 73, Pl. 7, Fig. 17

Crucella sanfilippoae PESSAGNO 1977a, p. 72, Pl. 2, Fig. 15–16. AITA 1982, Pl. 3, Fig. 9.
Pseudocrucella sanfilippoae (PESSAGNO), BAUMGARTNER 1980, p. 291, Pl. 8, Fig. 1, 23, 24. KOCHER 1981, p. 88, Pl. 16, Fig. 1. Not: DE WEVER & CABY 1981, Pl. 2, Fig. 2J.

Genus *Pseudodictyomitra* PESSAGNO

Pseudodictyomitra PESSAGNO 1977b, p. 50.
Type species: Pseudodictyomitra pentacolaensis PESSAGNO 1977b.

Pseudodictyomitra carpatica (LOZNYAK)

Data 107, range 105, pob 293, rk –, Pl. 8, Fig. 1

Dictyomitra carpatica LOZNYAK 1969, p. 38, Pl. 2, Fig. 11–12. FOREMAN 1973, p. 263, Pl. 10, Fig. 1–3, Pl. 16, Fig. 5. FOREMAN 1975, p. 614, Pl. 2G, Fig. 12–14, not 11, Pl. 7, Fig. 7 not 6.
Pseudodictyomitra carpatica (LOZNYAK), SCHAAF 1981, p. 436, Pl. 3, Fig. 1a–c, 2, Pl. 20, Fig. 4a–b. NAKASEKO & NISHIMURA 1981, p. 158, Pl. 9, Fig. 6, 11. DE WEVER & THIÉBAULT 1981, p. 590, Pl. 2, Fig. 2. MATSUYAMA et al. 1982, Pl. 1, Fig. 7. YAO 1984, Pl. 4, Fig. 18.
Pseudodictyomitra sp. cf. *P. carpatica* (LOZNYAK), NISHIZONO et al. 1982, Pl. 3, Fig. 9.
Pseudodictyomitra sp. KANIE et al. 1984, Pl. 4, Fig. 14.

Pseudodictyomitra depressa BAUMGARTNER n. sp.

Data 97, range 101, pob 284, rk –, Pl. 8, Fig. 2, 7–8, 11

Pseudodictyomitra sp. OKAMURA 1980, Pl. 20, Fig. 6, 11.
Unnamed nassellariid F, WU HAO-RUO & LI HONG-SHENG 1982, Pl. 2, Fig. 19.
Archaeodictyomitra carpatica (LOZNYAK). OKAMURA & UTO 1982, Pl. 2, Fig. 3 (only).
Pseudodictyomitra carpatica (LOZNYAK). OKAMURA & UTO 1982, Pl. 8, Fig. 7a–b.

Description. – Overall shape of test broadly conical proximally and slightly constricted distally, the widest segments being the 7th to 9th segment. Cephalis, thorax and abdomen together smooth, conical, without external strictures. Thorax and abdomen with one horizontal row of pores at base. First postabdominal segment cylindrical, with weak ornamentation and one row of pores at base. Following five to six postabdominal segments cylindrical, with very pronounced circumferential ridges separated by deeply depressed grooves at segmental divisions in which one or two rows of pores are visible. The circumferential ridges are of round cross section and bear costae (about 12 visible per half circumference) which are regularly spaced between the pores. Well preserved specimens show faint horizontal ribs between costae. Last postabdominal segment clearly narrower than second last, with two well exposed, staggered rows of pores and less pronounced circumferential ridge and costae at base.

Remarks. – This species differs from other *Pseudodictyomitra* by having deeply depressed segmental divisions and a distally constricted overall shape.

Etymology. – *depressa:* referring to the depressed segmental divisions (Latin).

Measurements (in μ)

	Holotype	Average of 6 spec.	min.	max.
Cephalis, thorax and abdomen				
Height:	51	53	51	55
Width:	48	53	48	60
Width of widest segment:	140	130	110	147
Width of last segment:	123	113	97	123
Total length of test:	239	245	202	306

Type locality. – Locality no. 16 of locality descriptions.

Genus *Ristola* PESSAGNO & WHALEN, emend.

Ristola PESSAGNO & WHALEN 1982, p. 148, emend.
Type species: Parvicingula (?) *procera* PESSAGNO 1977a.

Emendation. – PESSAGNO & WHALEN (1982) erected this genus to include all forms questionably assigned to *Parvicingula* lacking a horn. It is herein emended to include only species which have a conical proximal portion, a very long cylindrical portion with several tenths of postabdominal segments and in addition have an outer layer, which, similar as with *Mirifusus,* tends to obscure the regular hexagonal pore frames of the inner layer in the proximal portion of the test (see Pl. 8, Fig. 3, 9, 10). Conical forms, lacking this outer layer are included with *Parvicingula,* whether they have a horn or not.

Ristola altissima (RÜST)

Data 32, range 47, pob 164, rk 52, Pl. 8, Fig. 3–4, 9

Lithocampe altissima RÜST 1885, p. 315 (45), Pl. 40, Fig. 2. not: MOORE 1973, p. 828, Pl. 3, Fig. 7. OZVOLDOVA 1979, p. 258, Pl. 5, Fig. 1.
Parvicingula altissima (RÜST), PESSAGNO 1977a, p. 85, Pl. 8, Fig. 9–10. ?NAKASEKO et al. 1979, Pl. 1, Fig. 9–10. BAUMGARTNER et al. 1980, p. 58, Pl. 5, Fig. 4–7. ?NAKASEKO & NISHIMURA 1981, Pl. 8, Fig. 14. KOCHER 1981, p. 81, Pl. 15, Fig. 9. YAO et al. 1982, Pl. 4, Fig. 19. ADACHI 1982, Pl. 1, Fig. 8. MURATA et al. 1982, Pl. 1, Fig. 13. YAO 1984, Pl. 2, Fig. 25.
Mirifusus sp., SATO et al. 1982, Pl. 4, Fig. 13.
Theoperid gen. et sp. indet. AOKI & TASHIRO 1982, Pl. 2, Fig. 7.

Ristola cretacea (BAUMGARTNER)

Data 101, range 93, pob 165, rk 23, Pl. 8, Fig. 5, 10

Lithocampe altissima RÜST, MUZAVOR 1977, p. 102, Pl. 8, Fig. 7.
Parvicingula cretacea BAUMGARTNER, BAUMGARTNER et al. 1980, p. 59, Pl. 5, Fig. 1–3, Pl. 6, Fig. 4.

Ristola procera (PESSAGNO)

Data 45, range 72, pob 163, rk 97, Pl. 8, Fig. 6

Parvincingula (?) *procera* PESSAGNO 1977a, p. 86, Pl. 9, Fig. 6–9.
Parvicingula procera PESSAGNO, BAUMGARTNER et al. 1980, p. 60, Pl. 5, Fig. 8. KOCHER 1981, p. 83, Pl. 15, Fig. 14.

Genus *Saitoum* PESSAGNO

Saitoum PESSAGNO 1977a, p. 96.

Type species: Saitoum pagei PESSAGNO 1977a.

Saitoum pagei PESSAGNO

Data 88, range 49, pob 20, rk 55, Pl. 8, Fig. 12

Saitoum pagei PESSAGNO 1977a, p. 98, Pl. 12, Fig. 11–14. KOCHER 1981, p. 89, Pl. 16, Fig. 2–3. DE WEVER & CABY 1981, Pl. 2, Fig. 2H. BAUMGARTNER et al. 1981, Fig. 4a–b.

Genus *Sethocapsa* HAECKEL

Sethocapsa HAECKEL 1881, p. 433.
Type species: Sethocapsa cometa (PANTANELLI) in RÜST 1885.

Sethocapsa cetia FOREMAN

Data 68, range 87, pob 203, rk 39, Pl. 8, Fig. 13

Sethocapsa cetia FOREMAN 1973, p. 267, Pl. 12, Fig. 1, Pl. 16, Fig. 19. FOREMAN 1975, p. 617, Pl. 2K, Fig. 1, Pl. 6, Fig. 14. MUZAVOR 1977, p. 114, Pl. 5, Fig. 4. FOREMAN 1978, p. 749, Pl. 2, Fig. 1. BAUMGARTNER et al. 1980, p. 61, Pl. 3, Fig. 14. KOCHER 1981, p. 89, Pl. 16, Fig. 4–5.
Sethocapsa cethia STEIGER 1981, Pl. 14, Fig. 6 (incorrect secondary spelling IRZN Art. 33b.).
Not: *Obesacapsula cetia* (FOREMAN), PESSAGNO 1977a, p. 87, Pl. 11, Fig. 4. Not: PESSAGNO 1977b, p. 52, Pl. 9, Fig. 11.

Sethocapsa leiostraca FOREMAN

Data 84, range 51, pob 62, rk 7

Sethocapsa leiostraca FOREMAN 1973, p. 268, Pl. 12, Fig. 5–6. FOREMAN 1975, p. 617, Pl. 2J Fig. 5. KOCHER 1981, p. 89, Pl. 16, Fig. 6.
?*Sethocapsa trachyostraca* FOREMAN, BAUMGARTNER et al. 1980, p. 61, Pl. 6, Fig. 2.

Sethocapsa trachyostraca FOREMAN

pob 63, rk 15, Pl. 8, Fig. 14

Sethocapsa trachyostraca FOREMAN 1973, p. 268, Pl. 12, Fig. 4. FOREMAN 1975, p. 617, Pl. 2J, Fig. 3, 4. MUZAVOR 1977, p. 119, Pl. 6, Fig. 5. FOREMAN 1978, p. 749, Pl. 1, Fig. 18. Not: BAUMGARTNER et al. 1980, Pl. 6, Fig. 2. SCHAAF 1981, p. 437, Pl. 21, Fig. 1a–b. Not: KOCHER 1981, Pl. 16, Fig. 9–10.

Remarks. – Although the illustrated material is insufficient, there is good evidence that forms assignable to both *S. leiostraca* and *S. trachyostraca* do range down to Zone A1 (middle to late Callovian).

Sethocapsa uterculus (PARONA)

Data 111, range 109, pob 297, rk –, Pl. 8, Fig. 15

Theocapsa uterculus PARONA 1890, p. 168, Pl. 5, Fig. 17.
Sethocapsa sp. cf. *Theocapsa uterculus* PARONA, FOREMAN 1975, p. 617, Pl. 21, Fig. 21–22. FOREMAN 1978, p. 749, Pl. 2, Fig. 8. KANIE et al. 1981, Pl. 1, Fig. 12.
Sethocapsa uterculus (PARONA), SCHAAF 1981, p. 437, Pl. 5, Fig. 8a–b, Pl. 26, Fig. 5a–b. OKAMURA & UTO 1982, Pl. 3, Fig. 15. YAO 1983, Pl. 4, Fig. 1–2.

Remarks. – Similar forms not included here, range down to the Berriasian.

Genus *Spongocapsula* PESSAGNO

Spongocapsula PESSAGNO 1977a, p. 88.
Type species: Spongocapsula palmerae PESSAGNO 1977a.

Spongocapsula palmerae PESSAGNO

Data 50, range 38, pob 199, rk 76, Pl. 8, Fig. 16

Spongocapsula palmerae PESSAGNO 1977a, p. 88, Pl. 11, Fig. 12–14, 16. KOCHER 1981, p. 93, Pl. 16, Fig. 17.

Spongocapsula perampla (RÜST)

Dat 85, range –, pob 267, rk 9, Pl. 8, Fig. 17

Lithocampe perampla RÜST 1885, p. 315, Pl. 39, Fig. 11. RIEDEL & SANFILIPPO 1974, p. 779, Pl. 7, Fig. 1–4.
Spongocapsula sp. aff. *S. perampla* (RÜST), PESSAGNO 1977a, p. 90, Pl. 11, Fig. 15.
Spongocapsula perampla (RÜST), KOCHER 1981, p. 94, Pl. 16, Fig. 18.

Remarks. – These, possibly several, morphotypes have a very spotty occurrence in the Late Jurassic and Early Cretaceous. Their data has been excluded from treatment for Unitary Association.

Genus *Staurosphaera* HAECKEL

Staurosphaera HAECKEL 1881, p. 450.
Type species: Staurosphaera crassa DUNIKOWSKI 1882.

Staurosphaera antiqua RÜST

Data 49, range 60, pob 218, rk 83, Pl. 8, Fig. 18

Staurosphaera antiqua RÜST 1885, p. 289, Pl. 28, Fig. 2.
Emiluvia antiqua (RÜST), PESSAGNO 1977a, p. 76, Pl. 4, Fig. 9–10. KOCHER 1981, p. 63, Pl. 13, Fig. 4.

Remarks. – This species lacks the typical raised axial outer layer of the central area of *Emiluvia*. It is therefore left with its original generic assignment until more is known about this group.

Genus *Stichocapsa* HAECKEL

Stichocapsa HAECKEL 1881, p. 1515.
Type species: Stichocapsa jaspidea RÜST 1885.

Stichocapsa convexa YAO

Data 61, range 16, pob 55, rk 56, Pl. 8, Fig. 19

Stichocapsa convexa YAO 1979, p. 35, Pl. 5, Fig. 14–16, Pl. 6, Fig. 1–7. KOCHER 1981, p. 95, Pl. 16, Fig. 21–22. WAKITA 1982, Pl. 3, Fig. 7. AITA 1982, Pl. 1, Fig. 6–7b.
Stichocapsa sp. J., AITA 1982, Pl. 1, Fig. 8–9b.

Stichocapsa japonica YAO

Data 22, range 19, pob 49, rk 74

Stichocapsa japonica YAO 1979, p. 36, Pl. 6, Fig. 9–12, Pl. 7, Fig. 1–15. KOCHER 1981, p. 96, Pl. 16, Fig. 23. YAO et al. 1982, Pl. 3, Fig. 16. KIDO et al. 1982, P. 5, Fig. 8. WAKITA & OKAMURA 1982, Pl. 8, Fig. 4.

Stichocapsa sp. aff. *S. japonica* YAO

Data 4, range 3, pob 48, rk –, Pl. 8, Fig. 20

Remarks. – The included form differs from the type material in having a nodose test surface. This morphotype seems to be limited to Zone A0 (and older) samples.

Genus *Stylocapsa* PRINCIPI

Stylocapsa PRINCIPI 1909, p. 20. Emend. TAN SIN HOK 1927, p. 32.
Type species: Stylocapsa exagonata PRINCIPI 1909.

Stylocapsa oblongula KOCHER

Data 6, range 53, pob 59, rk 111, Pl. 9, Fig. 1–2

Stylocapsa oblongula KOCHER in BAUMGARTNER et al. 1980, p. 62, Pl. 6, Fig. 1. KOCHER 1981, p. 97, Pl. 17, Fig. 27–29. AITA 1982, Pl. 1, Fig. 18a–b. MATSUOKA 1983, p. 19, Pl. 6, Fig. 5–7.

Genus *Syringocapsa* NEVIANI

Syringocapsa NEVIANI 1900, p. 662.
Type species: Theosyringium robustum VINASSA 1900, p. 343.

Syringocapsa agolarium FOREMAN

Data 105, range 104, pob 291, rk –, Pl. 9, Fig. 3–4

Syringocapsa agolarium FOREMAN 1973, p. 268, Pl. 1, Fig. 5, Pl. 16, Fig. 17.

Syringocapsa lucifer BAUMGARTNER n. sp.

Data 96, range 91, pob 283, rk –, Pl. 9, Fig. 5

Description. – Very large form with spiny spherical postabdominal segment. Cephalis, thorax and abdomen together conical, externally smooth, with small, sparsely distributed pores. Following few (1–3?) postabdominal segments densely porous, forming a conical proximal portion together with the first three segments almost without external segmental strictures. Final postabdominal segment inflated spherical, three times as wide as conical proximal portion and forming more than half of the total height of test; the surface is densely porous, with an irregular system of rounded bars wearing numerous short, sharp spines of rounded cross section. Final segment terminates in a slender, short, imperforate terminal tube.

Remarks. – This species differs from *Syringocapsa limatum* FOREMAN 1973 in having a densely porous, spiny final segment and in having only a thin, short, imperforate terminal extension.

Etymology. – *lucifer* (Latin) refers to a weapon used by the Middle-Age Swiss.

Measurements (in μ)

	Holotype	Average of 9 spec.	min.	max.
Proximal conical portion				
Height:	200	173	156	200
Width:	170	151	128	177
Final p.a. segment				
Height:	340	368	334	405
Width:	390	401	362	461
Terminal tube				
Lenght:	90	104	50	135
Width:	66	67	43	113
Length of spines:	60	69	50	85

Type locality. – Locality no. 23 of locality descriptions.

Genus *Tetraditryma* BAUMGARTNER

Tetraditryma BAUMGARTNER 1980, p. 296.
Type species: Tetraditryma pseudoplena BAUMGARTNER 1980.

Tetraditryma corralitosensis (PESSAGNO)

Data 20, range 17, pob 124, rk 58, Pl. 9, Fig. 6–7

Crucella (?) *corralitosensis* PESSAGNO 1977a, p. 72, Pl. 2, Fig. 10–13.
Tetraditryma corralitosensis (PESSAGNO), BAUMGARTNER 1980, p. 296, Pl. 7, Fig. 12–15, Pl. 11, Fig. 13. KOCHER 1981, p. 98. Pl. 16, Fig. 31. DE WEVER & CABY 1981, Pl. 2, Fig. 2G. ISHIDA 1983, Pl. 11, Fig. 8.
Tetraditryma sp. cf. *T. corralitosensis* (PESSAGNO), WAKITA 1982, Pl. 5, Fig. 9–10.

Tetraditryma praeplena BAUMGARTNER n. sp.

Data 5, range 6, pob 125, rk –, Pl. 9, Fig. 8–9, 13–13a

Description. – General construction of test and central area very similar to *T. pseudoplena*. The four rays are of equal length, stand nearly at right angle and end in a ray tip which differs from *T. pseudoplena* in being not thickened, and having two slender, sharp, triradiate lateral spines standing at an angle of 60–70 degrees to the ray axis and several secondary lateral and small central spines. The cortical wall (arrow Pl. 9, Fig. 13a) is very delicate, porous, or may be totally absent.

Remarks. – *T. praeplena* is the immediate ancestor of *T. pseudoplena* and cooccurs with the former in Zones A0–A1. *T. praeplena* differs from *T. pseudoplena* in lacking bulbous ray tips, in having finer lateral spines which stand at an angle of 60–70, instead of 90 degrees to ray axis and in having a delicate instead of a massive imperforate cortical wall.

Etymology. – Referring to the evolutionary relationship with *T. pseudoplena*.

Measurements (in μ)

	Holotype	Average of 4 spec.	min.	max.
Length of rays				
AX:	246	243	198	277
BX:	246			
CX:	270			
DX:	252			
Width of rays:	54	44	36	54
Length of longest central spine:	42	27	12	42
Length of longest lateral spine:	69	62	69	54

Type locality. – Locality no. 40 of locality descriptions.

Tetraditryma pseudoplena BAUMGARTNER

Data 57, range 34, pob 123, rk 59, Pl. 9, Fig. 12, 14

Hagiastrum plenum (RÜST), PESSAGNO 1977a, p. 72, Pl. 2, Fig. 14.
Tetraditryma pseudoplena BAUMGARTNER 1980, p. 297, Pl. 1, Fig. 9, Pl. 7, Fig. 1–11. BAUMGARTNER et al. 1980, p. 63, Pl. 2, Fig. 1. KOCHER 1981, p. 98, Pl. 16, Fig. 32–33. SATO et al. 1982, Pl. 3, Fig. 7. ISHIDA 1983, Pl. 11, Fig. 7.

Genus *Tetratrabs* BAUMGARTNER

Tetratrabs BAUMGARTNER 1980, p. 294.
Type species: Tetratrabs gratiosa BAUMGARTNER 1980.

Tetratrabs bulbosa BAUMGARTNER

Data 62, range 74, pob 122, rk 60, Pl. 9, Fig. 11

Tetratrabs bulbosa BAUMGARTNER 1980, p. 295, Pl. 5, Fig. 1, Pl. 6, Fig. 1–3, 8. KOCHER 1981, p. 99, Pl. 16, Fig. 34.

Tetratrabs zealis (OZVOLDOVA)

Data 36, range 24, pob 121, rk 61, Pl. 9, Fig. 10

Crucella zealis OZVOLDOVA 1979, p. 34, Pl. 2, Fig. 1.
Tetratrabs gratiosa BAUMGARTNER 1980, p. 295, Pl. 1, Fig. 11, Pl. 5, Fig. 2–7, Pl. 6, Fig. 4–7, 9–14, Pl. 11, Fig. 7–9. BAUMGARTNER et al. 1980, p. 63, Pl. 2, Fig. 6. SATO et al. 1982, Pl. 3, Fig. 8. ISHIDA 1983, Pl. 11, Fig. 9.
Tetratrabs zealis (OZVOLDOVA), KOCHER 1981, p. 99, Pl. 17, Fig. 1.

Genus *Thanarla* PESSAGNO

Thanarla PESSAGNO 1977b, p. 45.
Type species: Phormocyrtis veneta SQUINABOL 1903.

Thanarla pulchra (SQUINABOL)

Data 109, range 107, pob 296, rk –, Pl. 9, Fig. 15

Sethamphora pulchra SQUINABOL 1904, p. 213, Pl. 5, Fig. 8. MOORE 1973, p. 826, Pl. 3, Fig. 5, 6, not 4.
Dictyomitra pulchra (SQUINABOL), DUMITRICA 1975, p. 87, Fig. 2.
Lithocampe elegantissima CITA, FOREMAN 1975, p. 616, Pl. 2G, Fig. 3–4. MUZAVOR 1977, p. 100, Pl. 8, Fig. 1. ?NAKASEKO et al. 1979, Pl. 4, Fig. 2. AOKI 1982, Pl. 3, Fig. 11–12.

Thanarla pulchra (SQUINABOL), PESSAGNO 1977b, p.46, Pl.7, Fig.7, 21, 26. SCHAAF 1981, p.439, Pl.4, Fig.10. ? Pl.19, Fig.7a–b. Nakaseko & Nishimura 1981, p.163, Pl.15, Fig.11 (not Pl.7, Fig.4–5, 7–8, Pl.15, Fig.12.). Taketani 1982, p.59, Pl.11, Fig.19.
?*Thanarla pacifica* NAKASEKO & NISHIMURA 1981, p.163, Pl.7, Fig.3a–b, 6 (same specimen as NAKASEKO et al. 1979, Pl.4, Fig.2), 9.
Thanarla elegantissima (CITA), MATSUYAMA et al. 1982, Pl.2, Fig.2.
Thanarla sp. cf. *T.pulchra* (SQUINABOL), OKAMURA & UTO 1982, Pl.5, Fig.6. YAO 1984, Pl.4, Fig.10.

Remarks. – Included are the forms with a broadly inflated, distally constricted, distal portion of the test. Transitional forms to *T.elegantissima,* with a more cylindrical distal portion have also been observed in the Neocomian but are here excluded.

Genus *Theocapsomma* HAECKEL, emend. FOREMAN

Theocapsomma HAECKEL 1887, p.1428, emend. FOREMAN 1968, p.29.
Type species: Theocapsa linnaei HAECKEL 1887.

Theocapsomma cordis KOCHER

Data 15, range 30, pob 227, rk 99, Pl.8, Fig.16–17

Theocapsomma cordis KOCHER 1981, p.100, Pl.17, Fig.2–4.

Genus *Triactoma* RÜST

Triactoma RÜST 1885, p.289.
Type species: Triactoma tithonianum RÜST 1885.

Triactoma blakei (PESSAGNO)

Data 25, range 46, pob 95, rk 64, Pl.10, Fig.3

Tripocyclia blakei PESSAGNO 1977a, p.80, Pl.6, Fig.15–16. MIZUTANI 1981, p.175, Pl.57, Fig.5–6.
Triactoma foremanae MUZAVOR 1977, p.55, Pl.1, Fig.11.
Triactoma blakei (PESSAGNO), FOREMAN 1978, p.743, Pl.1, Fig.15. KOCHER 1981, p.101, Pl.17, Fig.5, not Fig.6.
Tripocyclina blakei (PESSAGNO), ISHIDA 1983, Pl.4, Fig.15.

Triactoma cornuta BAUMGARTNER

Data 89, range 65, pob 166, rk 78, Pl.10, Fig.1

Gen. et sp. indet. OZVOLDOVA 1979, p.260, Pl.2, Fig.3.
Triactoma cornuta BAUMGARTNER, BAUMGARTNER et al. 1980, p.63, Pl.2, Fig.2–3. KOCHER 1981, p.101, Pl.17, Fig.7. DE WEVER & CABY 1981, Pl.2, Fig.2F. ISHIDA 1983, Pl.4, Fig.12–13.

Triactoma echiodes FOREMAN

Data 81, range 89, pob 94, rk 19, Pl.10, Fig.2

Triactoma echiodes FOREMAN 1973, p.260, Pl.3, Fig.1. P.16, Fig.21. FOREMAN 1975, p.609, Pl.2F, Fig.9–10. Pl.3, Fig.10. BAUMGARTNER et al. 1980, p.64, Pl.2, Fig.10. KOCHER 1981, p.101, Pl.17, Fig.8–9. KANIE et al. 1981, Pl.1, Fig.7.

Triactoma jonesi (PESSAGNO)

Data 29, range 25, pob 96, rk 33, Pl. 10, Fig. 4

Tripocyclia jonesi PESSAGNO 1977a, p. 80, Pl. 7, Fig. 1–5.
Tripocyclia trigonum RÜST, PESSAGNO 1977a, p. 80, Pl. 7, Fig. 6–7. SASHIDA et al. 1982, Pl. 1, Fig. 5.
Triactoma jonesi (PESSAGNO); ?FOREMAN 1978, p. 743, Pl. 1, Fig. 13–14. KOCHER 1981, p. 102, Pl. 17, Fig. 10.
Triactoma sp. WAKITA & OKAMURA 1982, Pl. 5, Fig. 11.
Tripocyclia trigonum RÜST, ISHIDA 1983, Pl. 4, Fig. 14.

Remarks. – In the studied material there are plenty of transitional forms between *T. jonesi* and *T. trigonum*. *T. tithonianum* is separated on the basis of slenderer, longer and more pointed spines (see also remarks in KOCHER 1981).

Triactoma tithonianum RÜST

Data 30, range 52, pob 97, rk 40, Pl. 10, Fig. 5

Triactoma tithonianum RÜST 1885, p. 289, Pl. 28, Fig. 5. FOREMAN 1973, p. 260, Pl. 2, Fig. 1. KOCHER 1981, p. 102, Pl. 17, Fig. 12.

Genus *Tricolocapsa* HAECKEL

Tricolocapsa HAECKEL 1881, p. 436.
Type species: Tricolocapsa theophrasti HAECKEL 1887.

Tricolocapsa plicarum YAO

Data 9, range 8, pob 51, rk –, Pl. 10, Fig. 6–7

Tricolocapsa plicarum YAO 1979, p. 32, Pl. 4, Fig. 1–11. YAO et al. 1982, Pl. 3, Fig. 12. SASHIDA et al. 1982, Pl. 2, Fig. 1, not: Pl. 1, Fig. 2. OWADA & SAKA 1982, Pl. 2, Fig. 15. KOJIMA 1982, Pl. 2, Fig. 1. WAKITA 1982, Pl. 3, Fig. 3. KIDO et al. 1982, Pl. 5, Fig. 1. IMOTO et al. 1982, Pl. 2, Fig. 1–2. NISHIZONO et al. 1982, Pl. 2, Fig. 16. WAKITA & OKAMURA 1982, Pl. 7, Fig. 9. ?ISHIDA 1983, Pl. 8, Fig. 9. MATSUOKA 1983, p. 20, Pl. 3, Fig. 1–2. KASHIMA 1983, Pl. 9, Fig. 1. Saka 1983, Pl. 6, Fig. 2–4. YAO 1984, Pl. 1, Fig. 11–12.

Remarks. – There are at least two morphotypes included: One is broadly spindle-shaped and has open plicae, about 17–20 per half circumference. The other is more slenderly spindle-shaped and has narrow plicae, more than 20 per half circumference. Forms with horizontal bars connecting plicae between each pore (e.g. SASHIDA et al. 1982, Pl. 1, Fig. 2) are excluded.

Genus *Trillus* PESSAGNO & BLOME

Trillus PESSAGNO & BLOME 1980, p. 248.
Type species: Trillus seidersi PESSAGNO & BLOME 1980.

Trillus sp. cf. *T. seidersi* PESSAGNO & BLOME

Data 1, range 1, pob 39, rk –, Pl. 10, Fig. 8

Trillus seidersi PESSAGNO & BLOME 1980, p. 249, Pl. 9, Fig. 2–4, 9, 19.
Trillus sp. A, PESSAGNO & BLOME 1980, p. 248, Pl. 11, Fig. 1. YAO et al. 1982, Pl. 3, Fig. 25. MIZUTANI & KOIKE 1982, Pl. 1, Fig. 5.

Trillus sp. C, HATTORI & YOSHIMURA 1982, Pl. 2, Fig. 3.
Trillus sp. WAKITA 1982, Pl. 7, Fig. 8–9. YAO 1984, Pl. 1, Fig. 22–23.

Remarks. – Under this name are included several morphotypes which may all cooccur in samples not younger than Zone A0. They share stout, coarse pore frames and a pronounced equatorial girdle.

Equally cooccurring in Zone A0 only are one or several morphotypes of *Zartus* PESSAGNO & BLOME 1980.

Genus *Tritrabs* BAUMGARTNER

Tritrabs BAUMGARTNER 1980, p. 293.
Type species: Paronaella (?) *casmaliaensis* PESSAGNO 1977a.

Tritrabs casmaliaensis (PESSAGNO)

Data 26, range 45, pob 117, rk 81, Pl. 10, Fig. 9

Paronaella (?) *casmaliaensis* PESSAGNO 1977a, p. 69, Pl. 1, Fig. 6–8.
Tritrabs casmaliaensis (PESSAGNO) BAUMGARTNER 1980, p. 293, Pl. 1, Fig. 10, Pl. 4, Fig. 11, Pl. 11, Fig. 10. KOCHER 1981, p. 105, Pl. 17, Fig. 18. ISHIDA 1983, Pl. 10, Fig. 6.
Tritrabs sp. A, ISHIDA 1983, Pl. 10, Fig. 8.
Tritrabs sp. cf. *T. casmaliaensis* (PESSAGNO) NISHIZONO & MURATA 1983, Pl. 3, Fig. 11.

Tritrabs ewingi (PESSAGNO)

Data 54, range 70, pob 113, rk 34, Pl. 10, Fig. 10

Paronaella (?) *ewingi* PESSAGNO 1971, p. 47, Pl. 19, Fig. 2–5. PESSAGNO 1977a, p. 70, Pl. 1, Fig. 14–15.
Tritrabs ewingi (PESSAGNO), BAUMGARTNER 1980, p. 293, Pl. 4, Fig. 5, 7, 17, 18. Not: KOCHER 1981, Pl. 17, Fig. 19.

Tritrabs exotica (PESSAGNO)

Data 27, range 37, pob 118, rk 35, Pl. 10, Fig. 11.

Paronaella (?) *exotica* PESSAGNO 1977a, p. 70, Pl. 1, Fig. 12–13.
Tritrabs exotica (PESSAGNO), BAUMGARTNER 1980, p. 294, Pl. 4, Fig. 16. ?KOCHER 1981, Pl. 17, Fig. 20.

Tritrabs hayi (PESSAGNO)

Data 28, range 20, pob 116, rk 101, Pl. 10, Fig. 12

Paronaella (?) *hayi* PESSAGNO 1977a, p. 70, Pl. 1, Fig. 16, Pl. 2, Fig. 1.
Tritrabs hayi (PESSAGNO), BAUMGARTNER 1980, p. 294, Pl. 4, Fig. 10, 21–22. KOCHER 1981, p. 106, Pl. 17, Fig. 21. ISHIDA 1983. Pl. 10, Fig. 7.

Tritrabs rhododactylus BAUMGARTNER

Data 27, range 26, pob 118, rk 35, Pl. 10, Fig. 13

Tritrabs rhododactylus BAUMGARTNER 1980, p. 294, Pl. 4, Fig. 12–15, Pl. 11, Fig. 15. ?ISHIDA 1983, Pl. 10. Fig. 10.
Tritrabs rhododactyla BAUMGARTNER, KOCHER 1981, p. 106, Pl. 17, Fig. 22.
Tritrabs sp. cf. *T. casmaliaensis* (PESSAGNO), SATO et al. 1982, Pl. 3, Fig. 5.

Genus *Unuma* ICHIKAWA & YAO

Unuma ICHIKAWA & YAO 1976, p. 111.
Type species: Unuma typicus ICHIKAWA & YAO 1976.

Unuma echinatus ICHIKAWA & YAO

Data 2, range 4, pob 231, rk –, Pl. 10, Fig. 14–15

Unuma echinatus ICHIKAWA & YAO 1976, p. 112, Pl. 1, Fig. 5–6, Pl. 2, Fig. 5–7. YAO et al. 1982, Pl. 3, Fig. 5. MIZUTANI & KOIKE 1982, Pl. 2, Fig. 6. WAKITA 1982, pl. 3, Fig. 11–12. MATSUOKA 1982, Pl. 1, Fig. 21. NISHIZONO et al. 1982, Pl. 2, Fig. 19 (not Fig. 20 as indicated in plate caption).
Unuma sp. cf. *U. echinatus* ICHIKAWA & YAO, KIDO et al. 1982, Pl. 3, Fig. 10.

Genus *Xitus* PESSAGNO

Xitus PESSAGNO 1976b, p. 55.
Type species: Xitus plenus PESSAGNO 1977b.

Xitus sp. cf. *X. spicularius* (ALIEV)

Data 106, range 98, pob 295, rk –, Pl. 10, Fig. 16–17

?*Dictyomitra spicularia* ALIEV, 1965, Pl. 6, Fig. 9.
Dictyomitra sp. cf. *D. spicularia* ALIEV, FOREMAN 1973, p. 264, Pl. 9, Fig. 8–9. NAKASEKO et al. 1979, Pl. 3, Fig. 5.
not: *Xitus spicularius* (ALIEV), PESSAGNO 1977a, p. 56, Pl. 9, Fig. 7, Pl. 10, Fig. 5.
Novixitus normalis WU HAO-RUO & LI HONG-SHENG 1982, Pl. 2, Fig. 5.
Xitus transversus WU HAO-RUO & LI HONG-SHENG 1982, Pl. 2, Fig. 7, not Fig. 8.
Novixitus sp. KANIE et al. 1981, Pl. 1, Fig. 17.
Xitus sp. OKAMURA & UTO 1982, Pl. 5. Fig. 4–5.
Xitus spicularius YAO 1984, Pl. 4, Fig. 17.

Remarks. – The studied form is broader than ALIEV's illustrations and tends to have a constricted last and second last segment.

6. Locality descriptions: topographic, litho- and biostratigraphic data of studied radiolarian localities

6.1 Introduction

In this chapter the data pertaining to the studied radiolarian localities are presented. The localities include primarily own collections and examination of material collected by the workers cited below. A very minor part of the data is taken from the literature. In order to have an idea of the areal extent of the study a geographic/paleogeographic overview is given below grouping the localities in terms of paleogeographic or Alpine tectonic units from west to east, starting in the Atlantic. This overview is followed by a listing of the localities in the same numerical order as they appear in the database (see appendix).

6.2 Geographic/paleogeographic overview of studied localities

Atlantic

Western Central Atlantic

Blake Bahama Basin: Loc. 30. DSDP Leg 76, Site 534.

Cat Gap: Loc. 39. DSDP Leg 1, Site 5.

Eastern Central Atlantic

Cape Verde Basin: Loc. 29. DSDP Leg 41, Site 367.

Western Mediterranean Tethys

Betic Cordilleras, Spain

Subbetic Zone: Loc. 45. Sierra de Ricote.

Central Alps, Switzerland, "northern" margin of Liguria–Piemont Ocean

Ultrahelvetic: Loc. 38. Veveyse de Châtel-St-Denis.

Southern and eastern Alps, "southern" margin of the Liguria–Piemont Ocean, Switzerland, Italy and Austria

Lombardy Basin and neighbouring zones:

Loc. 22. Sangiano, loc. 23. Cava Rusconi, loc. 20. Valmaggiore, loc. 17. Besozzo II, loc. 21. Besozzo I, loc. 25. Saltrio, loc. 24. Breggia Gorge, loc. 18. Monte Generoso.

Trento Plateau: Loc. 6. Serrada, loc. 44. Ceniga.

Northern Calcareous Alps: Loc. 36. Glasenbach Gorge, loc. 43. Trattberg.

Liguria and Central Apennines, Italy

Ligurid Ophiolite Units – oceanic Western Tethys:

Loc. 46. Monte Campannello, Elba, loc. 47. San Felo, Elba, loc. 48, Roccetta di Vara, Liguria.

Tuscan Zone: Loc. 27. Monte Cetona.

Umbrian Zone: Loc. 26. Fiume Bosso.

Sicily, Italy

Loc. 28. Santa Anna near Caltabellotta.

Eastern Mediterranean Tethys

Carpathians, Romania

Drocea Mountains: Loc. 15. Gomielor Valley.

Rarau Mountains: Loc. 12. Pojorita, loc. 14. Piatra Soimului.

Haghimas Mountains: Loc. 13. Laen Rosu.

Sirinia Zone: Loc. 16. Svinita, Banat, S-Carpathians.

Hellenides, Greece

Pindos Zone: Loc. 10., loc. 11. Marathos, Central Greece.

Pelagonian (s.l.) *Zone:*

Adhami Basal Sequence, Argolis Peninsula: Loc. 5. Kandhia, loc. 8. Theokafta.

Dhidhimi–Trapezona Basal Sequence, Argolis Peninsula: Loc. 3. Prosimni, loc. 4. Taxiarchis, loc. 1. Dhimaina, loc. 2. Angelokastron.

Northern Evvoia Basal Sequence: Loc. 51. Near Achladi.

Asklipion Unit, Argolis Peninsula: Loc. 7. Koliaki Chert.

Migdhalitsa Ophiolite Unit, Argolis Peninsula: Loc. 9. Rhadon.

Ophiolites of northern Evvoia: Loc. 49.

Middle Eastern Tethys

Central Oman Mountains, Oman

Hawasina Nappes

"Halfa Formation": Loc. 42. OM 191, 200, near Sur.

Al Aridh Formation: Loc. 50. Jebel Al Hasi.

Far Eastern Tethys, Japan

Mino Belt, Central Japan

Inuyama Area: Loc. 40. near Unuma. IN 7.

Pacific

Northwest Pacific

Abyssal plain southeast of Japan: Loc. 34. DSDP Leg 20, Site 195, loc. 35. DSDP Leg 20, Site 196.

Shatsky Rise: Loc. 32. DSDP Leg 32, Site 306, loc. 33. DSDP Leg. 32, Site 307.

Central Pacific

Magellan Rise: loc. 31. DSDP Leg 17, Site 167.

Western North America

Californian Coast Range

Point Sal Ophiolite: Loc. 37. Point Sal.

South Central America

Pacific coast of Costa Rica

Nicoya Ophiolite Complex: Loc. 41. Guatemala, Santa Rosa.

6.3 Listing of localities included in the database

Remarks. – Under *Locality data* the exact geographic location and access to the locality are described. Many of the following radiolarian localities have been described as such in earlier papers and this information is not repeated here. Instead, *References* are given including page numbers and original locality designations. The authorship of a locality is ascribed to the first publication presenting radiolarian data. The collector(s) of samples is (are) cited if differing from the author(s).

Under *Lithology* and *sample location* samples and measured sections are located with respect to lithology or the reader is referred to Plate 12. Where possible, earlier lithologic descriptions are referenced. *Biostratigraphy* summarizes or references biostratigraphic information excluding radiolarians.

Radiolarian data provides reference to earlier radiolarian data of the locality and gives the source(s) of the data presented in this paper. *Zonal assignment* gives sequential sample number, original sample number and assignment to Unitary Associations (U.A.) of sample for those localities not illustrated in Plate 12. For many of the new localities additional samples are under study and will be presented at a later date.

Items of the format are omitted, where the references are the same as the first mentioned. The two most used references are abbreviated: BAUMGARTNER et al. 1980 (= BG. et al. 1980) and KOCHER 1981 (= KO. 1981).

1. Dhimaina, Argolis Peninsula, Peloponnesus, Greece: 9.
   References. – DE WEVER in VRIELYNCK 1978, p. 39, loc. T-13. BG. et al. 1980, p. 64, loc. a. Coll. B. Vrielynck.
   Lithology and sample location. – VRIELYNCK 1978, BG. et al. 1980. See Plate 12.
   Biostratigraphy. – BG. et al. 1980, p. 28.
   Radiolarian data. – Not: DE WEVER in VRIELYNCK 1978. BG. et al. 1980, DE WEVER in KO. 1981 and own observations.

2. Angelokastron, Argolis Peninsula, Peloponnesus, Greece: 8.
References. – BAUMGARTNER 1980, p. 314–316, loc. A–B. BG. et al. 1980, p. 65, loc. C0–C2. See Plate 12.
Biostratigraphy. – As loc. 1.
Radiolarian data. – Own observations: BAUMGARTNER 1980, BG. et al. 1980. in KO. 1981.
3. Prosimni, Argolis Peninsula, Peloponnesus, Greece: 3.
References. – DE WEVER in VRIELYNCK 1978, p. 36, loc. T-11. BG. et al 1980, p. 66, loc. d. Coll. B. Vrielynck. See Plate 12.
Biostratigraphy. – As loc. 1.
Radiolarian data. – Not: DE WEVER in VRIELYNCK 1978. BG. et al. 1980, DE WEVER in KO. 1981, own examination of DE WEVER's residues.
4. Taxiarchis, Argolis Peninsula, Peloponnesus, Greece: 3.
References. – BAUMGARTNER 1980, p. 316, loc. C. BG. et al. 1980, p. 64, loc. b.
Radiolarian data. – Own data: BAUMGARTNER 1980, BG. et al. 1980, in KO. 1981.
5. Kandhia, Argolis Peninsula, Peloponnesus, Greece: 2.
References. – BG. et al 1980, p. 66, loc. e.
Radiolarian data. – Own data: BG. et al 1980, in KO. 1981.
6. Serrada, Trento Province, northern Italy: 1.
Locality data. – New locality. The section was measured along the Serrada–Terragnolo–Rovereto road in the first hairpin curve at the entrance of Serrada (opposite to the road sign "Serrada"), about 300 m uproad from the section measured by D. Bernoulli & C. Sturani (unpubl. manuscript).
Lithology and sample location. – The section is floored by cream colored massive oolitic grainstones (San Vigilio Oolites), overlain by about 3 m of pelagic, *Bositra*-rich pink limestones topped by a Fe–Mn-crust. This hardground is overlain by a 3.7 m thick radiolarian-rich unit consisting of 3–6 cm-bedded, pink cherty limestones with thin greenish marly partings. Four soft, pale green bentonite layers are found at 1.30, 1.40, 1.60 and 1.70 m above the hardground. The radiolarian sample cited here, POB 1403, is located 3.50 m above hardground or 1.80 m above the highest bentonite. This unit is overlain by 30 cm of flat bedded beige pelagic limestone, then about 10 m of nodular marly limestone and then white *Calpionella*-bearing nannofossil limestones.
Biostratigraphy. – BERNOULLI & STURANI (unpubl. manuscript) concluded, based on a regional survey of ammonites found in the enclosing units an early Kimmeridgian age for the cherty limestones.
Radiolarian data. – Own data, POB 1403 is assigned to U. A. 8–10, Zones B to C2.
7. Koliaki Chert, Argolis Peninsula, Peloponnesus, Greece: 4.
References. – BAUMGARTNER 1981, p. 70–72, 88, Pl. 6, section A. See Plate 12.
Lithology and sample location. – The samples included under this locality are a composite of the cited section A, Koliaki Chert, Theokafta Subunit and one sample (POB 325) from the Koliaki Chert of the Main Asklipion Unit. Sample 1, POB 1263 was collected a few m above the brecciated top of the Adhami Limestone (Upper Liassic–?Middle Jurassic) in red, thinbedded siliceous mudstones and chert. Locality: 1.5 km north of Asklipion, along dirt road linking Asklipion limestone quarries with new national road (under construction in 1980), 30 m from entrance to new road, on east side of dirt road (x: 06.83.13; y: 41.63.75, topographic map of Greece 1:50,000, sheet Ligourion). Sample 2, POB 1262 was collected 100 m south of sample 1, 30 m north of last outcrops of Asklipion limestone olistoliths (x: 06.83.16; y: 41.63.55). Sample 3, POB 325 was collected in the Main Asklipion Unit, within a sequence of red siliceous mudstones and chert of at least 100 m thickness in the little valley below Koutroumbeika, between Trakhia and Bafi (x: 06.91.20; y: 41.59.00). Sample 4, POB 1261 was collected from the chert matrix of a breccia with conodont-bearing Triassic Asklipion Limestone fragments (BAUMGARTNER 1981, Fig. 35a) which borders the main body of Asklipion Limestone, just below the contact with the tectonically overlying keratophyric tuffs at the little col of the forementioned dirt road (x: 06.83.18; y: 41.63.40).
Radiolarian data. – Own data.
8. Theokafta, Argolis Peninsula, Peloponnesus, Greece: 1.
References. – BAUMGARTNER 1980, p. 316, loc. D. BG. et al. 1980, p. 66, loc. f.
Lithology and location. – BAUMGARTNER 1981, Pl. 2, 3, section F. See Plate 12.
Radiolarian data. – Own data, see also in KO. 1981.
9. Rhadon, Argolis Peninsula, Peloponnesus, Greece: 1.
References. – BAUMGARTNER 1981, p. 97–98.
Lithology and sample location. – The main road Trakhia–Kranidhi cuts across the Migdhalitsa Ophiolite Unit and has a culmination approximately 3.5 km west of Radhon, where the road cut exposes nice pillow

lavas with ocean floor characteristics (BAUMGARTNER 1981, samples POB 300, 301, Fig. 48, 49). 100 m south of the pass the road cuts through small outcrops of pillows, pillow breccias and overlying red radiolarian chert, siliceous mudstones and siliceous limestones (redeposited). Sample POB 926 was collected about 10 m above pillow breccias. See Plate 12.
Radiolarian data. – Own data.

10. Pindos, Central Greece: 3.
References. – BG. et al. 1980, p. 66, loc. g, coll. M. Baltuck.
Lithology and sample location. – BALTUCK 1982. See Plate 12.
Radiolarian data. – Own data: BG. et al. 1980; in KO. 1981.
11. Marathos, Central Greece: 6.
References. – BG. et al. 1980, p. 66, loc. h, coll. N. Lyberis, preparation: E. A. Pessagno.
Lithology and sample location. – LYBERIS 1978.
Radiolarian data. – Own data based on observations in PESSAGNO's residues: BG. et al. 1980, in KO. 1981.
12. Pojorita, Rarau Mountains, Romania: 2.
13. Laen Rosu, Haghimas Mountains, Romania: 1.
14. Piatra Soimului, Rarau Mountains, Romania: 1.
15. Gomielor Valley, Drocea Mountains, Romania: 1.
References. – DUMITRICA 1970, p. 45 (for locality 12.) BG. et al. 1980, p. 67, loc. i, coll. P. Dumitrica.
Biostratigraphy. – Discussed in BG. et al. 1980.
Radiolarian data. – Own data based on examination of DUMITRICA's residues. KO. 1981.
16. Svinita, Banat, Danube section, southern Carpathians, Romania: 9.
References. – BG. et al. 1980, p. 67, loc. k, coll. P. Dumitrica.
Lithology and sample location. – AVRAM 1976. See Plate 12.
Biostratigraphy. – Presented in BG. et al. 1980.
Radiolarian data. – Own data based on examination of DUMITRICA's residues and personal comm. P. Dumitrica: BG. et al. 1980, in KO. 1981.
17. Besozzo II, Prov. Varese, Lombardy, northern Italy: 3.
References. – BG. et al. 1980, p. 67, loc. l, KO. 1981, p. 38, loc. l, coll. R. Kocher.
Radiolarian data. – KO. 1981.
Zonal assignments. – Sample 1: RK 95: U.A. 1–5; sample 2: RK 92: U.A. 5; sample 3: RK 101: U.A. 8.
18. Monte Generoso, Ticino, southern Switzerland: 3.
References. – KO. 1981, p. 40, loc. t.
Radiolarian data. – KO. 1981 and own revision of KOCHER's residues.
Zonal assignments. – Sample 1: BB 1: U.A. 3–5; sample 2: A-2: U.A. 7–8; sample 3: A-1: U.A. 8–10.
19 Torre de Busi, Prov. Como, Lombardy, northern Italy: 9.
References. – BG. et al. 1980, p. 67, loc. n. KO. 1981, p. 39, loc. n, coll. R. Kocher, Sample 1: POB 1341, own collection.
Lithology and sample location. – Sample 1: POB 1341 was collected 4.10 m below sharp base of basal radiolarites in top part of Sogno Formation, in cherty, *Bositra*-rich limestones. Locality: Along road Torre di Busi–Sogno, several 100 m below Colle di Sogno, where road cuts again down into the Sogno Formation. See Plate 12.
Radiolarian data. – BG. et al. 1980, KO. 1981 and own revision of KOCHER's residues. POB 1341: own data.
20. Valmaggiore, Brenta, Prov. Varese, northern Italy: 4.
References. – BG. et al. 1980, p. 67, loc. o. KO. 1981, p. 39, loc. o. Coll. R. Kocher.
Radiolarian data. – KO. 1981.
Zonal assignments. – Sample 1: RK 1095: U.A. 4–5; sample 2: RK 1088: U.A. 6–8; sample 3: RK 1086: U.A. 8; sample 4: RK 1085: U.A. 9–10.
21. Besozzo I, Besozzo Sup., Prov. Varese, northern Italy: 5.
References. – BG. et al. 1980, p. 67, loc. p. KO. 1981, p. 39, loc. p. Coll. R. Kocher.
Radiolarian data. – KO. 1981.
Zonal assignments. – Sample 1: RK 106: U.A. 8, sample 2: RK 109: U.A. 8, sample 3: RK 110: U.A. 8–9, sample 4: RK 111: U.A. 8–9, sample 5: RK 115: U.A. 9.
22. Sangiano, Prov. Varese, northern Italy: 7.
References. – BG. et al. 1980, p. 68, loc. q. KO. 1981, p. 39, loc. q. Coll. R. Kocher. See Plate 12.
Radiolarian data. – KO. 1981.
23. Cava Rusconi, Cittiglio, Prov. Varese, northern Italy: 1.

References. – BG. et al. 1980, p. 68, loc. s. POB 1205. See Plate 12.
Radiolarian data. – Own data: BG. et al. 1980, and KO. 1981.

24. Breggia Gorge, Ticino, southern Switzerland: 24.
References. – BG. et al. 1980, p. 68, loc. r. KO. 1981, p. 40, loc. r. Coll. R. Kocher. Topmost sample 24: POB 1330: own collection.
Lithology and sample location. – KO. 1981 includes the entire outcrop back to the waterfall in the lower Breggia gorge with the basal radiolarites. The lower 20 m of his section (samples B 61 and B 100) are, however, marly and contain abundant *Bositra*. We include this part of the section with the Marne a Posidonia, an equivalent of the Sogno Formation. This is confirmed by the revised radiolarian zonation. Sample 24: POB 1330 was collected in the quarry of Maiolica Lombarda, 10.50 m above the top of the Rosso ad Aptici (steeply dipping bedding plane at entrance of narrow gorge), at the base of the second slump unit. See Plate 12.
Radiolarian data. – BG. et al. 1980, KO. 1981, this paper: reexamination of KOCHER's residues.
25. Saltrio, Prov. Varese, northern Italy: 12.
References. – BG. et al. 1980, p. 67, loc. m. KO. 1981, p. 38, loc. m. Coll. R. Kocher. See Plate 12.
Radiolarian data. – BG. et al. 1980, KO. 1981, this paper: reexamination of KOCHER's residues.
26. Fiume Bosso, near Pianello, Umbria, Central Italy: 17.
References. – KO. 1981, p. 41, loc. n (samples RK). Samples W79: Coll. E. L. Winterer. Sample POB BO230.8: own collection. See Plate 12. Earlier lithologic and biostratigraphic work includes CENTAMORE et al. 1971, MICARELLI et al. 1977 (Maiolica), MCBRIDE & FOLK 1979 (Radiolarites), BERNOULLI et al. 1979.
Radiolarian data. – KO. 1981, revision of KOCHER's residues and own data.
27. Monte Cetona, Tuscany, central Italy: 9.
References. – KO. 1981, p. 41, loc. v.
Lithology and sample location. – BERNOULLI et al. 1979.
Radiolarian data. – KO. 1981.
Zonal assignment. – Sample 1: RK 1038: U.A. 3–5, sample 2: RK 1039: U.A. 4–5, samples 3–8: RK 1043, 1045, 1046, 1047, 1048, 1049: U.A. 4, sample 9: RK 1051: U.A. 4–8.
28. Santa Anna, near Caltabellotta, Sicily, Italy: 4.
References. – RIEDEL & SANFILIPPO 1974, p. 774, WRE 67–74. BG. 1980, p. 68, loc. t1–t2. Samples 1–3: S1–S4: Coll. B. McGill.
Radiolarian data. – RIEDEL & SANFILIPPO 1974, BG. et al. 1980, KO. 1981 and own revisions of S1–S4 and WRE 67–74.
Zonal assignment. – Samples 1–4: S1–S4, WRE 67–74: U.A. 8.
29. DSDP Leg 41, Site 367, Cape Verde Basin, East Atlantic: 7.
References. – FOREMAN 1978, p. 739. See Plate 12.
Biostratigraphy. – Summarized in BG et al. 1980.
Radiolarian data. – FOREMAN 1978, BG. et al. 1980 and own revisions of FOREMAN's residues.
30. DSDP Leg 76, Site 534, Blake Bahama Basin, West Atlantic: 28.
References. – BAUMGARTNER 1983 (lithology and zonal assignment of samples).
Lithology and sample location. – See Plate 12.
Biostratigraphy. – HABIB & DRUGG 1983 (dinoflagellates), ROTH et al. 1983 and ROTH 1983 (nannofossils), GRADSTEIN 1983 (foraminifers), REMANE 1983 (calpionellids).
Radiolarian data. – Own data.
31. DSDP Leg 17, Site 167, Magellan Rise, Central Pacific: 6.
References. – RIEDEL & SANFILIPPO 1974, p. 773.
Radiolarian data. – RIEDEL & SANFILIPPO 1974, BG. et al. 1980, in KO. 1981, own observations in RIEDEL & SANFILIPPO's residues.
Zonal assignment. – Sample 1: 167-94-2-40: U.A. 10, sample 2: 167-93-2-22: U.A. 11, sample 3: 167-88-CC: U.A. 13-14, samples 4–6: 167-76-2-65, 167-74-2-65, 167-69-3-36: U.A. 14.
32, 33. DSDP Leg 32, Shatsky Rise, Northwest Pacific, Site 306: 7, Site 307: 6.
References. – FOREMAN 1975, p. 579.
Radiolarian data. – FOREMAN 1975, BG. et al. 1980, and own revision of FOREMAN's residues.
Zonal assignment. – Loc. 32, samples 1–4: 306-42-1-116, -42-1-103, -41-CC, -40-1-119: U.A. 11; samples 5–7: 306-21-CC, -16-CC, -14-CC: U.A. 11-14. Loc. 33, samples 1–2: 307-12-1-120, -10-1-119: U.A. 11–14; samples 3–6: 307-9-1-80, -8-CC, -7-1-75, -6-CC: U.A. 14.
34, 35. DSDP Leg 20, Southeast Japan Abyssal Plain, Northwest Pacific, Site 195: 4, Site 196: 3.

References. – FOREMAN 1973, p. 249.
Radiolarian data. – FOREMAN 1973, BG. et al. 1980, in KO. 1981, and own revision of FOREMAN'S residues.
Zonal assigment. – Loc. 34, samples 1–4: 195-B2-CC, -B1-CC, -5-CB, 4-CC, 3-CC: U.A. 14. Loc. 35, sample 1: 196-5-CC: U.A. 11, samples 2–3: 196-4-1-P3, 196-3-1: U.A. 14.

36. Glasenbach Gorge, near Salzburg, Austria: 2.
References. – KO. 1981, p. 42.
Lithology. – BERNOULLI & JENKYNS 1970.

37. Point Sal, Santa Barbara County, California, USA: 3.
References. – RIEDEL & SANFILIPPO 1974, p. 773: Pt. Sal, coll. C.A. Hopson and D.E. Karig, WR 73-4. PESSAGNO 1977, p. 102: samples NSF 900F–NSF 911.5 and own collection.
Radiolarian data. – Idem and own revisions of the above residues and raw samples.
Zonal assignment. – Sample 1: NSF 907: U.A. 7, sample 2: NSF 908: U.A. 7–8, sample 3: NSF 909: U.A. 7–8, Zone B.

38. Veveyse de Châtel-St-Denis, Cant. Vaud, Switzerland: 1.
Locality data. – New radiolarian locality. Earlier work includes CHAROLLAIS & RIGASSI 1961 (calpionellids, nannoconids and other microfossils), BUSNARDO et al. (in preparation, ammonite high resolution stratigraphy). Locality: 2.5 km southeast of the town Châtel-St-Denis, gorge of Veveyse river several 100 m upriver from motorway and road bridges in river bed.
Lithology and sample location. – The sequence spans the Kimmeridgian to Barremian with siliceous limestones, marly, partly turbiditic limestones and marls. The studied sample comes from the middle part of the section, and corresponds to bed 67-4 of BUSNARDO et al. (in preparation). Lithology: dark gray, mottled, clayey limestone, with abundant burrows in which radiolarians and other microfossil fragments are preserved as pyrite. Samples from other Lower Cretaceous levels are in preparation.
Biostratigraphy. – Bed 67-4 belongs to the *Callidiscus* Ammonite-zone of the terminal Valanginian (R. Busnardo, personal communication).
Radiolarian data. – Own data.
Zonal assignment. – Sample POB 1134: U.A. 14, Zone E2.

39. DSDP Leg 1, Site 5, Blake Bahama Basin, West Atlantic: 1.
References. – PESSAGNO 1971. Sample 5A-7-1-top.
Radiolarian data. – Own examination of PESSAGNO'S residue.
Zonal assignment. – U.A. 11, Zone D.

40. In 7, near Unuma, Inuyama area, central Japan: 1.
References. – YAO 1972, ICHIKAWA & YAO 1976, YAO 1979, YAO et al. 1980, YAO et al. 1982.
Radiolarian data. – Idem and own observations in residues prepared from a raw sample provided by A. Yao.
Zonal assignment. – Sample IN 7: U.A. 0, Zone A1.

41. Guatemala, near Santa Rosa, Nicoya Peninsula, Costa Rica: 1.
References. – New radiolarian locality. See KUYPERS 1979, Fig. 21. Locality: Lower part of Quebrada Triste, near Guatemala, 2.75 km east of Santa Rosa. Coll. E. Kuypers.
Lithology and sample location. – Dark brown Mn-rich chert sampled a few meters above contact with basalt.
Radiolarian data. – Own data, many other samples from Nicoya Peninsula are in preparation.
Zonal assignment. – Sample 2-18-1-79: U.A. 3–5, Zones A1–A2.

42. OM 191, OM 200, near Sur, Hawasina Complex, southeastern Oman: 2.
References. – TIPPIT 1981. Coll. R.G. Coleman.
Radiolarian data. – Own observations in TIPPIT'S residues.
Zonal assignment. – Sample 1: OM 191: U.A. 11, Zone D, sample 2: OM 200: U.A. 14, Zone E2.

43. Trattberg, Salzburg, Austria: 2.
Locality data. – New radiolarian locality. For geology: STEIGER 1981. Localities: Along road Hallein–Trattberg. Sample 1: above "Gletscherschliff" Natural Monument, sample 2: Quarry below Trattbergalp. Coll. P.O. B. and T. Steiger.
Lithology. – Light gray, clayey nannofossil limestones with gray replacement chert nodules and layers, "Aptychenschichten".
Radiolarian data. – Own data.
Zonal assignment. – Sample 1: U.A. 11, sample 2: U.A. 12, Zone D.

*44. Ceniga, near Arco, Trento, northern Italy: 4.

Locality data. – New radiolarian locality. Section described by FOGELGESANG 1975 (p. 29). From Arco follow small road on right side of Sarca river about 3.5 km northwards to little hill south of Ceniga. Outcrops in road cut and on slope of hill west of road. Coll. P.O. Baumgartner and E. L. Winterer.

Lithology and sample location. – See Plate 12. FOGELGESANG (1975) mentions 3 m of siliceous limestones and 1.5 m of Aptychus limestones. We observed 9 m of thinbedded pink siliceous limestones with lenses of red to reddishbrown replacement chert. The bentonites observed in other sections of the Trento swell (see loc. 6) have not been found – probably due to poor outcrops in the middle part of section.

Biostratigraphy. – FOGELGESANG (1975, p. 24) reports a late Oxfordian chaetetid species from a comparable section at Colme di Vignola, recovered from the Aptychus limestones, and concludes from his regional study on a late Oxfordian–early Kimmeridgian age for the siliceous limestones.

Radiolarian data. – Own data.

*45. Sierra de Ricote, Subbetic, Prov. Murcia, Spain: 3.

Locality data. – New radiolarian locality. Lithologic description: SEYFRIED 1978. Several detailed sections measured and collected after indications of H. Seyfried: Bathonian cherty limestones, green calcareous radiolarites, red siliceous marls and Late Jurassic–Early Cretaceous cherty limestones were collected 7 km southwest of the town Albaran, on the hill immediately west and southwest of Casas de Vite (Mapa Militar 26–36 "Mula" in the vicinity of x: 6-357, y: 42-247). An additional section of the red siliceous marls and overlying marly cherty limestone was collected in creek 400 m south of Cortijos de la Cuesta Alta (x: 6-379, y: 42-255):

Lithology and sample location. – See Plate 12.

Biostratigraphy. – Biostratigraphy given in Plate 12 after SEYFRIED 1978 (Fig. 20). SEYFRIED (1981, p. 342) mentions the recovery of *Ataxioceras* sp., basal Kimmeridgian, from the transition between the red siliceous radiolarian marls and the overlying white cherty limestones (see Pl. 12), recovered between the studied sections (x: 6-372.5, y: 42-254; H. Seyfried, pers. comm.).

Radiolarian data. – The presently studied samples are indicated on Plate 12, other samples from the entire section are in preparation.

*46. South of Monte Campannello near Volterraio, Elba, Italy: 2.

Locality data. – New radiolarian locality. Lithologic description by BARRETT 1979, 1982. The base of the section collected lies 300 m west of Le Panche, the col of the Rio nell'Elba–Magazzini road, at about 300 m altitude. Variolitic pillow lavas are overlain by Mn–Fe crusts and dark red ferrugineous siliceous mudstones. The lowest sample with determinable radiolarians was collected in the first cm-thick white radiolarian sands 80 cm above basement. Coll. P.O.B. and E. L. Winterer. See Plate 12.

Radiolarian data. – Presently studied samples are indicated on Plate 12. A sequence of samples, including the top of the radiolarites near Nisporto are in preparation.

*47. S. Felo–Namia, Elba, Italy: 1.

Locality data. – New radiolarian locality. Previous illustration of section in FOLK & MCBRIDE 1978 and BERNOULLI et al. 1979. The extremely reduced section of radiolarites is exposed in a small quarry located on the Porto Azzurro–Rio Marina road between the localities Namia and San Felo, on the north side of the road. Along the road on the east side of the quarry the base of the section is exposed: Sheared but fresh serpentinite is overlain by about 8 m of weathered serpentinite including large boulder-like bodies of fresh serpentinite. The following 16 m thickness to the entrance of the quarry include very altered serpentinite penetrated by abundant calcite veins and in the upper 10 m dikes of red to pink siliceous muddy sediment. On the east wall of quarry this is overlain along a very irregular contact by an ophiolite breccia containing basalt fragments of dominantly 2–10 cm size but also entire pillows, basaltic sandstone-clasts and rare gabbro fragments embedded in a shaly matrix of siliceous mudstone and overlain by mainly thinbedded siliceous mudstone. The sample POB 1615 is the lowest sample containing determinable radiolarians, 1.50 m above basalt breccia. Coll. P.O.B. and E. L. Winterer.

Radiolarian data. – See Plate 12; more samples in preparation.

*48. Rocchetta di Vara, Liguria, Italy: 2.

Locality data. – New radiolarian locality. Earlier descriptions of the locality include ABBATE 1969 and FOLK & MCBRIDE 1978. The section is along the Brugnato–Roccetta di Vara road, the overturned base of the section is exposed east of the first river bridge and on a gravel road (our lowest sample POB 1661) just west of the big radiolarite quarry (sample POB 1662) on the south side of the road. The lowest sample with determinable radiolarians (POB 1661) was collected 1.40 m above the graded top of the underlying gabbro breccia and 60 cm below a graded gabbroic sandstone poorly exposed on the east side of gravel road. POB 1662 was sampled 29.20 m above the gabbro breccia in the southeast corner of quarry. Coll P.O.B. and E. L. Winterer.

Radiolarian data. – See Plate 12, more samples of whole section in preparation.

*49. C 31, northern Evvoia, eastern Greece: 1.

Sample data. – Residue provided by J. Simantov, Geneva, described as interpillow sediment of the Pelagonian (s.l.) ophiolites of northern Evvoia.

Radiolarian data. – Own data: C31: U.A. 4–5, Zones A1–A2.

*50. DB 6214, Al Aridh Formation, Jebel al Hasi, Hawasina Nappes, Central Oman: 1.

References. – BERNOULLI & WEISSERT [manuscript]. The sample comes from bedded lime-free radiolarites and shales in the type area of the Al Aridh Formation (GLENNIE et al. 1974). Coll. D. Bernoulli.

Radiolarian data. – Own data: DB 6214: U.A. 0, Zone A0.

*51. DB 4575, near Achladi, northern Evvoia, eastern Greece: 1.

Reference. – BAUMGARTNER & BERNOULLI 1976.

Radiolarian data. – Own data: DB 4575: U.A. 7–8, Zone B (not early Neocomian as supposed in the reference).

Acknowledgments

This paper is the result of eight years of collaboration and exchange with numerous fellow radiolarian workers which is gratefully acknowledged. Years of joint field work with Daniel Bernoulli in Greece and the collaboration with Jerry Winterer aboard *Glomar Challenger* and in the field in Italy have encouraged my research and inspired the conception of the paleooceanographic interpretations in this paper. The biochronologic concept has profited from continuous exchange with Jean Guex and Eric Davaud who computed the Unitary Associations.

The elaboration of the Middle Jurassic–Early Cretaceous radiolarian database greatly profited from the contribution of raw samples and radiolarian residues and the opportunity to study preparations from a number of colleagues: M. Baltuck, D. Bernoulli, C.D. Blome, P. De Wever, P. Dumitrica, the late Helen Foreman, F. Gradstein, R. Kocher, J. Ogg, E.A. Pessagno, W.R. Riedel, A. Sanfilippo, J. Simantov, P.R. Tippit, E.L. Winterer and A. Yao.

I am very thankful to Claudia R. Mora Rojas who assisted in all stages of this work, especially in compiling the database and references and in working out the measurements of new species. The SEM-Laboratory at the University of Basel, directed by R. Guggenheim produced much of the SEM-illustrations, which is gratefully acknowledged.

I owe thanks to the Deep Sea Drilling Project inviting me to participate in shorebased analysis of the Leg 76 samples for radiolarian paleontology. Field work in Greece in the years 1973–80 was funded by the Swiss National Science Foundation, projects no. 2.1620.74 and no. 2.762-0.77. Field work in Italy in 1983 was financed by the US National Science Foundation, grant no. EAR82-18477.

Patrick De Wever and Akira Yao kindly reviewed the systematic part and Daniel Bernoulli critically read the geologic part of this paper. I greatly appreciate their helpful corrections and criticism.

REFERENCES

ABBATE, E. (1969): Geologia delle Cinque Terre e dell'entroterra di Levanto (Liguria orientale). – Mem. Soc. geol. ital. *8*, 923–1014.

ADACHI, M. (1982): Some considerations on the *Mirifusus baileyi* Assemblage in the Mino terrain, central Japan. – Proc. first jap. radiolarian Symp.: Spec. Vol. News Osaka Micropaleont. *5*, 211–226.

AGTERBERG, F.P., & Nel, L.D. (1982a): Algorithms for the ranking and scaling of stratigraphic events. – Computers Geosci. *8*/1, 69–90.

— (1982b): Algorithms for the scaling of stratigraphic events. – Computers Geosci. *8*/2, 163–189.

AITA, Y. (1982): Jurassic radiolarian biostratigraphy in Irazuyama district, Kochi Prefecture, Japan – A preliminary report. – Proc. first jap. radiolarian Symp.: Spec. Vol. News Osaka Micropaleont. *5*, 255–270.

ALIEV, K.S. (1965): Radiolarians of the Lower Cretaceous deposits of northeastern Azerbaidzhan and their stratigraphic significance. – Izdat. Akad. Azerbaidz. SSR, Baku, p. 3–124.

AOKI, T. (1982): Upper Jurassic to Lower Cretaceous radiolarians from the Tsukimiyama and Tei Mélanges of the Northern Shimanto Belt in Kochi Prefecture, Shikoku. – Proc. first jap. radiolarian Symp.: Spec. Vol. News Osaka Micropaleont. *5*, 339–352.

AOKI, T., & TASHIRO, M. (1982): Stratigraphic study of the Shanto Belt (Cretaceous Kamigumi Formation equivalent to the Doganaro Formation) near Kamigumi, Kagami-cho, Kagami-gun, Kochi Prefecture. – Sci. Rep. Kochi Univ. *31*, 1–24.

AVRAM, E. (1976): La succession des dépôts Tithoniques supérieurs et Crétacés inférieurs de la région de Svinita (Banat). – Dări Seamă Şedint. Inst. Geol. Geofiz. *62*/4 (1974–5), 53–71.

AZÉMA, J. (1977): Etude géologique des zones externes des Cordillères Bétiques aux confins des provinces d'Alicante et de Murcie (Espagne). – Thesis Univ. Paris VI, 1–395.

BALTUCK, M. (1982): Provenance and distribution of Tethyan pelagic and hemipelagic siliceous sediments, Pindos Mountains, Greece. – Sediment. Geol. *31*, 63–88.

BARRETT, T.J. (1979): Origin of bedded cherts overlying ophiolitic rocks in the Italian North Apennines, and implication of the ophiolitic-pelagic sediment sequences for seafloor processes. – Unpublished Ph. D. Thesis. Oxford Univ., Oxford, England, p. 1–419.

— (1982): Stratigraphy and sedimentology of Jurassic bedded chert overlying ophiolites in the North Apennines, Italy. – Sedimentology *29*, 353–373.

BAUMGARTNER, P.O. (1980): Late Jurassic Hagiastridae and Patulibracchiidae (Radiolaria) from the Argolis Peninsula (Peloponnesus, Greece). – Micropaleontology *26*/3, 274–322.

— (1981): Jurassic sedimentary evolution and nappe emplacement in the Argolis Peninsula (Peloponnesus, Greece). – Unpubl. Doctoral Thesis, Basel Univ. Basel, Switzerland, p. 1–137.

— (1983): Summary of Middle Jurassic–Early Cretaceous radiolarian biostratigraphy of Site 534 (Blake-Bahama Basin) and correlation to Tethyan sections. – Init. Rep. Deep Sea Drill. Proj. *76*, 569–571.

— (1984): Comparison of Unitary Associations and probabilistic ranking and scaling as applied to Mesozoic Radiolaria. – Computers Geosci. *10*/1, 167–183.

BAUMGARTNER, P.O., & BERNOULLI, D. (1976): Stratigraphy and radiolarian fauna in a Late Jurassic–Early Cretaceous section near Achladi (Evvoia, Eastern Greece). – Eclogae geol. Helv. *69*/3, 601–626.

BAUMGARTNER, P.O., BJØRKLUND, K.R., CAULET, J-P., DE WEVER, P., KELLOGG, D., LABRACHERIE, M., NAKASEKO, K., NISHIMURA, A., SCHAAF, A., SCHMIDT-EFFING, R., & YAO, A. (1981): EURORAD II, 1980 – Second European meeting of radiolarian paleontologists: Current research on Cenozoic and Mesozoic radiolarians. – Eclogae geol. Helv. *74*/3, 1027–1061.

BAUMGARTNER, P.O., DE WEVER, P., & KOCHER, R. (1980): Correlation of Tethyan Late Jurassic–Early Cretaceous radiolarian events. – Cah. Micropaléont. *2*, 23–72.

BERNOULLI, D. (1964): Zur Geologie des Monte Generoso (Lombardische Alpen). – Beitr. geol. Karte Schweiz [N.F.] *118*, 1–134.

— (1972): North Atlantic and Mediterranean Mesozoic facies: a comparison. – Init. Rep. Deep Sea Drill. Proj. *11*, 801–871.

BERNOULLI, D., & JENKYNS, H.C. (1970): A Jurassic basin: The Glasenbach Gorge, Salzburg, Austria. – Verh. geol. Bundesanst. (Wien) *1970*/4, 504–531.

BERNOULLI, D., KÄLIN, O., & PATACCA, E. (1979): A sunken continental margin of the Mesozoic Tethys: The Northern and Central Apennines. – Symp. "Sédimentation jurassique W-européen". Publ. spéc. Assoc. Sédimentol. franç. *1*, 197–210.

BERNOULLI, D., & WEISSERT, H. (unpubl. manuscr.): Preliminary notes on the stratigraphy of the upper Hawasina Nappes and of the Oman Exotics.

BIGAZZI, C., BONADONNA, F.P., FERRARA, G., & INNOCENTI, F. (1973): Fission track ages of zircons and apatites from Northern Apennine ophiolites. – Fortschr. Mineral. (Kristallogr. Petrogr.) *50*, 51–53.

BLOME, C.D. (in press): Middle Jurassic (Callovian) Radiolaria from southern Alaska and eastern Oregon. – Micropaleontology.

BOSELLINI, A., & WINTERER, E.L. (1975): Pelagic limestone and radiolarite of the Tethyan Mesozoic: A genetic model. – Geology *3*/5, 279–282.

BUSNARDO, R., CHAROLLAIS, J., & WEIDMANN, M. (in prep.): Le Crétacé inférieur de la Vevèyse de Châtel-St-Denis (Fribourg): stratigraphie et ammonites.

CENTAMORE, E., CHIOCCHINI, M., DEIANA, G., MICARELLI, A., & PIERUCCINI, U. (1971): Contributo alla conoscenza del Giurassico dell'Appennino Umbro-Marchigiano. – Studi geol. Camerti *1*, 7–89.

CHAROLLAIS, J., & RIGASSI, D. (1961): Répartition de quelques microfossiles dans le Jurassique supérieur et le Crétacé de Châtel-St-Denis. – Arch. Sci. (Genève) *14*/2, 265–279.

CITA, M.B. (1964): Ricerche micropaleontologiche e stratigrafiche sui sedimenti pelagici del Giurassico superiore e del Cretaceo inferiore nella catena del Monte Baldo. – Riv. ital. Paleont. (Stratigr.) Mem. *10*, 1–182.

CITA, M.B., & PASQUARÈ, G. (1959): Osservazioni micropaleontologiche sul Cretaceo delle Dolomiti. – Riv. ital. Paleont. (Stratigr.) *65*/4, 385–442.

DAVAUD, E., & GUEX, J. (1978): Traitement analytique manuel et algorithmique de problèmes complexes de corrélations biochronologiques. – Eclogae geol. Helv. *71*/3, 581–610.

DE WEVER, P. (1981): Hagiastridae, Patulibracchiidae et Spongodiscidae (Radiolaires Polycystines) du Lias de Turquie. – Rev. Micropaléont. *24*/1, 27–50.

DE WEVER, P., & CABY, R. (1981): Datation de la base des schistes lustrés postophiolitiques par des radiolaires (Oxfordien supérieur–Kimméridgien moyen) dans les Alpes Cottiennes (Saint Veran, France). – C.R. Acad. Sci. (Paris) *292* (Sér. 2), 467–472.

DE WEVER, P., RIEDEL, W.R., BAUMGARTNER P., DUMITRICA, P., BJORKLUND, K., CAULET, J.P., DROBNE, K., GRANLUND, A., KOCHER, R., & SCHAAF, A. (1979): Recherches actuelles sur les radiolaires en Europe. – Ann. Soc. géol. Nord *98*, 205–222.

DE WEVER, P., & THIÉBAULT, F. (1981): Les radiolaires d'âge Jurassique supérieur à Crétacé supérieur dans les radiolarites du Pinde–Olonos (près qu'île de Koroni; Péloponnèse méridional, Grèce). – Geobios *14*/5, 577–609.

DONOFRIO, D.A., & MOSTLER, H. (1978): Zur Verbreitung der Saturnalidae (Radiolaria) im Mesozoikum der Nördlichen Kalkalpen und Südalpen. – Geol.-paläont. Mitt. Innsbruck *7*/5, 1–55.

DUMITRICA, P. (1970): Cryptocephalic and cryptothoracic Nassellaria in some Mesozoic deposits of Romania. – Rev. roumaine Géol. Géophys. Géogr. (sér. Géol.) *14*/1, 45–124.

— (1978): Family Eptingiidae, n. fam., extinct Nassellaria (Radiolaria) with sagittal ring. – Dări Seamă Şedint. Inst. Geol. Geofiz. *64*/3 (1976–7), 27–38.

DUNIKOWSKI, E. v. (1882): Die Spongien, Radiolarien und Foraminiferen der unterliassischen Schichten vom Schafberg bei Salzburg. – Denkschr. (kais.) Akad. Wiss. Wien, math.-natw. Kl. *45*, 163–194.

EHRENBERG, C.G. (1844): Einige vorläufige Resultate seiner Untersuchungen der ihm von der Südpolreise des Capitain Ross, so wie von den Herren Schayer und Darwin zugekommenen Materialien über das Verhalten des kleinsten Lebens in den Oceanen und den grössten bisher zugänglichen Tiefen des Weltmeeres. – Ber. k. preuss. Akad. Wiss. Berlin *1844*, 182–207.

FLEURY, J.J. (1974): Précisions sur la série de la Nappe du Pinde; l'âge des «radiolarites» (Dogger–Malm) et des «Marnes rouges à radiolaires – Premier Flysch» (Eocrétacé–Sénonien basal) (Grèce). – C.R. Acad. Sci. (Paris) *278*, 201–204.

— (1975): Le «Premier Flysch du Pinde» témoin de l'ensemble des événements orogéniques mésozoïques antécrétacé supérieur ayant affecté les Hellénides internes (Grèce). – C.R. Acad. Sci. (Paris) *281*, 1459–1461.

FOGELGESANG, J.F. (1975): Géologie du Monte Baldo septentrional (Prov. de Trente, Italie) et aspects géochimiques de la sédimentation pélagique tridentine et lombarde au Jurassique. – Unpubl. thesis 3e cycle. Univ. Pierre et Marie Curie, Paris, France, p. 1–178.

FOLK, R.L., & MCBRIDE, E.F. (1978): Radiolarites and their relation to subjacent "ocean crust" in Liguria, Italy. – J. sediment. Petrol. *48*/4, 1069–1102.

FOREMAN, H. (1968): Upper Maestrichtian Radiolaria of California. – Spec. Pap. Paleontol. Assoc. London *3*, 1–82.

— (1971): Cretaceous Radiolaria, Leg 7 DSDP. – Init. Rep Deep Sea Drill. Proj. *7*, 1673–1693.

— (1973): Radiolaria from DSDP Leg 20. – Init. Rep. Deep Sea Drill. Proj. *20*, 249–305.

— (1975): Radiolaria from the North Pacific, DSDP, Leg 32. – Init. Rep. Deep Sea Brill. Proj. *32*, 579–676.

— (1978): Mesozoic Radiolaria in the Atlantic Ocean off the northwest coast of Africa. – Init. Rep. Deep Sea Drill. Proj. *41*, 739–761.

GLENNIE, K.W., BOEUF, M.G.A., HUGHES-CLARKE, M.W., MOODY-STUART, M., PILAAR, W.F.H., & REINHARDT, B.M. (1974): Geology of the Oman Mountains, – Verh. k. nederl. geol. mijnbouwkd. Genoot. *31*, 1–423.

GRADSTEIN, F.M. (1983): Paleoecology and stratigraphy of Jurassic abyssal Foraminifera in the Blake-Bahama Basin, Deep Sea Drilling Project Site 534. – Init. Rep. Deep Sea Drill. Proj. *76*, 537–560.

GUEX, J. (1977): Une nouvelle méthode d'analyse biochronologique. – Bull. Soc. vaud. Sci. nat. *73*, 309–322.

— (1979): Terminologie et méthodes de la biostratigraphie moderne: commentaires critiques et propositions. – Bull. Soc. vaud. Sci. nat. no. *74*/3, 169–216.

— (1984): Estimations numériques de la qualité de l'enregistrement fossile des espèces. – Bull. Soc. vaud. Sci. nat. *77*, 79–89.

GUEX, J., & DAVAUD, E. (1982): Recherche automatique des associations unitaires en biochronologie. – Bull. Soc. vaud. Sci. nat. *76*, 53–69.

— (1984): The Unitary Associations method. – Computer Geosci. *10*/1, 69–96.

GYGI, R., & MARCHAND, D. (1982): Les faunes de Cardioceratinae (Ammonoidea) du Callovien terminal et de l'Oxfordien inférieur et moyen (Jurassique) de la Suisse septentrionale: Stratigraphie, paléoécologie, taxonomie préliminaire. – Geobios *15*/4, 517–571.

HABIB, D., & DRUGG, W.S. (1983): Dinoflagellate age of Middle Jurassic–Early Cretaceous sediments in the Blake-Bahama Basin. – Init. Rep. Deep Sea Drill. Proj. *76*, 623–638.

HAECKEL, E. (1881): Entwurf eines Radiolarien-Systems auf Grund von Studien der Challenger-Radiolarien. – Z. Natw. med. naturw. Ges. Jena *15* [N.F.] *8*/3, 418–472.

— (1887): Report of the Radiolaria collected by H.M.S. Challenger during the years 1873–76. – Rep. Sci. Result. Voyage H.M.S. Challenger, Zool. *18*/1–2, 1–1803.

HATTORI, I., & YOSHIMURA, M. (1982): Lithofacies distribution and radiolarian fossils in the Nanjo area in Fukui Prefecture, Central Japan. – Proc. first jap. radiolarian Symp.: Spec. Vol. News Osaka Micropaleont. *5*, 103–116.

HEITZER, I. (1930): Die Radiolarienfauna der mitteljurassischen Kieselmergel im Sonnwendgebirge. – Jb. geol. Bundesanst. Wien *80*, 381–406.

HINDE, G.J. (1900): Descriptions of fossil Radiolaria from the rocks of Central Borneo. In: MOLENGRAAFF, G.A. (Ed.): Borneo-Expeditie: Geol. Verkenningstochten in Central Borneo (1893–94) (p. 1–51). – E.L. Brill, Leiden, H. Gerlings, Amsterdam.

HOJNOS, R. (1916): Beiträge zur Kenntnis der ungarischen fossilen Radiolarien. – Földt. Közl. *46*, 340–364.

ICHIKAWA, K., & YAO, A. (1976): Two new genera of Mesozoic cyrtoid radiolarians from Japan. In: TAKAYANAGI, Y., & SAITO, T. (Ed.): Progress in micropaleontology (p. 110–117). – Micropaleontology Press, New York.

IMOTO, N., TAMAKI, A., TANABE, T., & ISHIGA, H. (1982): Deposit at the Yumiyama Mine in the Tamba District, Southwest Japan. – Proc. first jap. radiolarian Symp.: Spec. Vol. News Osaka Micropaleont. *5*, 227–236.

ISHIDA, H. (1983): Stratigraphy and radiolarian assemblages of the Triassic and Jurassic siliceous sedimentary rocks in Konose Valley, Tokushima Prefecture, Southwest Japan. – J. Sci. Univ. Tokushima *16*, 111–141.

JENKYNS, H.C., & WINTERER, E.L: (1982): Paleooceanography of Mesozoic ribbon radiolarites. – Earth and planet. Sci. Lett. *60*, 351–375.

JONES, D.L., COX, A., CONEY, P., & BECK, M. (1982): The growth of Western North America. – Sci. American *247*/5, 70–84.

KÄLIN, O., PATACCA, E., & RENZ, O. (1979): Jurassic pelagic deposits from southeastern Tuscany; aspects of sedimentation and new biostratigraphic data. – Eclogae geol. Helv. *72*/3, 715–762.

KÄLIN, O., & TRÜMPY, D.M. (1977): Sedimentation und Paläotektonik in den westlichen Südalpen: Zur triassisch-jurassischen Geschichte des Monte Nudo-Beckens. – Eclogae geol. Helv. *70*/2, 295–350.

KANIE, Y., TAKETANI, Y., SAKAI, A., & MIYATA, Y. (1981): Lower Cretaceous deposits beneath the Yezo group in the Urakawa area, Hokkaido. – J. geol. Soc. Japan *87*, 527–533.

KASHIMA, N. (1983): Geology of the aqueduct tunnel No. 6 at "the Chichibu Belt", western Shikoku. – Ehime Chigaku (Geology of Ehime), Mem. Vol. Prof. Miyahisa, p. 169–176.

KIDO, S., KAWAGUCHI, I., ADACHI, M., & MIZUTANI, S. (1982): On the *Dictyomitrella* (?) *kamoensis–Pantanellium foveatum* Assemblage in the Mino area, central Japan. – Proc. first jap. radiolarian Symp.: Spec. Vol. News Osaka Micropaleont. *5*, 195–210.

KOCHER, R.N. (1981): Biochronostratigraphische Untersuchungen oberjurassischer radiolarienführender Gesteine insbesondere der Südalpen. – Mitt. geol. Inst. ETH u. Univ. Zürich. [N.F.] *234*, 1–184.

KOJIMA, S. (1982): Some Jurassic, Triassic and Permian radiolarians from the eastern part of Takayama City, central Japan. – Proc. first jap. radiolarian Symp.: Spec. Vol. News Osaka Micropaleont. *5*, 81–92.

KOZUR, H., & MOSTLER, H. (1979): Beiträge zur Erforschung der mesozoischen Radiolarien. Teil III: Die Oberfamilien Actinommacea HAECKEL 1862, emend., Artiscacea HAECKEL 1882, Multiarcusellacea nov. der Spumellaria und triassische Nassellaria. – Geol.-paläont. Mitt. Innsbruck *9*/1–2, 1–132.

KUYPERS, E. (1979): La geología del Complejo Ofiolítico de Nicoya, Costa Rica. – Informe Sem. Inst. Geogr. Nac. Julio–Diciembre, p. 15–76.

LANCELOT, Y., SEIBOLD, E., DEAN, W.E., JANSA, L.F., EREMEEV, V., GARDNER, J., CEPEK, P., KRASHENINNIKOV, V.A., PFLAUMANN, U., JOHNSON, D., RANKIN, J.G., & TRABANT, P. (1978): Site 367: Cape Verde Basin (Site Chapter). – Init. Rep. Deep Sea Drill. Proj. *41*, 163–232.

LAUBSCHER, H., & BERNOULLI, D. (1977): Mediterranean and Tethys. In: NAIRN, A.E.M., KANES, W.H., & STEHLI, F.G. (Ed.): The Eastern Mediterranean (p. 1–28). The ocean basins and margins 4A. – Plenum Publishing Corp, New York.

LEJEUNE, M. (1936): Sur un moyen d'isoler les microfossiles inclus dans les silex. – C.R. Acad. Sci. (Paris) *203*/7, 435–437.

LOZNYAK, P.Y. (1969): Radiolarii nizhnemelovykh otlozhenii Ukrainskikh Karpat. (Radiolaria of the Lower Cretaceous sediments of the Ukrainian Carpathians.) In: VYALOV, O.C. (Ed.): Iskopaemye i Sovremennye Radiolarii (Fossil and Recent Radiolaria) (p. 29–40). – L'vov. geol. O-vo., L'vov. Univ.

LYBERIS, N. (1978): Etude géologique de la partie méridionale des montagnes d'Agrapha (Euritanie, Grèce). – Thesis 3e cycle, Paris, p. 1–145.

MATSUOKA, A. (1981): Middle to Late Jurassic radiolarian assemblage in the Sakawa area of the southern subbelt of the Chichibu Belt. – Proc. Kansai Branch, geol. Soc. Japan *90*, 3–4.

— (1982): Jurassic two-segmented Nassellarians (Radiolaria) from Shikoku, Japan. – J. Geosci. Osaka City Univ. *25*/5, 71–86.

— (1983): Middle and Late Jurassic radiolarian biostratigraphy in the Sakawa and adjacent areas, Shikoku, Southwest Japan. – J. Geosci. Osaka City Univ. *26*/1, 1–48.

MATSUYAMA, H., KUMON, F., & NAKAJO, K. (1982): Cretaceous radiolarian fossils from the Hidakagawa Group in the Shimanto Belt, Kii Peninsula, Southwest Japan. – Proc. first jap. radiolarian Symp.: Spec. Vol. News Osaka Micropaleont. *5*, 371–382.

MCBRIDE, E.F., & FOLK, R.L. (1979): Features and origin of Italian Jurassic radiolarites deposited on continental crust. – J. sediment. Petrol. *49*/3, 837–868.

MICARELLI, A., POTETTI, M., & CHIOCCHINI, M. (1977): Ricerche microbiostratigrafiche sulla Maiolica della regione Umbro-Marchigiana. – Stud. geol. Camerti *3*, 57–86.

MIZUTANI, S. (1981): A Jurassic formation in the Hida-Kanayama area, Central Japan. – Bull. Mizunami Fossil Mus. *8*, 147–190.

MIZUTANI, S., & KOIKE, T. (1982): Radiolarians in the Jurassic siliceous shale and in the Triassic bedded chert of Unuma, Kagamigahara City, Gifu Prefecture, Central Japan. – Proc. first jap. radiolarian Symp.: Spec. Vol. News Osaka Micropaleont. *5*, 117–134.

MIZUTANI, S., NISHIYAMA, H., & ITO, T. (1982): Radiolarian biostratigraphic study of the Shimanto Group in the Nanto-Nansei Area, Mie Prefecture, Kii Peninsula, Central Japan. – J. Earth Sci. Nagoya Univ. *30*, 31–107.

MOORE, T.C. (1973): Radiolaria from Leg 17 of the Deep Sea Drilling Project. – Init. Rep. Deep Sea Drill. Proj. *17*, 797–869.

MURATA, M., OHISHI, A., NISHIZONO, Y., SATO, T., & TAKEHARA, T. (1982): Late Mesozoic radiolarian fauna from the Sakaguchi Formation. – Proc. first jap. radiolarian Symp.: Spec. Vol. News Osaka Micropaleont. *5*, 327–337.

MUZAVOR, S.N.X. (1977): Die Oberjurassische Radiolarienfauna von Oberaudorf am Inn. – Diss. Fachber. Geowiss. Ludwig-Maximilians-Univ., München, p. 1–163.

NAKASEKO, K. (Ed., 1982): Proceedings of the first japanese radiolarian symposium. – Spec. Vol. News Osaka Micropaleont. *5*, 1–485.

NAKASEKO, K., & NISHIMURA, A. (1981): Upper Jurassic and Cretaceous Radiolaria from the Shimanto Group in Southwest Japan. – Sci. Rep. College gen. Educ. Osaka Univ. *30*/2, 133–203.

NAKASEKO, K., NISHIMURA, A., & SUGANO, K. (1979): Cretaceous Radiolaria in the Shimanto Belt, Japan. – Spec. Vol. News Osaka Micropaleont. *2*, 1–49.

NEVIANI, A. (1900): Supplemento alla fauna a radiolari delle rocce mesozoiche del Bolognese. – Boll. Soc. geol. ital. *19*, 645–671.

NISHIZONO, Y., & MURATA, M. (1983): Preliminary studies on the sedimentary facies and radiolarian biostratigraphy of Paleozoic and Mesozoic sediments, exposed along the mid-stream of the Kuma River, Kyushu, Japan. – Kumamoto J. Sci. Geol. *12*, 1–40.

NISHIZONO, Y., OHISHI, A., SATO, T., & MURATA, M. (1982): Radiolarian fauna from the Paleozoic and Mesozoic Formations distributed along the mid-stream of Kuma River, Kyushu, Japan. – Proc. first jap. radiolarian Symp.: Spec. Vol. News Osaka Micropaleont. *5*, 311–326.

OKAMURA, M. (1980): Radiolarian fossils from the northern Shimanto Belt (Cretaceous) in Kochi Prefecture, Shikoku. – Geology and Paleontology of the Shimanto Belt (p. 153–178): Rinya-Kosekai.

OKAMURA, M., & UTO, H. (1982): Notes on stratigraphic distributions of radiolarians from the Lower Cretaceous sequence of chert in the Yokonami Melange of Shimanto Belt, Kochi Prefecture, Shikoku. – Res. Rep. Kochi Univ, Nat. Sci. *31*, 87–94.

OWADA, K., & SAKA, Y. (1982): Preliminary note on the Paleozoic and Mesozoic formations in the Chichibu Belt, Okutama District, Kwanto Mountains, Japan. – Proc. first jap. radiolarian Symp.: Spec. Vol. News Osaka Micropaleont. *5*, 67–80.

OZVOLDOVA, L. (1975): Upper Jurassic radiolarians from the Kysuca Series in the Klippen Belt. – Zap. Karpaty, Ser. Paleont. *1*, 73–86.

— (1979): Radiolarian assemblage of radiolarian cherts at Podbiel locality (Slovakia). – Čas. Miner. Geol. *24*/3, 249–266.

PARONA, C. F. (1890): Radiolarie nei noduli selciosi del calcare giurese di Cittiglio presso Laveno. – Boll. Soc. geol. ital. *9*, 1–167.

PESSAGNO, E. A., Jr. (1969): Mesozoic planktonic Foraminifera and Radiolaria. – Init. Rep. Deep Sea Drill. Proj. *1*, 607–621.

— (1971): Jurassic and Cretaceous Hagiastridae from the Blake-Bahama Basin (Site 5A, JOIDES Leg 1) and the Great Valley Sequence, California Coast Ranges. – Bull. amer. Paleont. *60*/264, 1–83.

— (1972): Cretaceous Radiolaria. Part I: The Phaseliformidae, new family, and other Spongodiscacea from the Upper Cretaceous portion of the Great Valley Sequence. Part II: Pseudoaulophacidae RIEDEL from the Cretaceous of California and the Blake-Bahama Basin (JOIDES Leg 1). – Bull. amer. Paleont. *61*/270, 269–314.

— (1973): Upper Cretaceous Spumellaria from the Great Valley Sequence, California Coast Ranges. – Bull. amer. Paleont. *63*/276, 49–102.

— (1976): Radiolarian zonation and stratigraphy of the Upper Cretaceous portion of the Great Valley Sequence, California Coast Ranges. – Spec. Publ. Micropaleont. *2*, 1–95; Micropaleontology Press, New York.

— (1977a): Upper Jurassic Radiolaria and radiolarian biostratigraphy of the California Coast Ranges. – Micropaleontology *23*/1, 56–113.

— (1977b): Lower Cretaceous radiolarian biostratigraphy of the Great Valley Sequence and Franciscan Complex, California Coast Ranges. – Spec. Publ. Cushman Found. foram. Res. *15*, 1–87.

PESSAGNO, E. A., Jr., & BLOME, C. D. (1980): Upper Triassic and Jurassic Pantanellinae from California, Oregon and British Columbia. – Micropaleontology *26*/3, 225–273.

— (1982): Bizarre Nassellariina (Radiolaria) from the Middle and Upper Jurassic of North America. – Micropaleontology *28*/3, 289–318.

PESSAGNO, E. A., Jr., & NEWPORT, R. L. (1972): A technique for extracting Radiolaria from radiolarian cherts. – Micropaleontology *18*/2, 231–234.

PESSAGNO, E. A., Jr., & POISSON, A. (1981): Lower Jurassic Radiolaria from the Gümüslü Allochthon of Southwestern Turkey (Taurides Occidentales). – Bull. miner. Res. Explor. Inst. Turkey *92*, 47–69.

PESSAGNO, E. A., Jr., & WHALEN, P. A. (1982): Lower and Middle Jurassic Radiolaria (multicyrtid Nassellariina) from California, east-central Oregon and the Queen Charlotte Islands, B.C. – Micropaleontology *28*/2, 111–169.

PRINCIPI, P. (1909): Contributo allo studio dei radiolari miocenici italiani. – Boll. Soc. geol. ital. *28*/1, 1–22.

REMANE, J. (1983): Calpionellids and the Jurassic/Cretaceous boundary at Deep Sea Drilling Project Site 534, Western North Atlantic Ocean. – Init. Rep. Deep Sea Drill. Proj. *76*, 561–568.

RENZ, G. W. (1974): Radiolaria from Leg 27 of the Deep Sea Drilling Project. – Init. Rep. Deep Sea Drill. Proj. *27*, 769–841.

RENZ, O. (1978): Aptychi (Ammonoidea) from the Late Jurassic and the Early Cretaceous of the eastern Atlantic, DSDP Site 367. – Init. Rep. Deep Sea Drill. Proj. *41*, 499–513.

RIEDEL, W. R., & SANFILIPPO, A. (1974): Radiolaria from the southern Indian Ocean, DSDP Leg 26. – Init. Rep. Deep Sea Drill. Proj. *26*, 771–814.

ROTH, P. H. (1983): Jurassic and Lower Cretaceous calcareous nannofossils in the western North Atlantlic (Site 534): Biostratigraphy, preservation and some observations on biogeography and paleooceanography. – Init. Rep. Deep Sea Drill. Proj. *76*, 587–622.

ROTH, P. H., MEDD, A. W., & WATKINS, D. K. (1983): Jurassic calcareous nannofossil zonation, an overview with new evidence from Deep Sea Drilling Project Site 534. – Init. Rep. Deep Sea Drill. Proj. *76*, 573–580.

RÜST, D. (1885): Beiträge zur Kenntnis der fossilen Radiolarien aus Gesteinen des Jura. – Palaeontographica *31* (3, 7), 269–322.

— (1898): Neue Beiträge zur Kenntnis der fossilen Radiolarien aus Gesteinen des Jura und der Kreide. – Palaeontographica *45*, 1–67.

SACHS, H. M., & FAIRBANKS HASSON, P. (1979): Comparison of species vs. character description for very high resolution biostratigraphy using cannartid radiolarians. – J. Paleont. *53*/5, 1112–1120.

SAKA, Y. (1983): Preliminary note on the Jurassic strata in the Chichibu Terrane, western Shima Peninsula, Southwest Japan. – Gakujutsu Kenkyu, School of Educ., Waseda Univ. *32*, 29–34.

SASHIDA, K., IGO, HISAHARU, IGO, HISAYOSHI, H., TAKIZAWA, S., HISADA, K., SHIBATA, T., TSUKADA, K., & NISHIMURA, H. (1982): On the Jurassic radiolarian assemblages in the Kanto district. – Proc. first jap. radiolarian Symp.: Spec. Vol. News Osaka Micropaleont. *5*, 51–66.

SATO, T., NISHIZONO, Y., & MURATA, M. (1982): Paleozoic and Mesozoic radiolarian faunas from the Shakumasan Formation. – Proc. first jap. radiolarian Symp.: Spec. Vol. News Osaka Micropaleont. *5*, 301–310.

SCHAAF, A. (1981): Late Early Cretaceous Radiolaria from Deep Sea Drilling Project Leg 62. – Init. Rep. Deep Sea Drill. Proj. *62*, 419–470.

SEYFRIED, H. (1978): Der subbetische Jura von Murcia (Südost-Spanien). – Geol. Jb. (B) *29*, 1–201.

— (1981): Ensayo sobre el significado paleogeográfico de los sedimentos del Jurásico de las Cordilleras Béticas Orientales. – Cuad. Geol. (iberica) *10*, 317–348.

SHERIDAN, R.E., GRADSTEIN, F.M., BARNARD, L.A., BLIEFNICK, D.M., HABIB, D., JENDEN, P.D., KAGAMI, H., KEENAN, E., KOSTECKI, J., KVENVOLDEN, K.A., MOULLADE, M., OGG, J., ROBERTSON, A.H.F., ROTH, P., SHIPLEY, T.H., BOWDLER, J.L., COTILLON, P.H., HALLEY, R.B., KINOSHITA, H., PATTON, J.W., PISCIOTTO, K.A., PREMOLI-SILVA, I., TESTARMATA, M.M., & WATKINS, D.K. (1983): Site 534: Blake-Bahama Basin (Site Chapter). – Init. Rep. Deep Sea Drill. Proj. *76*, 141–340.

SQUINABOL, S. (1903): Le Radiolarie dei noduli selciosi nella Scaglia degli Euganei: Contribuzione 1. – Riv. ital. Paleont. *9*, 105–150.

— (1904): Radiolarie cretacee degli Euganei. – Atti Mem. r. Accad. Sci. Lett. Arti Padova [n.s.] *20*, 171–244.

— (1914): Contributo alla conoscenza dei Radiolarii fossili del Veneto. Appendice – Di un genere dei Radiolari caratteristico del Secondario. – Mem. Ist. Geol. Univ. Padova *2*, 249–306.

STEIGER, T. (1981): Kalkturbidite im Oberjura der Nördlichen Kalkalpen (Barmsteinkalke, Salzburg, Österreich). – Facies *4*, 215–348.

STURANI, C. (1964): La successione delle faune ad ammoniti nelle formazioni mediogiurassiche delle Prealpi venete occidentali. – Mem. Ist. Geol. Mineral. Univ. Padova *24*, 1–63.

TAKETANI, Y. (1982): Cretaceous Radiolaria from Hokkaido. – Proc. first jap. radiolarian Symp.: Spec. Vol. News Osaka Micropaleont. *5*, 361–370.

TAN SIN HOK (1927): Over de samenstelling en het onstan van krijt- en mergel-gesteenten van de Molukken. In: BROUWER, H.A. (Ed.): Geologische onderzoekingen in den oostelijken Oost-Indischen Archipel. – 5. Jb. Mijnwezen nederl. (Oost-)Indië *55* (1926), pt.3, 5–156.

THIÉBAULT, F., DE WEVER, P., FLEURY, J.J., & BASSOULET, J.B. (1981): Précisions sur la série stratigraphique de la nappe du Pinde de la presqu'île de Koroni (Péloponnèse méridional – Grèce): l'âge des radiolarites (Dogger–Crétacé supérieur). – Ann. Soc. géol. Nord, Lille *100*, 91–105.

TIPPIT, P.R. (1981): Radiolarian biostratigraphy of the Hawasina Complex. – Thesis, Progr. Geosci. Univ. Texas, Dallas *200*, 201–339.

VAIL, P.R., MITCHUM, R.M., Jr., & THOMPSON, S. III (1977): Global cycles of relative changes of sea level. In: PAYTON, C.E. (Ed.): Seismic stratigraphy – applications to hydrocarbon exploration (p.83–97). – Mem. amer. Ass. Petroleum Geol. *26*.

VINASSA DE REGNY, P.E. (1900): I Radiolari delle ftaniti titoniane di Carpena (Spezia). – Palaeontographia ital. *4* (1898), 217–238.

VRIELYNCK, B. (1978): Données nouvelles sur les zones internes du Péloponnèse. Grèce. Les massifs à l'est de la plaine d'Argos. – Thesis 3e cycle, Univ. Sci. Tech. Lille, p.1–115.

WAKITA, K. (1982): Jurassic radiolarians from Kuzuryu-ko–Gujo-hachiman area. – Proc. first jap. radiolarian Symp.: Spec. Vol. News Osaka Micropaleont. *5*, 153–172.

WAKITA, K., & OKAMURA, M. (1982): Mesozoic sedimentary rocks containing allochthonous blocks, Gujo-hachiman, Gifu Prefecture, Central Japan. – Bull. geol. Surv. Japan *33*, 161–185.

WINTERER, E.L., & BOSELLINI, A. (1981): Subsidence and sedimentation on Jurassic passive continental margin, Southern Alps, Italy. – Bull. amer. Assoc. Petroleum Geol. *65*, 394–421.

WISNIOWSKI, T. (1889): Beitrag zur Kenntnis der Mikrofauna aus den oberjurassischen Feuersteinknollen der Umgebung von Krakau. – Jb. k.k. geol. Reichsanst. *38*/4 (1888), 657–702.

WU HAO-RUO & LI HONG-SHENG (1982): Radiolaria from the olistostrome of the Zongzhuo Formation, Gyangze, Southern Xizang (Tibet). – Acta palaeont. sinica *21*/1, 64–74.

YAO, A. (1972): Radiolarian fauna from the Mino Belt in the northern part of the Inuyama area, Central Japan. Part I: Spongosaturnalids. – J. Geosci. Osaka City Univ. *15*, 21–64.

— (1979): Radiolarian fauna from the Mino Belt in the northern part of the Inuyama area, Central Japan. Part II: Nassellaria 1. – J. Geosci. Osaka City Univ. *22*, 21–72.

— (1983): Late Paleozoic and Mesozoic radiolarians from Southwest Japan. In: IJIMA, A., HEIN, J.R., & SIEVER, R. (Ed.): Siliceous deposits in the Pacific Region (p. 361–376). – Elsevier, Amsterdam.

— (1984): Subdivision of the Mesozoic Complex in Kii-Yura area, Southwest Japan and its bearing on the Mesozoic basin development in the southern Chichibu Terrane. – J. Geosci. Osaka City Univ. *27*, Art. 2, 41–103.

YAO, A., MATSUDA, T., & ISOZAKI, Y. (1980): Triassic and Jurassic radiolarians from the Inuyama area, central Japan. – J. Geosci. Osaka City Univ. *23*, 135–154.

YAO, A., & MATSUOKA, A. (1981): *Unuma echinatus* Assemblage in the Inuyama area of the Mino Belt. – Proc. Kansai Branch, Geol. Soc. Japan *90*, 5–6.

YAO, A., MATSUOKA, A., & NAKATANI, T. (1982): Triassic and Jurassic radiolarian assemblages in Southwest Japan. – Proc. first jap. radiolarian Symp.: Spec. Vol. News Osaka Micropaleont. *5*, 27–43.

APPENDIX: DATABASE

DATABASE OF MIDDLE JURASSIC - EARLY CRETACEOUS RADIOLARIA

Includes first and final occurrences of 111 species in 51 localities (245 samples). Version 30A, updated: May 1984.

* - new data not used in computation of Unitary Associations of this paper.
** - revised data as used for computation of U. A. in January 1984, presented in this paper.

Format: Number. Name of locality: Number of sequential samples.
Species number. Lowest sample - highest sample.
Total number of species at locality.

1. Dhimaina, Argolis Peninsula, Peloponnesus, Greece: 9.

17.7-9, 18.3-3, 20.3-3, 21.1-8, 25.1-1, 27.1-3, 28.3-3, 29.3-6, 32.3-5, 40.1-3, 46.2-2, 49.1-1, 56.2-9, 57.1-1, 60.3-3, 62.3-3, 64.1-4, 72.3-3, 73.3-3, 75.1-8, 76.2-9, 77.3-3, 78.2-9, 79.2-3, 84.1-5, 88.2-3. 26.

2. Angelokastron, Argolis Peninsula, Peloponnesus, Greece: 8.

16.2-2, 18.2-7, 19.2-4, 20.4-6, 23.1-8, 24.2-8, 25.1-6, 26.2-8, 27.1-6, 28.2-4, 29.1-8, 30.4-4, 31.2-4, 32.1-8, 33.2-8, 35.2-4, 36.1-8, 37.1-6, 38.2-6, 40.2-8, 43.2-5, 44.2-4, 45.1-4, 46.2-6, 47.1-8, 48.1-5, 49.2-4, 50.1-4, 51.2-5, 52.2-4, 53.2-6, 54.2-4, 55.2-4, 56.2-8, 57.1-8, 58.2-4, 59.2-4, 60.1-8, 62.2-8, 64.2-8, 65.1-4, 66.4-4, 67.2-4, 70.2-4, 72.2-4, 73.2-5, 74.2-4, 75.1-8, 76.1-6, 77.4-8, 78.5-5, 79.2-5, 84.2-4, 86.2-4, 88.6-6, 89.1-5, 90.2-8, 91.1-1. 58.

3. Prosimni, Argolis Peninsula, Peloponnesus, Greece: 3.

21.1-3, 25.1-1, 29.1-1, 32.3-3, 33.1-1, 37.1-1, 40.1-3, 49.3-3, 56,1-3, 60.1-3, 62.1-1, 64.1-3, 71.1-3, 73.3-3, 75.1-3, 76.1-3, 77.1-1, 84.1-1, 86.1-1. 19.

4. Taxiarchis, Argolis Peninsula, Peloponnesus, Greece: 3.

18.2-3, 20.2-2, 21.3-3, 23.1-3, 24.1-2, 25.3-3, 27.1-3, 29.1-3, 30.1-3, 32.1-3, 33.1-3, 36.2-2, 37.1-3, 40.1-1, 43.1-1, 44.1-1, 47.1-3, 49.1-1, 50.1-3, 53.1-1, 54.3-3, 56.1-3, 60.1-3, 62.1-3, 64.1-1, 71.3-3, 72.1-1, 73.1-2, 75.1-3, 76.1-3, 77.1-2, 85.3-3, 88.1-1, 89.1-1, 90.1-2. 35.

5. Kandhia, Argolis Peninsula, Peloponnesus, Greece: 2.

18.1-2, 21.1-2, 23.1-2, 24.2-2, 25.1-2, 26.2-2, 27.2-2, 29.1-2, 30.1-2, 32.1-2, 33.1-2, 40.1-2, 44.1-1, 46.1-1, 54.2-2, 56.1-2,

57.2-2, 59.1-1, 60.1-2, 62.1-2, 64.1-2, 69.1-2, 71.1-1, 72.2-2, 73.1-2, 75.1-2, 76.1-2, 86.1-1, 90.1-2. 29.

6. Serrada, Trento Province, Northern Italy: 1.

24.1-1, 25.1-1, 30.1-1, 33.1-1, 55.1-1, 60.1-1, 64.1-1, 69.1-1, 75.1-1, 76.1-1, 84.1-1. 11.

7. Kolıaki, Argolis Peninsula, Peloponnesus, Greece: 4.

1.1-2, 2.1-2, 3.1-1, 4.1-2, 6.3-3, 9.2-3, 11.3-3, 12.3-3, 14.3-3, 15.3-3, 17.1-4, 18.3-3, 20.3-3, 21.3-4, 23.2-4, 24.1-3, 27.4-4, 28.4-4, 29.4-4, 32.3-3, 34.2-3, 35.3-3, 36.2-4, 37.3-3, 39.3-3, 40.4-4, 43.3-3, 47.3-3, 49.3-3, 56.3-4, 57.3-4, 60.4-4, 61.3-3, 63.1-1, 71.4-4, 75.4-4, 76.4-4, 88.3-3, 90.3-3. 39.

8. Theokafta, Argolis Peninsula, Peloponnesus, Greece: 1.

20.1-1, 23.1-1, 24.1-1, 25.1-1, 27.1-1, 28.1-1, 29.1-1, 30.1-1, 31.1-1, 33.1-1, 36.1-1, 38.1-1, 40.1-1, 43.1-1, 54.1-1, 56.1-1, 57.1-1, 58.1-1, 59.1-1, 60.1-1, 62.1-1, 65.1-1, 67.1-1, 68.1-1, 69.1-1, 71.1-1, 73.1-1, 75.1-1, 76.1-1, 78.1-1, 79.1-1, 80.1-1, 81.1-1, 86.1-1, 88.1-1, 90.1-1. 36.

9. Rhadon, Argolis Peninsula, Peloponnesus, Greece: 1.

21.1-1, 27.1-1, 29.1-1, 37.1-1, 47.1-1, 88.1-1, 91.1-1. 7.

10. Pindos, Central Greece: 3.

25.2-2, 27.2-2, 32.2-2, 36.2-2, 37.2-2, 40.2-2, 44.2-2, 45.2-2, 48.1-1, 54.1-1, 56.1-1, 60.2-2, 62.2-2, 64.2-2, 76.2-2, 86.2-2, 97.3-3, 106.3-3, 109.3-3. 19.

11. Marathos, Central Greece: 6.

23.2-2, 32.3-4, 33.2-3, 47.1-1, 53.1-1, 62.3-4, 68.4-4, 69.2-3, 76.2-4, 99.5-5, 106.5-6, 109.5-6. 12.

12. Pojorita, Rarau Mountains, Roumania: 2.

18.2-2, 19.2-2, 21.1-2, 23.1-2, 24.2-2, 25.2-2, 26.2-2, 27.2-2, 28.2-2, 29.2-2, 32.2-2, 33.2-2, 35.2-2, 36.1-2, 37.2-2, 43.1-2, 45.2-2, 47.2-2, 54.1-1, 56.2-2, 57.1-2, 60.2-2, 62.2-2, 64.2-2, 67.1-1, 75.2-2, 76.2-2, 91.2-2. 28.

13. Laen Rosu, Haghimas Mountains, Roumania: 1.

16.1-1, 23.1-1, 29.1-1, 36.1-1, 37.1-1, 46.1-1, 47.1-1, 88.1-1, 91.1-1. 9.

14. Piatra Soimului, Rarau Mountains, Roumania: 1.

21.1-1, 23.1-1, 27.1-1, 29.1-1, 32.1-1, 35.1-1, 36.1-1, 43.1-1, 44.1-1, 56.1-1, 60.1-1, 62.1-1, 75.1-1, 76.1-1, 85.1-1, 87.1-1,

91.1-1. 17.

15. Gomielor Valley, Drocea Mountains, Roumania: 1

8.1-1, 35.1-1, 36.1-1, 37.1-1, 57.1-1. 5.

16. Svinita, Banat, Danube section, S-Carpathians, Roumania: 9.

29.1-1, 54.1-9, 59.5-5, 68.1-2, 69.1-1, 71.1-1, 75.1-7, 79.1-8, 80.1-8, 81.1-8, 82.1-8, 83.1-8, 84.3-8, 94.1-8, 95.1-8, 97.2-7, 98.2-8, 99.1-9, 100.2-8, 101.1-3, 102.1-1, 103.1-8, 104.2-8, 105.1-8, 106.2-7, 108.2-8, 109.2-8, 110.6-8, 111.6-8. 29.

17. Besozzo II, Prov. Varese, Lombardy, Northern Italy: 3.

6.2-2, 7.2-2, 11.2-2, 12.2-2, 13.1-2, 17.2-2, 18.2-2, 19.2-2, 21.3-3, 24.1-3, 26.3-3, 27.2-3, 29.3-3, 31.2-2, 32.3-3, 33.2-3, 36.2-3, 37.2-2, 41.2-2, 42.2-2, 44.3-3, 47.3-3, 50.3-3, 55.2-2, 56.3-3, 57.3-3, 60.3-3, 61.2-2, 64.3-3, 65.2-2, 67.3-3, 69.3-3, 71.3-3, 73.2-2, 74.2-2, 76.3-3, 84.3-3, 85.2-2, 86.1-1. 39.

18. Monte Generoso, Ticino, Southern Switzerland: 3.

6.1-1, 15.1-1, 17.2-2, 18.2-2, 23.2-2, 24.2-2, 25.2-2, 26.2-2, 27.2-2, 31.2-2, 36.2-3, 37.1-2, 38.2-2, 40.2-2, 43.2-2, 48.2-2, 49.2-2, 50.2-2, 51.2-2, 53.2-2, 55.2-2, 56.2-3, 57.2-2, 60.2-2, 64.2-2, 65.2-2, 69.3-3, 71.2-3, 72.2-2, 73.2-2, 74.2-2, 75.2-2, 76.2-2, 85.2-2, 88.2-2. 35.

19. Torre de Busi, Prov. Como, Lombardy, Northern Italy: 9.

1.1-1, 2.1-1, 3.1-1, 4.1-1, 5.1-1, 6.4-5, 7.3-6, 10.1-1, 11.2-2, 12.1-6, 15.3-5, 16.6-6, 17.1-6, 21.7-7, 23.1-6, 24.1-6, 29.1-1, 32.6-8, 33.3-4, 35.4-6, 36.1-1, 37.6-6, 38.4-4, 40.1-1, 43.2-6, 46.4-6, 47.2-2, 50.6-6, 51.7-7, 56.7-7, 60.7-7, 61.2-9, 63.1-1, 66.1-2, 69.7-9, 70.7-7, 71.7-7, 72.7-9, 75.9-9, 76.7-7, 77.7-7, 82.9-9, 86.2-6, 88.4-9. 44.

20. Valmaggiore, Brenta, Prov. Varese, Northern Italy: 4.

6.1-1, 7.1-1, 11.1-1, 15.1-1, 17.1-1, 19.1-1, 22.1-1, 23.1-1, 24.1-3, 26.3-3, 27.2-2, 29.2-2, 33.3-3, 37.1-1, 40.2-2, 41.3-3, 47.1-1, 49.2-2, 55.2-2, 60.3-3, 61.1-1, 62.3-4, 64.2-3, 67.2-2, 69.3-4, 74.1-1, 75.4-4, 82.4-4, 84.3-4, 85.3-3, 88.2-2. 31.

21. Besozzo I, Besozzo Sup., Prov. Varese, Northern Italy: 5.

17.1-1, 19.1-1, 21.1-5, 22.5-5, 25.2-2, 27.2-5, 30.5-5, 32.4-5, 33.1-5, 41.1-2, 44.2-2, 48.4-5, 49.1-1, 50.1-1, 51.5-5, 52.5-5, 53.2-5, 54.2-5, 55.1-5, 56.1-5, 60.1-5, 61.4-4, 64.4-5, 69.1-5, 71.1-5, 72.1-1, 73.1-1, 74.1-1, 75.1-5, 76.2-5, 77.5-5, 82.5-5, 84.1-1. 33.

22. Sangiano, Prov. Varese, Northern Italy: 7.

7.1-3, 8.1-3, 11.1-3, 12.1-3, 13.2-3, 15.3-4, 16.1-1, 17.1-4,

18.1-4, 19.1-3, 20.1-3, 21.1-7, 23.1-4, 24.1-4, 25.4-4, 26.1-5,
27.2-4, 29.2-4, 31.4-4, 32.4-7, 33.2-7, 35.4-4, 36.1-4, 37.1-4,
41.6-6, 42.2-3, 43.2-2, 44.4-4, 46.4-4, 47.1-4, 48.4-4, 50.1-2,
54.2-4, 55.4-7, 56.1-6, 57.3-4, 58.3-6, 60.4-6, 61.1-7, 62.4-7,
64.3-3, 68.7-7, 69.5-7, 71.5-7, 72.3-7, 74.2-7, 75.4-7, 76.6-6,
77.2-7, 80.7-7, 82.6-7, 84.6-6, 85.1-4, 86.1-3, 88.4-4, 89.4-4.
56.

23. Cava Rusconi, Cittiglio, Prov. Varese, Northern Italy: 1.

27.1-1, 29.1-1, 30.1-1, 33.1-1, 50.1-1, 54.1-1, 68.1-1, 69.1-1,
71.1-1, 72.1-1, 73.1-1, 74.1-1, 75.1-1, 78.1-1, 79.1-1, 80.1-1,
81.1-1, 82.1-1, 83.1-1, 84.1-1, 93.1-1, 94.1-1, 95.1-1, 96.1-1,
97.1-1, 98.1-1, 99.1-1, 101.1-1, 102.1-1, 103.1-1, 106.1-1. 31.

24. Breggia Gorge, Ticino, Southern Switzerland: 24.

2.2-2, 6.3-9, 7.1-13, 8.3-10, 9.7-7, 11.3-14, 12.5-13, 13.5-12,
14.3-7, 15.3-9, 16.3-14, 17.1-15, 18.3-13, 19.5-15, 20.3-15,
21.5-20, 22.12-12, 23.3-14, 24.1-21, 25.5-21, 26.3-20, 27.12-18,
28.3-5, 29.2-19, 30.18-21, 31.5-18, 32.5-23, 33.3-23, 34.2-2,
35.9-21, 36.3-12, 37.3-14, 38.2-16, 39.3-7, 40.5-19, 41.4-19,
42.5-15, 43.1-20, 44.10-14, 46.12-12, 47.7-17, 48.15-18,
49.19-19, 50.14-19, 51.4-19, 53.12-16, 54.7-24, 56.10-23,
57.2-18, 58.4-10, 59.24-24, 60.15-18, 61.4-20, 62.8-19, 63.2-5,
64.14-20, 65.14-17, 66.8-8, 68.24-24, 69.19-24, 71.10-24,
72.8-12, 73.18-18, 74.7-24, 75.15-24, 76.7-23, 77.12-21,
80.24-24, 81.24-24, 82.22-24, 83.24-24, 84.12-24, 85.1-19,
86.1-20, 87.3-10, 88.17-17, 89.14-18, 90.2-3, 91.4-4, 92.4-4,
93.24-24, 94.24-24, 95.24-24, 96.24-24, 97.24-24, 98.24-24,
99.24-24, 100.24-24, 101.24-24, 102.24-24, 103.24-24, 104.24-24.
92.

25. Saltrio, Prov. Varese, Northern Italy: 12.

2.1-1, 5.3-5, 6.6-12, 7.1-12, 8.2-12, 9.3-11, 10.1-2, 11.1-12,
12.2-12, 13.1-11, 14.1-11, 15.1-12, 16.2-11, 17.1-12, 18.1-12,
19.2-11, 20.2-11, 21.1-11, 22.10-10, 23.1-11, 24.1-12, 25.3-11,
26.6-12, 27.12-12, 28.3-4, 29.1-11, 31.5-5, 32.2-12, 33.2-12,
35.7-12, 36.2-12, 37.11-11, 38.7-11, 39.2-12, 40.2-10, 42.7-11,
43.4-12, 46.6-11, 47.5-11, 49.3-11, 50.1-1, 52.1-11, 57.2-8,
58.1-11, 61.1-12, 63.1-2, 66.3-9, 67.4-4, 70.11-11, 73.5-11,
74.6-12, 84.3-11, 86.4-11, 87.1-11, 88.5-11, 89.6-7, 91.5-9,
92.5-11. 58.

26. Fiume Bosso, near Pianello, Umbria, Central Italy: 17.
** Sample 1 added -> old sample number + 1 = new.
1.1-1, 2.1-2, 3.1-1, 6.3-3, 8.5-5, 9.2-3, 10.1-1, 11.7-7, 12.6-6,
13.4-4, 14.1-1, 15.3-3, 16.3-6, 17.2-5, 18.2-6, 19.1-7, 20.1-3,
21.2-14, 22.2-3, 23.1-8, 24.2-10, 25.3-15, 26.7-7, 27.2-9,
28.1-1, 29.1-16, 30.8-9, 31.7-8, 32.3-8, 33.4-11, 35.6-6, 36.3-9,
37.3-11, 38.7-7, 39.3-3, 41.7-7, 43.15-15, 47.3-5, 49.6-6,
50.7-9, 54.8-16, 55.8-9, 56.5-15, 57.3-14, 59.8-8, 60.8-15,
61.2-5, 62.8-15, 63.1-1, 64.8-11, 65.7-7, 67.3-3, 68.16-16,
69.8-16, 70.16-16, 71.15-16, 72.6-8, 73.6-6, 74.14-15, 75.8-15,
76.7-15, 79.16-16, 80.16-16, 81.16-16, 82.15-17, 83.16-16,

84.10-10, 85.4-12, 86.4-4, 87.3-6, 88.7-7, 89.6-6, ** not 99.8-8, 102.16-17, 103.16-16. 74.

27. Monte Cetona, Tuscany, Central Italy: 9.

6.1-8, 7.8-8, 8.2-2, 11.2-8, 12.4-4, 13.8-8, 15.3-8, 16.8-8, 17.2-9, 18.8-8, 19.6-6, 20.3-9, 22.6-6, 23.4-4, 24.1-9, 26.1-7, 29.3-4, 32.8-8, 33.1-8, 36.8-8, 38.2-3, 39.8-8, 42.5-8, 43.3-8, 47.4-8, 50.3-8, 56.9-9, 57.8-8, 61.2-9, 65.2-2, 66.3-3, 86.1-6. 32.

28. Santa Anna, near Caltabellotta, Sicily, Italy: 4.

16.2-3, 18.3-3, 19.4-4, 21.4-4, 23.4-4, 24.1-1, 25.4-4, 27.4-4, 29.1-1, 30.3-3, 32.1-4, 33.4-4, 36.2-3, 37.1-3, 38.4-4, 40.4-4, 50.3-4, 54.3-3, 56.1-4, 57.1-3, 59.4-4, 60.3-4, 62.3-4, 64.1-4, 65.4-4, 69.1-3, 71.2-3, 72.1-3, 73.4-4, 74.3-3, 75.4-4, 76.1-4, 77.4-4, 78.3-3, 84.4-4, 85.4-4, 86.4-4, 90.3-3, 91.4-4. 39.

29. DSDP Leg 41, Site 367, Cape Verde Basin, E-Atlantic: 7.

16.3-3, 18.1-3, 21.1-6, 23.1-6, 24.1-1, 25.1-5, 30.2-6, 31.1-3, 32.4-4, 33.1-3, 37.1-1, 40.1-3, 43.4-4, 47.1-1, 52.1-1, 54.6-6, 55.1-6, 56.1-5, 57.3-3, 59,3-3, 60.1-4, 62.1-1, 64.1-7, 68.4-7, 69.2-6, 70.4-4, 71.3-5, 73.1-3, 74.2-4, 75.1-5, 76.1-6, 79.1-7, 82.6-6, 86.1-6, 89,4-4, 90.6-6, 99.7-7. 37.

30. DSDP Leg 76, Site 534, Blake Bahama Basin, W-Atlantic: 28.

5.1-2, 6.5-23, 7.1-23, 8.1-23, 9.1-23, 10.2-2, 11.2-23, 12.2-19, 13.2-22, 14.2-18, 15.2-23, 16.2-20, 17.2-23, 18.2-23, 19.2-21, 20.2-20, 21.2-23, 22.2-20, 23.2-23, 24.1-23, 25.1-24, 26.2-19, 27.2-22, 28.17-18, 29.2-24, 30.2-24, 31.2-24, 32.2-24, 33.2-24, 34.3-23, 35.3-23, 36.3-23, 37.5-20, 38.7-20, 39.3-12, 40.3-24, 41.11-11, 42.12-20, 43.14-20, 44.19-19, 45.16-20, 47.1-23, 48.4-20, 49.24-24, 50.19-20, 53.16-18, 54.16-24, 55.16-24, 56.17-21, 57.18-18, 58.18-19, 59.18-26, 60.24-24. 61.1-20, 63.3-3, 64.24-24, 65.12-12, 69.24-25, 71.24-24, 74.25-25, 75.24-28, 76.24-24, 79.25-25, 80.24-28, 81.24-25, 82.25-28, 84.2-28, 85.8-20, 86.12-19, 87.1-23, 88.2-24, 90.24-24, 91.2-23, 92.2-12, 93.25-25, 94.25-28, 95.25-25, 96.25-25, 97.25-28, 98.25-25, 100.26-28, 102.25-26, 103.25-25, 105.25-28, 106.26-28, 107.26-28, 108.26-28, 109.26-26. 88.

31. DSDP Leg 17, Site 167, Magellan Rise, Central Pacific: 6.

27.2-2, 30.3-3, 64.1-1, 68.6-6, 69.1-2, 78.2-2, 79.2-3, 80.3-3, **82.2-6, **85.1-5, 86.1-5, 88.1-1, 99.1-6, 100.2-6, 102.2-3, 103.3-3, **107.2-6, **109.3-6, **110.4-6, **111.6-6. 20.

32. DSDP Leg 32, Site 306, Shatsky Rise, northwest Pacific: 7.

30.1-4, 54.4-4, 59.1-7, 68.1-5, 69.1-4, 75.1-7, 79.1-7, 80.1-7, 81.3-7, 82.1-4, 83.1-4, 84.1-4, 93.2-2, 97.2-3, 98.2-3, 99.1-6, 100.3-3, 101.2-3, 102.1-4, 103.2-2, 104.6-7, 106.2-3, 107.2-7. 23.

33. DSDP Leg 32, Site 307, Shatsky Rise, northwest Pacific: 6.

30.1-2, 59.2-5, 68.1-4, 75.1-5, 78.5-5, 79.5-5, 80.2-6, 81.3-6, 82.1-6, 83.2-4, 84.2-4, 94.4-4, 99.1-4, 100.4-5, 102.1-4, 104.3-6, 106.4-5, 107.1-6, 109.5-5, 110.3-6, 111.4-5. 21.

34. DSDP Leg 20, Site 195, SE-Japan Abyssal Plain, NW-Pacific: 4.

59.1-3, 79.4-4, 80.1-3, 83.1-2, 84.1-3, 102.1-4, 104.3-4, 105.3-3, 107.3-4, 110.1-3. 10.

35. DSDP Leg 20, Site 196, SE-Japan Abyssal Plain, NW-Pacific: 3.

30.1-1, 54.1-1, 59.1-3, 68.1-1, 69.1-1, 84.1-3, 71.1-1, 75.1-1, 78.2-2, 79.1-3, 80.1-3, 81.2-3, 82.1-3, 83.1-3, 93.1-1, 98.1-2, 99.1-1, 100.1-1, 102.1-1, 104.2-3, 105.2-3, 106.2-2, 107.1-3, 110.2-3. 24.

36. Glasenbach Gorge, near Salzburg, Austria: 2.

6.1-2, 8.2-2, 11.2-2, 12.2-2, 13.1-2, 15.2-2, 17.1-2, 19.2-2, 20.2-2, 23.2-2, 24.1-2, 26.1-1, 27.1-2, 28.1-1, 29.1-1, 31.1-2, 33.1-2, 35.1-2, 36.1-1, 37.2-2, 38.1-2, 43.2-2, 46.1-2, 50.1-1, 53.1-2, 54.2-2, 61.1-2, 65.1-1, 66.1-2, 67.2-2, 74.2-2, 86.1-2. 32.

37. Point Sal, Santa Barbara County, California, USA: 3.

16.1-1, 18.1-1, 19.1-1, 20.1-2, 24.1-2, 25.1-2, 26.1-3, 27.1-1, 28.1-2, 29.1-3, 30.2-2, 31.1-2, 32.1-2, 33.1-2, 36.1-1, 37.1-1, 38.2-2, 42.1-1, 43.1-1, 44.1-2, 45.1-2, 47.1-3, 48.1-1, 49.1-1, 50.1-3, 51.1-2, 53.1-3, 54.1-2, 56.1-2, 57.1-2, 58.2-2, 64.1-2, 65.1-2, 67.1-1, 70.1-1, 71.2-2, 72.1-3, 73.1-2, 74.1-3, 75.1-2, 76.1-3, 77.1-1, 78.1-1, 85.1-1, 86.1-1, 88.1-2, 89.1-1. 47.

38. Veveyse de Chatel S. Denis, Cant. Vaud, Switzerland: 1.

59.1-1, 77.1-1, 80.1-1, 83.1-1, 84.1-1, 97.1-1, 98.1-1, 99.1-1, 104.1-1, 106.1-1, 109.1-1, 110.1-1, 111.1-1. 13.

39. DSDP Leg 1, Site 5, Blake Bahama Basin, W-Atlantic: 1.

54.1-1, 69.1-1, 71.1-1, 80.1-1, 83.1-1, 98.1-1, 101.1-1, 103.1-1. 8.

40. IN 7, near Unuma, Inuyama area, Central Japan: 1.

2.1-1, 3.1-1, 5.1-1, 9.1-1, 10.1-1, 14.1-1, 17.1-1, 18.1-1, 19.1-1, 20.1-1, 22.1-1, 24.1-1, 27.1-1, 28.1-1, 29.1-1, 34.1-1, 58.1-1, 61.1-1, 86.1-1. 19.

41. Guatemala, near Santa Rosa, Nicoya Peninsula, Costa Rica: 1.

7.1-1, 9.1-1, 18.1-1, 23.1-1, 24.1-1, 37.1-1, 61.1-1, 87.1-1. 8.

42. OM 191/200, near Sur, Halfa Fm., Hawasina Nappes, SE-Oman: 2.

29.2-2, 68.1-1, 69.1-1, 71.1-1, 80.2-2, 81.2-2, 82.1-2, 99.1-1, 100.1-2, 104.2-2, 105.1-2, 106.2-2, 109.2-2, ** 110.2-2 not 1-2, 111.2-2. 15.

43. Trattberg, Salzburg, Austria: 2.

30.1-1, 50.1-1, 54.1-1, 59.2-2, 68.1-2, 69.1-1, 71.1-1, 75.2-2, 79.1-2, 80.1-2, 81.2-2, 82.1-2, 84.2-2, 93.1-2, 94.1-2, 95.1-1, 96.1-1, 97.1-2, 98.1-1, 99.1-2, 100.2-2, 101.1-1, 102.1-2, 104.1-1, 106.2-2, 107.1-2, 108.2-2. 27.

* 44. Ceniga, near Arco, Trento, N-Italy: 4.

16.1-1, 23.1-3, 24.1-3, 25.1-4, 27.2-2, 29.2-2, 31.1-1, 32.1-2, 33.2-4, 35.1-1, 36.1-1, 43.1-2, 46.1-2, 47.1-1, 55.1-4, 59.3-3, 60.1-4, 62.1-3, 64.1-4, 69.2-4, 71.2-2, 72.2-2, 75.1-1, 76.1-4, 24.

* 45. Sierra de Ricote, Subbetic, Prov. Murcia, Spain: 3.

10.1-1, 13.2-2, 14.1-3, 16.1-3, 18.1-3, 23.1-2, 25.2-2, 27.3-3, 29.1-3, 32.1-3, 33.3-3, 36.3-3, 37.2-3, 43.2-2, 47.2-2, 57.2-2, 87.1-2, 89.2-3, 92.1-1, 19.

* 46. S of Monte Campannello near Volterraio, Elba, Italy: 2.

23.1-1, 24.1-1, 28.1-1, 32.1-1, 35.1-1, 36.1-1, 37.2-2, 43.1-1, 60.1-2, 62.1-2, 71.1-1, 75.1-1, 76.1-2, 13.

* 47. S. Felo - Namia, Elba, Italy: 1.

25.1-1, 27.1-1, 32.1-1, 33.1-1, 46.1-1, 60.1-1, 62.1-1, 64.1-1, 71.1-1, 75.1-1, 76.1-1, 11.

* 48. Rocchetta di Vara, Liguria, Italy: 2.

6.1-1, 14.1-1, 25.1-2, 27.1-1, 29.1-2, 40.1-1, 43.1-1, 57.2-2, 87.1-1, 9.

* 49. C 31 Simantov, N-Evvoia, Eastern Greece: 1.

8.1-1, 9.1-1, 11.1-1, 12.1-1, 19.1-1, 20.1-1, 23.1-1, 27.1-1, 32.1-1, 36.1-1, 43.1-1, 56.1-1, 61.1-1, 90.1-1, 14.

* 50. DB 6214, Jebel al Hasi, Al Aridh Formation, Hawasina Nappes, Central Oman: 1.

2.1-1, 5.1-1, 14.1-1, 18.1-1, 23.1-1, 24.1-1, 29.1-1, 34.1-1, 51.1-1, 63.1-1, 87.1-1, 90.1-1, 12.

* 51. DB 4575, near Achladi, N-Evvoia, Eastern Greece: 1.

17.1-1, 23.1-1, 43.1-1, 56.1-1, 75.1-1, 90.1-1, 6.

Plate explanations

The illustrations are in accordance with the alphabetic listing of genera and species arranged in alphabetical order, where space on the plates permitted.

Each illustrated specimen is designated with two numbers of the following format: Sample number/year/SEM-negative number, C-number. The sample number refers to locality descriptions and Plate 12. Year and SEM-number refer to the collection of negatives stored at the *Labor für Raster-Elektronenmikroskopie,* Geological Institute, University of Basel. Negative numbers larger than 81/9000 and 82/9000 refer to negatives taken at the Scripps Institution of Oceanography and are stored in the author's collection.

C-numbers refer to the collection of all illustrated material deposited at the *Naturhistorisches Museum Basel, Switzerland.*

Magnifications are indicated for each illustration, they are standardized where possible to allow visual comparisons.

Plate 1

Scanning electron micrographs of Middle Jurassic to Early Cretaceous siliceous (si) and pyritized (py) Radiolaria from Blake-Bahama Basin (DSDP Site 534), Lombardy (POB 1205, 1330, 1341), Romania (MO, V), Greece (POB 899) and Japan (IN 7) (see locality descriptions).

Fig. 1–2 *Acaeniotyle diaphorogona* FOREMAN, s.l.
(data 59, range 77, pob 90, rk –), 1: 534A-106-1-29/81/9028, C 35739, py, ×100. 2: 534A-106-1-29/81/9002, C 35740, py, ×100.

Fig. 3–4 *Acaeniotyle diaphorogona dentata* BAUMGARTNER, n. subsp.
(data 94, range 99, pob 281, rk –), 3: holotype POB 1205/79/5254, C 35741, si, ×100; 4: paratype MO 22/79/4112, C 35742, broken specimen, note triradiate base of internal beam connecting to (lacking) medullary shell; external spines have no inward continuation as for all *Acaeniotyle*. py, ×100.

Fig. 5 *Acaeniotyle umbilicata* (RÜST)
(data 80, range 88, pob 92, rk 18), MO 46/79/4161, C 35743, py, ×100.

Fig. 6 *Acanthocircus suboblongus* (YAO)
(data 24, range 22, pob 85, rk 41), POB 899/78/6123, C 35744, si, ×75.

Fig. 7 *Acanthocircus dicranacanthos* (SQUINABOL)
(data 82, range 86, pob 87, rk 17), MO 46/79/3095, C 35745, py, ×75.

Fig. 8–10 *Alievum helenae* SCHAAF
(data 104, range 103, pob 228, rk 20), 8, 10: V 34/80/2798, C 35746, py, 8, ×100, 10, ×165; 9: POB 1330/81/9086, C 35747, si, ×100.

Fig. 11–12 *Andromeda podbielensis* (OZVOLDOVA)
(data 16, range 43, pob 8, rk 87), 10: 534A-126-2-125/81/9142, C 35748, py, ×100; 11: 534A-125-5-111/81/9141, C 35749, py, ×100.

Fig. 13–15 *Andromeda praepodbielensis* BAUMGARTNER n. sp.
(data 3, range 2, pob 6, rk –), 13, 15: holotype POB 1341/81/2978, C 35750, si, ×100; 14: paratype IN 7/79/4431, C 35751, si, ×100.

Fig. 16–18 *Andromeda praecrassa* BAUMGARTNER n. sp.
(data 10, range 5, pob 7, rk –), 16: paratype POB 1341/81/2880, si, × 100; 17: holotype POB 1341/81/2975, C 35752, si, ×100; 18: paratype 534A-126-2-125/81/9143, C 35753, segmental divisions are marked with arrows, py, ×100.

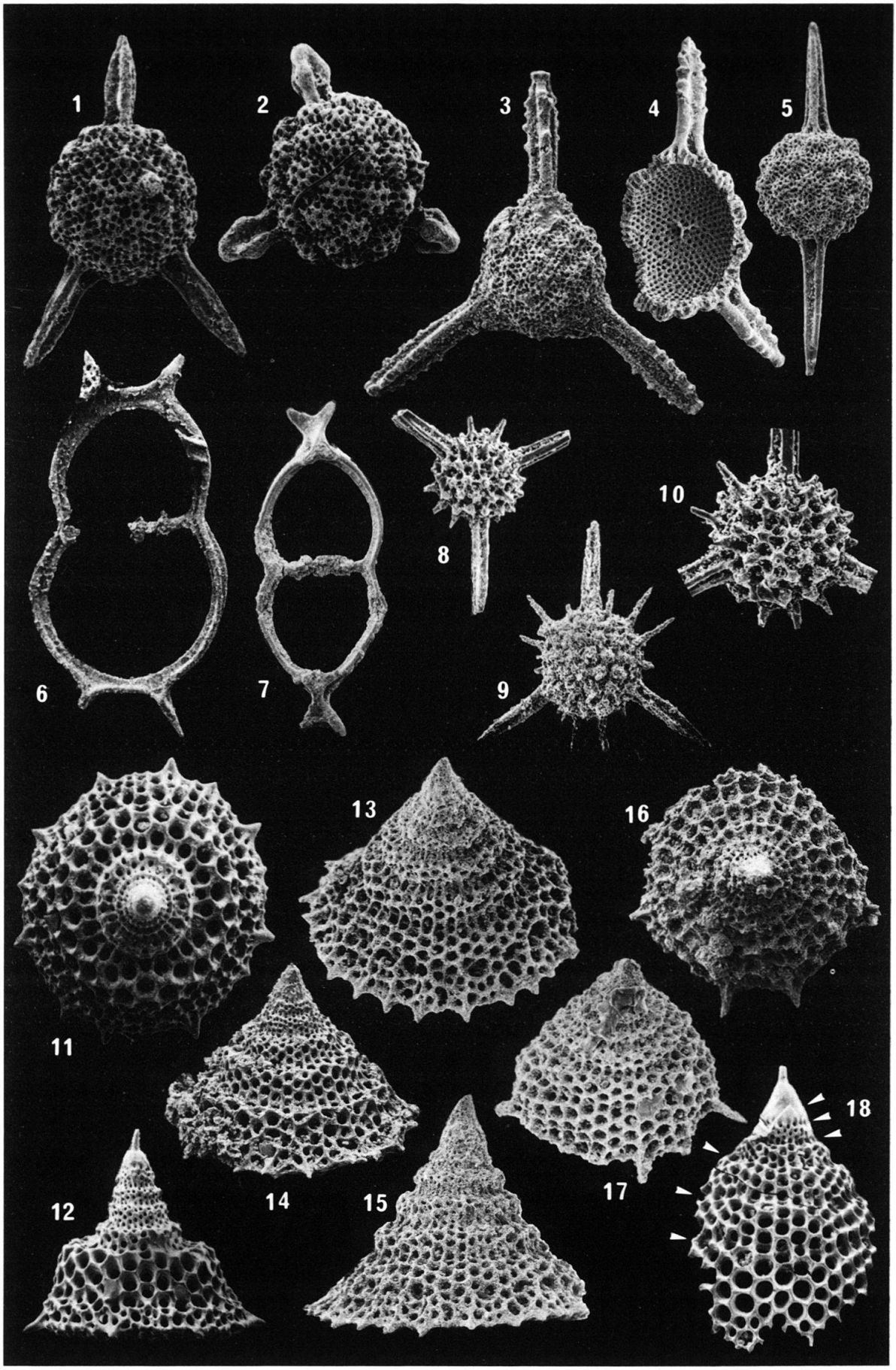
1
2
3
4
5
6
7
8
9
10
11
12
13
14
15
16
17
18

Plate 2

Scanning electron micrographs of Middle Jurassic to Early Cretaceous siliceous (si) and pyritized (py) Radiolaria from Blake-Bahama Basin (DSDP Site 534), Lombardy (POB 1205, 1330, 1341), Romania (MO, V), Greece (POB 28, 1262) and western Switzerland (POB 1134) (see locality descriptions).

Fig. 1–3 *Angulobracchia* (?) *portmanni* BAUMGARTNER n. sp.
(data 98, range 97, pob 285, rk –), 1: holotype POB 1330/81/9091, C 35754, si, ×100; 2: paratype MO 46/79/3121, C 35755, py, ×100; 3: paratype POB 1205/79/5741, C 35756, si, ×100.

Fig. 4 *Angulobracchia purisimaensis* (PESSAGNO)
(data 67, range 57, pob 144, rk 42), POB 28/78/3762, C 34809, si, ×75.

Fig. 5–6 *Archaeodictyomitra apiara* (RÜST)
(data 75, range 82, pob 263, rk 14), 5: MO 22/79/4101, C 35757, py, ×150; 6: 534A-81-2-64/81/9118, C 35758, py, ×150.

Fig. 7–8 *Archaeodictyomitra excellens* (TAN SIN HOK)
(data 100, range 102, pob 287, rk –), 7: MO 46/79/4292, C 35759, py, ×150; B: 534A-81-2-3/81/9101, C 35760, py, ×150.

Fig. 9–13 *Archaeohagiastrum munitum* BAUMGARTNER n. gen. n. sp.
(data 92, range 40, pob 271, rk –), 9: holotype 534A-125-5-111/81/9140, C 35761, py, ×150; 10, 13: paratype 534A-126-2-125/81/9175, C 35762, py, 10: ×150, 13: ×500; 11–12: 534A-126-2-125/81/9151, C 35763, lateral view of a specimen with broken spine showing three primary canals arranged around primary beam and six external beams, note also highly raised nodes of central area, typical for this species; py, 11: ×150, 12: ×500.

Fig. 14–15 *Bernoullius cristatus* BAUMGARTNER n. gen. n. sp.
(data 39, range 39, pob 221, rk 109), 14: holotype 534A-125-5-72/82/9197, C 35764, py, ×100; 15: paratype 534A-125-5-72/81/9198, C 35765, py, ×100.

Fig. 16 *Bernoullius dicera* (BAUMGARTNER)
(data 35, range 56, pob 223, rk 69), 534A-125-5-72/81/9200, C 35766, py, ×100.

Fig. 17–18 *Cecrops septemporatus* (PARONA)
(data 110, range 108, pob 229, rk 24), 17: POB 1134/80/2168, C 35767, py, ×100; 18: MO 46/79/4278, C 35768, py, ×100.

Fig. 19 *Diboloachras chandrika* KOCHER
(data 55, range 75, pob 265, rk 43), 534A-106-1-29/81/9039, C 35769, py, ×100.

Fig. 20 *Diacanthocapsa normalis* YAO
(data 34, range 10, pob 54, rk –), POB 1262/80/3961, C 35770, si, ×250.

Fig. 21 *Ditrabs sansalvadorensis* (PESSAGNO)
(data 103, range 96, pob 227, rk 21), MO 46a'/81/0962, C 35771, py, ×100.

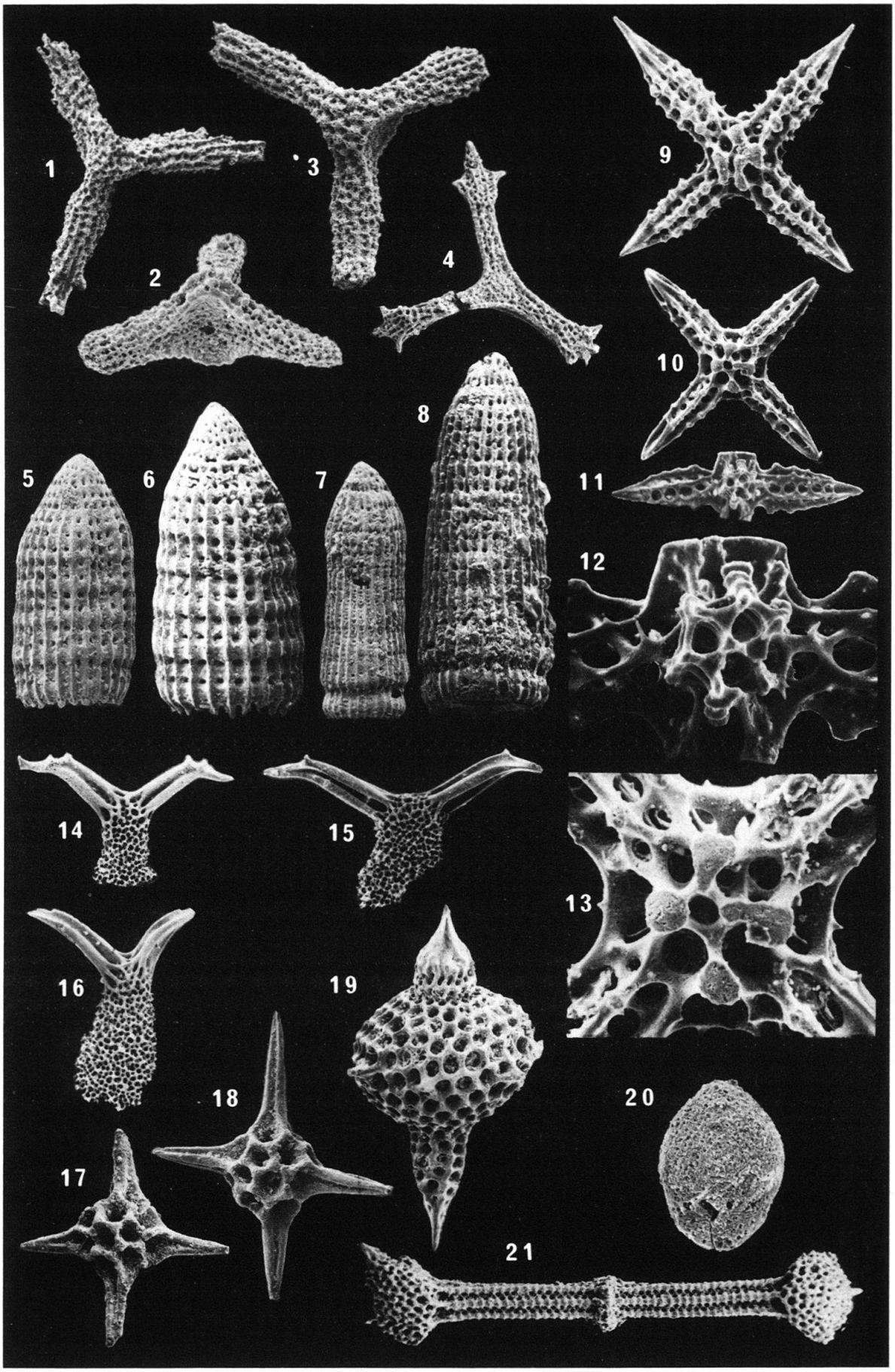
1
3
9
2
4
10
8
5
6
7
11
12
14
15
13
16
19
18
20
17
21

Plate 3

Scanning electron micrographs of Middle Jurassic to Early Cretaceous siliceous (si) and pyritized (py) Radiolaria from Blake-Bahama Basin (DSDP Site 534), Lombardy (POB 1341), Greece (POB 899, 986, 1262) (see locality descriptions)

Fig. 1 *Emiluvia hopsoni* PESSAGNO
(data 74, range 69, pob 225), POB 899/79/1656, C 35772, si, ×100.

Fig. 2 *Emiluvia sedecimporata elegans* (WISNIOWSKI)
(data 40, range 18, pob 216, rk –), POB 986/78/8107, C 35773, si, ×100.

Fig. 3 *Emiluvia pessagnoi* FOREMAN s.l.
(data 71, range 71, pob 226, rk 36), POB 986/78/8201, C 35774, si, ×100.

Fig. 4, 7 *Emiluvia sedecimporata salensis* PESSAGNO
(data 33, range 50, pob 215, rk 44 & 45), 4: 534A-126-2-125/81/9167, C 35775, py, ×100; 7: POB 899/78/8204, C 35776, si, ×100.

Fig. 5 *Emiluvia orea* BAUMGARTNER
(data 60, range 81, pob 224, rk 63), topotype POB 899/78/6106, C 35777, si, ×75.

Fig. 6, 8–9, 11, 12 *Emiluvia premyogii* BAUMGARTNER n. sp.
(data 19, range 14, pob 210, rk 88), 6: paratype 534A-124-1-52/81/2423, C 35778, py, ×100; 8, 11–12: holotype 534A-124-1-52/81/2424, C 35779, py, note perfect preservation in pyrite, showing the smooth surface of bars and spines and the knobby surface of nodes known from recent opaline polycystins, 8: ×100, 11: ×250, 12: ×1000; 9: paratype POB 899/79/1654, C 35780, si, ×100.

Fig. 10 *Emiluvia* (?) sp. P.
(data 41, range 59, pob 219, rk 90), 534A-125-2-36/81/1397, C 35781, py, ×150.

Fig. 13–16 Eucyrtid gen. et sp. indet.
(data 63, range 7, pob 74, rk –), 13–14: POB 1341/81/2958, C 35782, si, 13: ×250, 14: ×100; 15: POB 1263/80/3787, C 35783, si, ×100, 16: POB 1341/81/2960, C 35784, si, ×100.

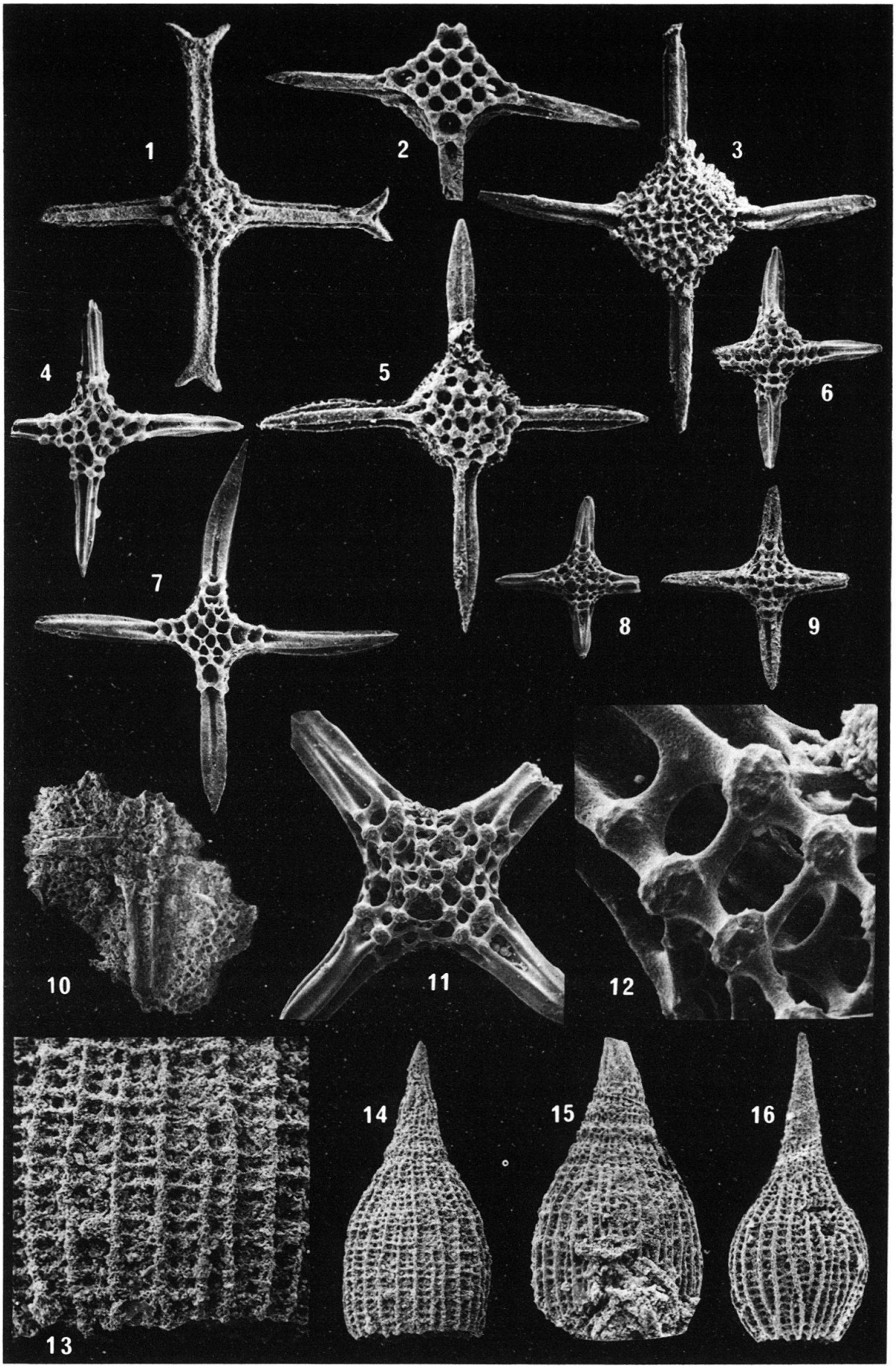
1
2
3
4
5
6
7
8
9
10
11
12
13
14
15
16

Plate 4

Scanning electron micrographs of Middle Jurassic to Early Cretaceous siliceous (si) and pyritized (py) Radiolaria from Blake-Bahama Basin (DSDP Site 534) and Greece (POB 325, 899) (see locality descriptions).

Fig. 1–3 *Eucyrtidiellum ptyctum* (RIEDEL & SANFILIPPO)
(data 56, range 66, pob 27, rk 46 [pars]), 1: POB 325/80/3798, C 35785, si, ×250; 2: 534A-122-1-43/81/2217, C 35786, py, ×250; 3: 534A-122-1-43/81/2212, C 35787, py, ×250.

Fig. 4–5 *Eucyrtidiellum pustulatum* BAUMGARTNER n. gen. n. sp.
(data 91, range 44, pob 13, rk –), 4: holotype 534A-124-1-52/81/2428, C 35788, py, ×250; 5: paratype 534A-124-1-52/81/2429, C 35789, py, ×250.

Fig. 6 *Eucyrtidiellum unumaensis* (YAO)
(data 17, range 12, pob 12, rk 89), 534A-126-2-125/81/9144, C 35790, py, ×250.

Fig. 7 *Gorgansium pulchrum* (KOCHER)
(data 11, range 28, pob 76, rk 105), 534A-125-2-36/81/1393, C 35791, py, ×250.

Fig. 8–9 Hagiastrid sp. A.
(data 8, range 41, pob 153, rk 107 and 108), 534A-124-1-52/81/2795, C 35792, py, fragment! 8: × 500, 9: × 150.

Fig. 10–11 *Haliodictya* (?) *hojnosi* RIEDEL & SANFILIPPO
(data 86, range –, pob 254, rk 3), 10: 534A-124-1-52/81/2672, C 35793, py, ×150; 11: POB 899/78/6147, C 35794, si, ×200.

Fig. 12 *Higumastra* sp. aff. *H. inflata* BAUMGARTNER
(data 66, range 15, pob 107, rk 47), 534A-126-2-125/81/9183, C 35795, py, ×150.

Fig. 13 *Higumastra imbricata* (OZVOLDOVA)
(data 13, range 29, pob 110, rk 92), 534A-125-5-72/81/9210, C 35796, py, ×150.

Fig. 14 *Holocryptocanium barbui* DUMITRICA
(data 108, range 106, pob 292, rk –), 534A-81-2-64/81/9119, C 35797, py, ×150.

Fig. 15 *Homoeoparonaella argolidensis* BAUMGARTNER
(data 43, range 37, pob 103, rk 30), topotype POB 899/78/6201, C 35798, si, ×75.

Fig. 16 *Homoeoparonaella elegans* (PESSAGNO)
(data 65, range 63, pob 104, rk 48), 534A-124-1-52/81/2417, C 35799, py, ×75.

Fig. 17 *Homoeoparonaella giganthea* BAUMGARTNER
(data 70, range 68, pob 105, rk 37), topotype POB 899/78/6216, C 35800, si, ×75.

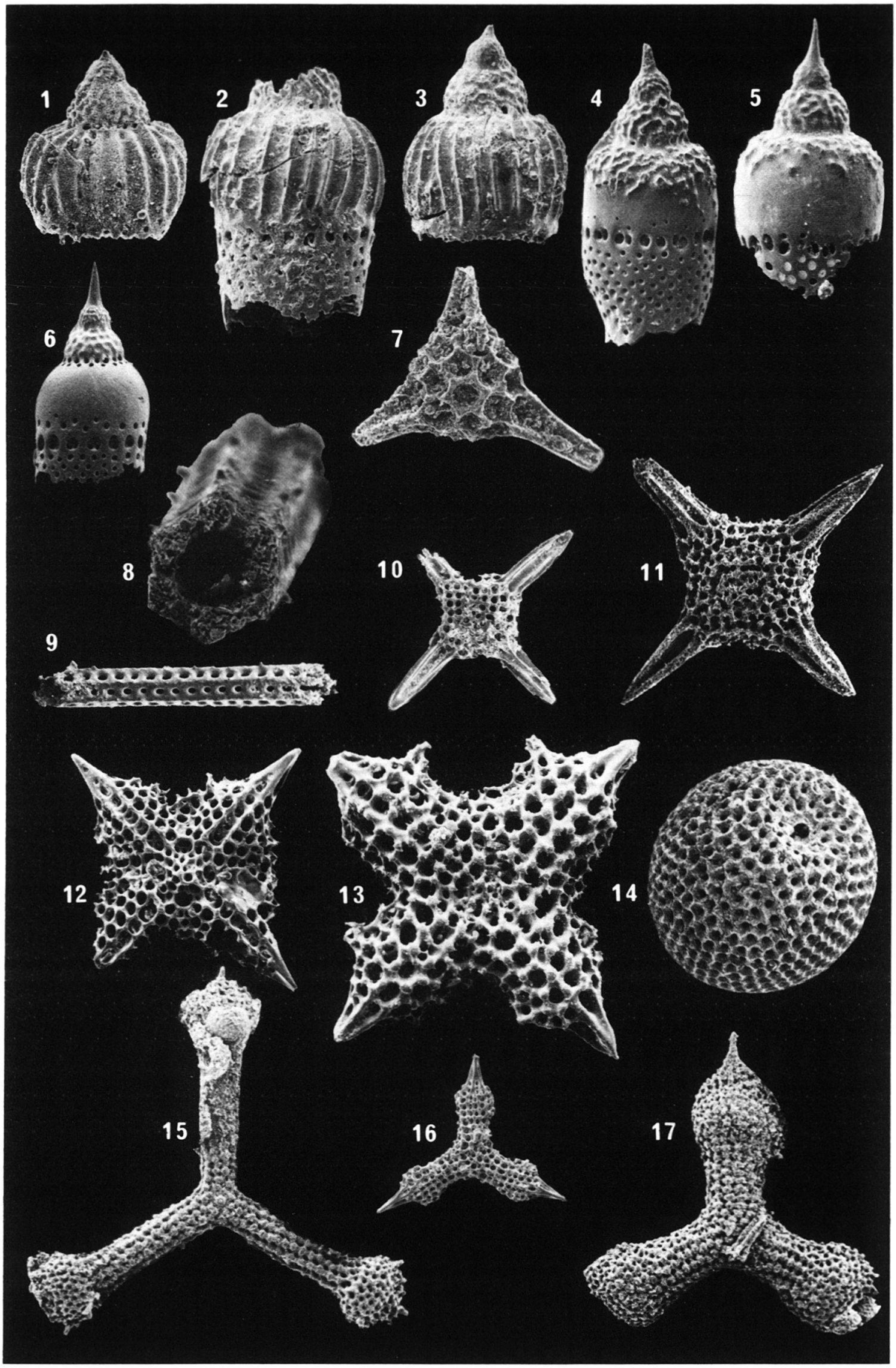
1
2
3
4
5
6
7
8
9
10
11
12
13
14
15
16
17

Plate 5

Scanning electron micrographs of Middle Jurassic to Early Cretaceous siliceous (si) and pyritized (py) Radiolaria from Blake-Bahama Basin (DSDP Site 534), Lombardy (POB 1205), Greece (POB 28, 899, 986), western Switzerland (POB 1134) and Japan (IN 7) (see locality descriptions).

Fig. 1–2 *Hsuum brevicostatum* (OZVOLDOVA)
(data 23, range , pob 181, rk 49), 1: 534A--125-3-29/81/2440, C 35801, py, ×150 2: POB 28/79/0360 C 35802, si, × 150.

Fig. 3–4 *Hsuum maxwelli* PESSAGNO group.
(data 47, range 42, pob 180, rk 93), 3: POB 28/78/3413, C 35803, si, ×150; 4: 534A-122-1-43/81/2274, C 35804, py, ×150.

Fig. 5–7 *Guexella nudata* (KOCHER)
(data 7, range 27, pob 61, rk 106), 534A-124-1-52/81/2667, C 35805, py, 5: ×300, 6: ×150, 7: ×450.

Fig. 8, 22 *Mirifusus guadalupensis* PESSAGNO
(data 37, range 55, pob 160, rk 50), 8: POB 28 /78/3587, C 35806, si, ×75; 22: POB 899/78/6261, C 35807, detail of inflated median part of test showing irregular outer layer, si, ×250.

Fig. 9, 15 *Mirifusus chenodes* (RENZ)
(data 77, range 80, pob 162, rk –), POB 899/79/1642, C 35808, si, note irregular outer layer of branching diagonal bars covering inner layer of small uniform pores in 4–5 rows per segment, 9: ×75, 15: ×250.

Fig. 10, 18 *Mirifusus mediodilatatus baileyi* PESSAGNO
(data 76, range 67, pob 161, rk 4 [pars]), 10: 534A-106-1-29/81/9053, C 35809, py, note slender conical proximal portion of test (above arrow) with several, well-defined segmental divisions, ×75; 18: POB 986/78/8183, C 34867, si, detail of inflated median portion of test with regular triangular pore frames, two rows of pores per segment and no covering outer layer, ×250.

Fig. 11, 14 *Mirifusus mediodilatatus minor* BAUMGARTNER n. subsp.
(data 99, range 90, pob 286, rk 4 [pars]), 11: holotype POB 1205/79/5038, C 35810, si, note short, blunt proximal conical portion of test (above arrow) with only one externally visible segmental division, ×75; 14: POB 1134/80/2182, C 35811, py, proximal conical portion of test shows outer layer entirely covering segmental divisions, ×75.

Fig. 12, 16–17, 20–21 *Mirifusus fragilis* BAUMGARTNER n. sp.
(data 14, range 9, pob 159, rk –), 12, 17, 20: holotype IN 7/79/4419, C 35812, si, note almost complete absence of outer layer, 12: ×75, 17: ×225, 20: ×250; 16: paratype 534A-126-2-125/81/9158, C 35813, py, note well-developed outer layer of diagonal bars, thin circumferential ridges, well visible inner layer of three rows of circular pores per segment, ×250; 21: 534A-125-3-29, C 35814, py, fragment of median inflated portion with weakly developed outer layer, thin circumferential ridges, ×250.

Fig. 13, 19 *Mirifusus mediodilatatus mediodilatatus* (RÜST)
(data 76, range 67, pob 161, rk 4 [pars]), 13: POB 28/78/3443, C 35815, si; 19: POB 899/78/6696, C 34866, si, detail of inflated median portion of test showing regular circular pore frames in two rows per segment and disappearing outer layer in upper part of Figure, ×250.

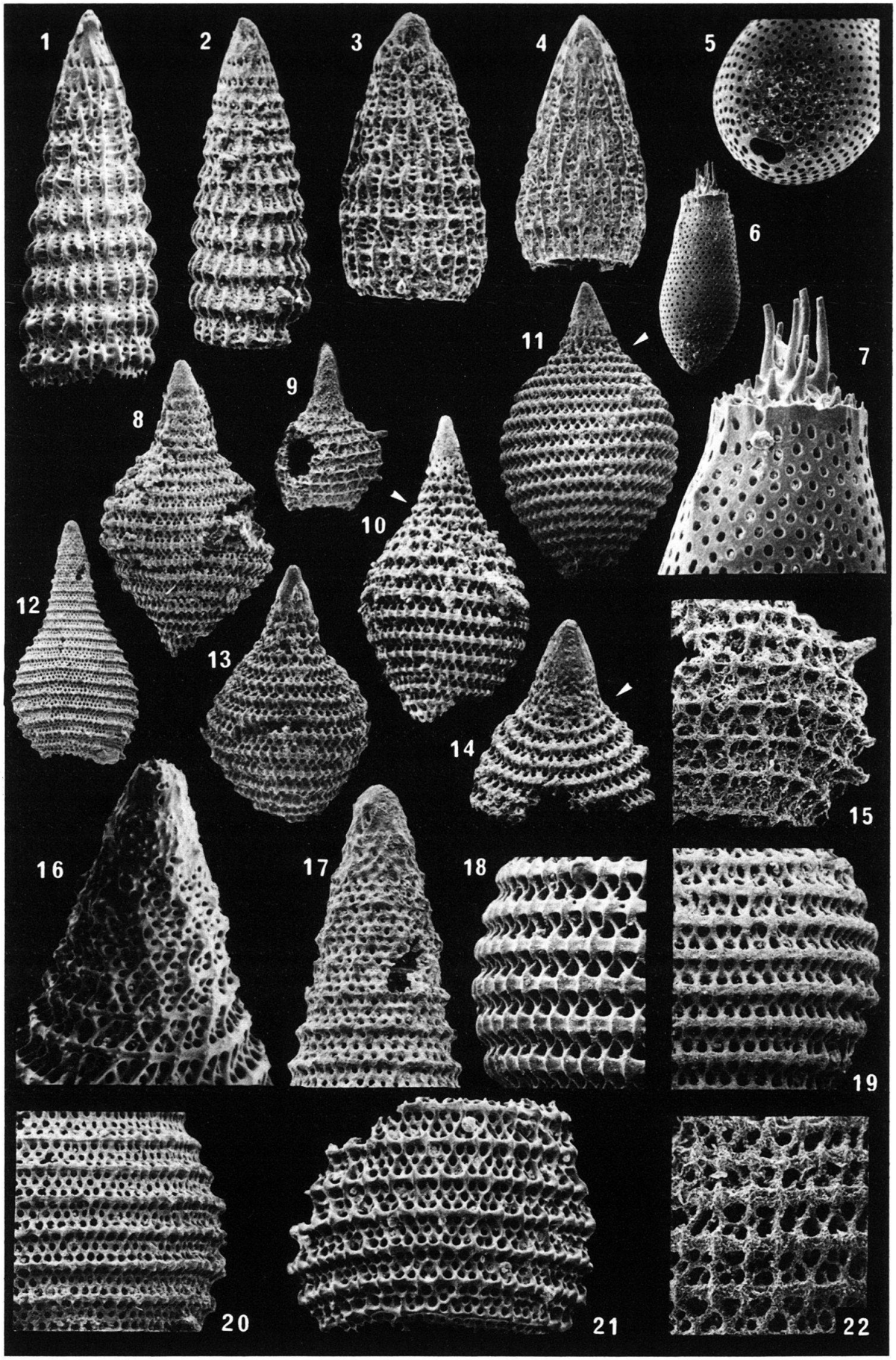
1
2
3
4
5
6
7
8
9
10
11
12
13
14
15
16
17
18
19
20
21
22

Plate 6

Scanning electron micrographs of Middle Jurassic to Early Cretaceous siliceous (si) and pyritized (py) Radiolaria from Blake-Bahama Basin (DSDP Sites 5, 534), Lombardy (POB 1205, 1330) and Greece (POB 28, 783, 899, 986) (see locality descriptions)

Fig. 1–2, 5 *Monotrabs plenoides* BAUMGARTNER n. gen. n. sp.
(data 42, range 54, pob 152, rk 91), holotype 534A-124-1-52/81/2686, C 35816, py; 2, 5: note long lateral spines and possible hagiastrid structure composed of beams and bars; 1: ×150, 2: ×250, 5: ×500.

Fig. 3 *Napora deweveri* BAUMGARTNER
(data 46, range 62, pob 35, rk 95), topotype POB 899/78/6462, C 35817, si, ×150.

Fig. 4 *Napora bukryi* PESSAGNO
(data 73, range 61, pob 34, rk 31), POB 899/78/6456, C 35818, si, ×150.

Fig. 6 *Napora lospensis* PESSAGNO
(data 72, range 76, pob 36, rk 32), POB 783/79/0105, C 35819, si, ×150.

Fig. 7–9 *Obesacapsula rusconensis* BAUMGARTNER n. sp.
(data 95, range 100, pob 282, rk –), 7: paratype POB 1205/79/5039, C 35820, si, ×75; 8: holotype POB 1205/80/2996, C 35821, si, ×75; 9: paratype 534A-89-2-47/81/9060, C 35822, si, ×75.

Fig. 11–12 *Napora pyramidalis* BAUMGARTNER n. sp.
(data 12, range 11, pob 33, rk 104), 11: holotype 534A-124-1-52/81/2704, C 35823, py, ×250; 12: paratype 534A-124-1-52/81/2656, C 35824, py, ×250.

Fig. 13 *Obesacapsula rotunda* (HINDE)
(data 83, range 95, pob 202, rk 16), 5A-7-1/79/4232, C 35825, si, ×75.

Fig. 14–15 *Pantanellium* (?) *berriasianum* BAUMGARTNER n. sp.
(data 93, range 92, pob 280, rk –), 14: holotype POB 1205/79/5265, C 35826, si, ×150; 15: paratype POB 1330/81/9085, C 35827, si, ×150.

Fig. 16 *Paronaella bandyi* PESSAGNO
(data 58, range 21, pob 135, rk 51), POB 899/78/6218, C 35828, si, ×75.

Fig. 17 *Paronaella broennimanni* PESSAGNO
(data 53, range 73, pob 137, rk 71), POB 28/78/3773, C 34792, si, ×75.

Fig. 18 *Formanella diamphidia* (FOREMAN)
(data 79, range 85, pob 112, rk 13), POB 28/78/3811, C 35829, si, ×75.

Fig. 19 *Formanella hipposidericus* (FOREMAN)
(data 78, range 83, pob 111, rk 12), POB 986/78/8152, C 34726, si, ×75.

Fig. 20 *Paronaella kotura* BAUMGARTNER
(data 48, range 64, pob 140, rk 85), topotype POB 899/79/6217, C 35830, si, ×75.

Fig. 21 *Paronaella mulleri* PESSAGNO
(data 38, range 32, pob 139, rk 96), POB 899/78/6229, C 35831, si, ×75.

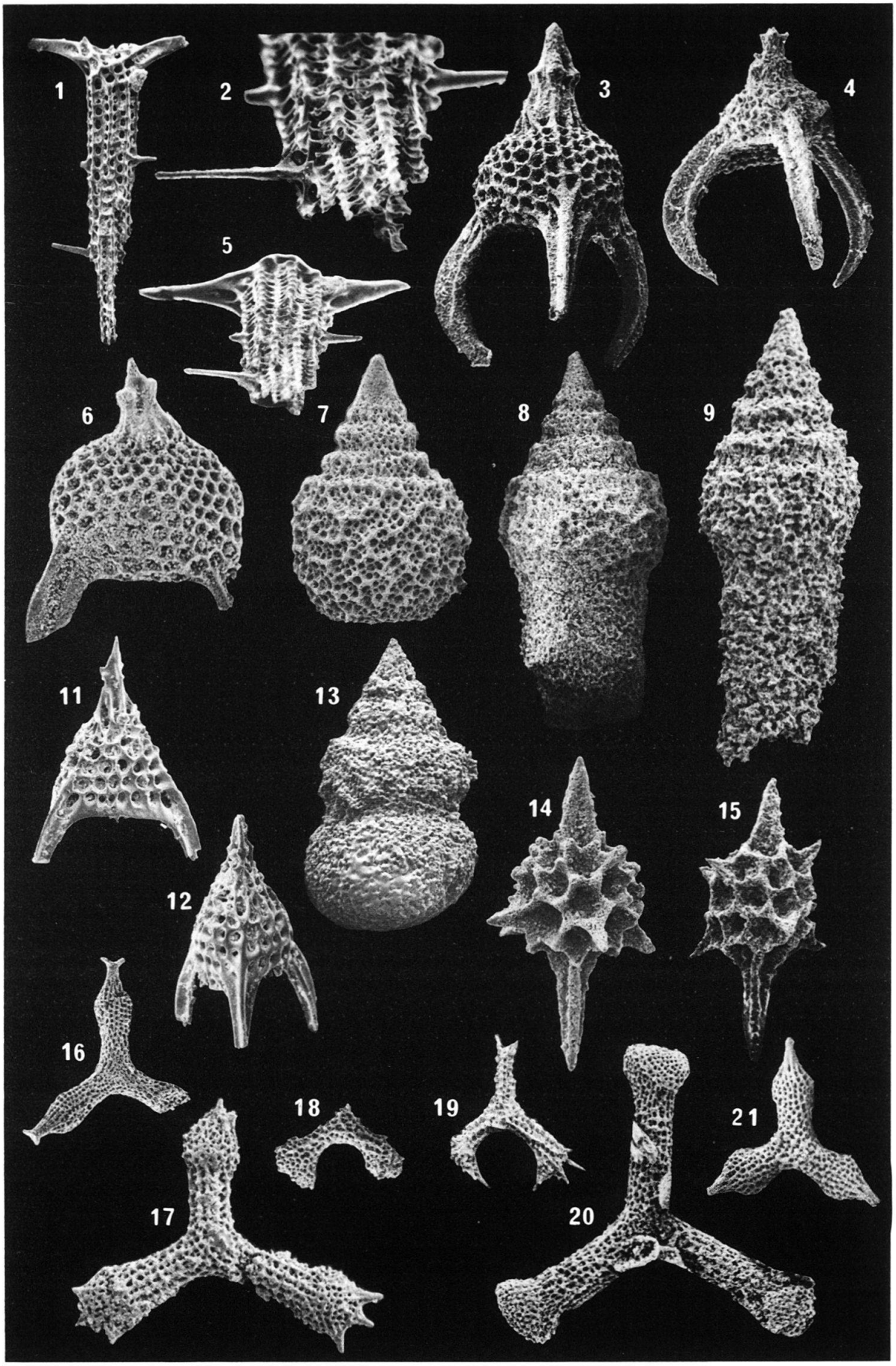
1
2
3
4
5
6
7
8
9
11
13
14
15
12
16
18
19
21
17
20

Plate 7

Scanning electron micrographs of Middle Jurassic to Early Cretaceous siliceous (si) and pyritized (py) Radiolaria from Blake-Bahama Basin (DSDP Site 534), Lombardy (POB 1205) Greece (POB 28, 284, 899, 986), Sicily (S 4) and California (NSF 907) (see locality descriptions)

Fig. 1 *Parvicingula cosmoconica* (FOREMAN)
(data 102, range 94, pob 255, rk 22), 534A-81-2-64/81/9111, C 35831, py, ×150.

Fig. 2–4 *Parvicingula dhimenaensis* BAUMGARTNER n. sp.
(data 90, range 33, pob 197, rk –), 2–3: holotype POB 284/79/0079, C 35833, si, 2: ×150, 3: ×250; 4: A-125-5-72/81/9214, C 35834, py, ×150.

Fig. 5–6 *Perispyridium ordinarium* (PESSAGNO)
(data 31, range 48, pob 100, rk 53), 5: POB 986/78/8147, C 35835, si, ×100; 6: 534A-124-1-52-81/2430, C 35836, py, ×100.

Fig. 7 *Podobursa helvetica* (RÜST)
(data 18, range 13, pob 169, rk 98), POB 28/78/3551, C 35837, si, ×100.

Fig. 8 *Podobursa spinosa* (OZVOLDOVA)
(data 64, range 78, pob 230, rk 54), S 4/79/4721, C 35838, si, ×100.

Fig. 9–10 *Podocapsa amphitreptera* FOREMAN
(data 69, range 84, pob 171, rk 38), 9: 534A-106-1-29/81/9009, C 35839, py, ×100; 10: POB 1205/80/2868, C 35840, si, ×100.

Fig. 11–14 *Praeconocaryomma* (?) *hexacubica* BAUMGARTNER n. sp.
(data 87, range 31, pob 244, rk –), 11: holotype 534A-126-2-125/81/9154, C 35841, py, ×150; 12: paratype 534A-126-2-125/81/9153, C 35842, py, spines supporting medullary shell are attached in center of squares of cortical shell, ×150; 13: 534A-126-2-125/81/9203, C 35843, py, note characteristic hexagonal pore arrangement, ×265; 14: paratype 534A-125-3-60/81/2451, C 35844, py, morphotype without spines, ×150.

Fig. 15 *Protunuma costata* (HEITZER)
(data 21, range 35, pob 232, rk 67), 534A-106-1-29, C 35845, py, ×150.

Fig. 16 *Pseudocrucella adriani* BAUMGARTNER
(data 52, range 34, pob 129, rk 72), topotype POB 899/78/6206, C 35846, si, ×75.

Fig. 17 *Pseudocrucella sanfilippoae* (PESSAGNO)
(data 51, range 58, pob 126, rk 73), topotype NSF 907/79/1695, C 35847, si, ×75.

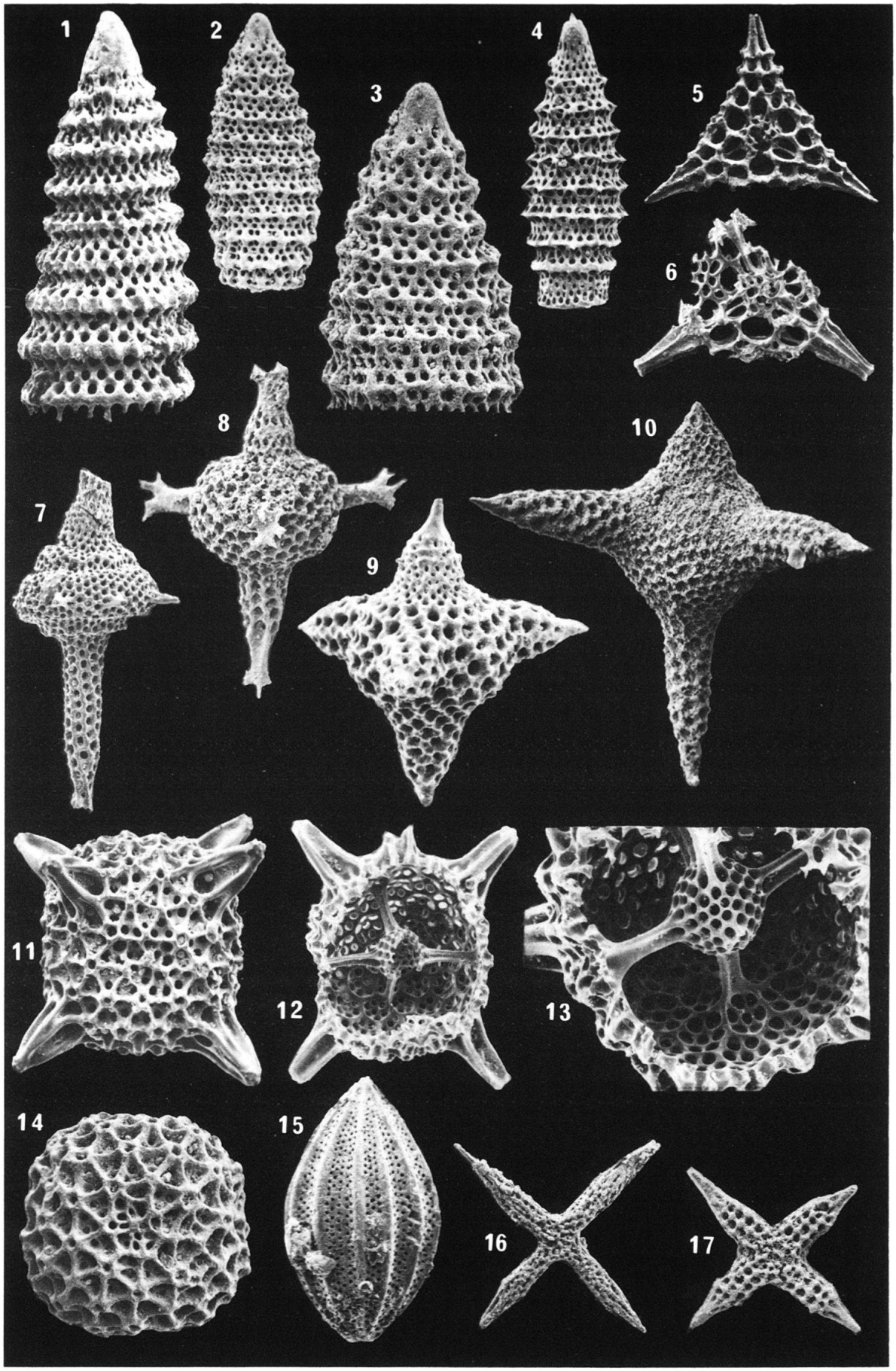
1
2
3
4
5
6
7
8
9
10
11
12
13
14
15
16
17

Plate 8

Scanning electron micrographs of Middle Jurassic to Early Cretaceous siliceous (si) and pyritized (py) Radiolaria from Blake-Bahama Basin (DSDP Site 534), Lombardy (POB 1205), Greece (POB 899, 986, 1263), western Switzerland (POB 1134) and Romania (MO) (see locality descriptions).

Fig. 1 *Pseudodictyomitra carpatica* (LOZNYAK)
(data 107, range 105, pob 293, rk –), 534A-81-2-64/81/9121, C 35848, py, ×150.

Fig. 2, 7–8, 11 *Pseudodictyomitra depressa* BAUMGARTNER n. sp.
(data 97, range 101, pob 284, rk –), 2, 11: holotype MO 22/79/0163, C 35849, py, 2: ×150, 11: ×250; 7: paratype 534A-81-2-3/81/9099, C 35850, py, ×150; 8: paratype 534A-81-2-3/81/9097, C 35851, ×150.

Fig. 3–4, 9 *Ristola altissima* (RÜST)
(data 32, range 47, pob 164, rk 52), 3: 534A-106-1-29/81/9011, C 35852, py, ×100; 4, 9: 534A-126-2-125/81/9133, C 35853, py, note distally disappearing outer layer, 4: ×100, 9: ×250.

Fig. 5, 10 *Ristola cretacea* (BAUMGARTNER)
(data 101, range 93, pob 165, rk 23), MO 26/80/1857, C 35854, py, 5: ×100, 6: ×250.

Fig. 6 *Ristola procera* (PESSAGNO)
(data 45, range 72, pob 163, rk 97), POB 899/78/6275, C 35855, si, ×100.

Fig. 12 *Saitoum pagei* PESSAGNO
(data 88, range 49, pob 20, rk 55), POB 986/78/8172, C 35/93, si, ×250.

Fig. 13 *Sethocapsa cetia* FOREMAN
(data 68, range 87, pob 203, rk 39), POB 1205/79/5745, C 35856, si, ×75.

Fig. 14 *Sethocapsa trachyostraca* FOREMAN
MO 46/79/4143, C 35857, py, ×150.

Fig. 15 *Sethocapsa uterculus* (PARONA)
(data 111, range 109, pob 297, rk –), POB 1134/80/2671, C 35858, py, ×150.

Fig. 16 *Spongocapsula palmerae* PESSAGNO
(data 50, range 38, pob 199, rk 76), 534A-125-5-72/81/9204, C 35859, py, ×100.

Fig. 17 *Spongocapsula perampla* (RÜST)
(data 85, range –, pob 267, rk 9), POB 986/79/0202, C 35860, si, ×100.

Fig. 18 *Staurosphaera antiqua* RÜST
(data 49, range 60, pob 218, rk 83), POB 899/78/6730, C 35861, si, ×100.

Fig. 19 *Stichocapsa convexa* YAO
(data 61, range 16, pob 55, rk 56), 534A-125-3-29/81/2440, C 35862, py, ×150.

Fig. 20 *Stichocapsa* sp. aff. *S. japonica* YAO
(data 4, range 3, pob 48, rk –), POB 1263/80/6730, C 35863, si, ×150.

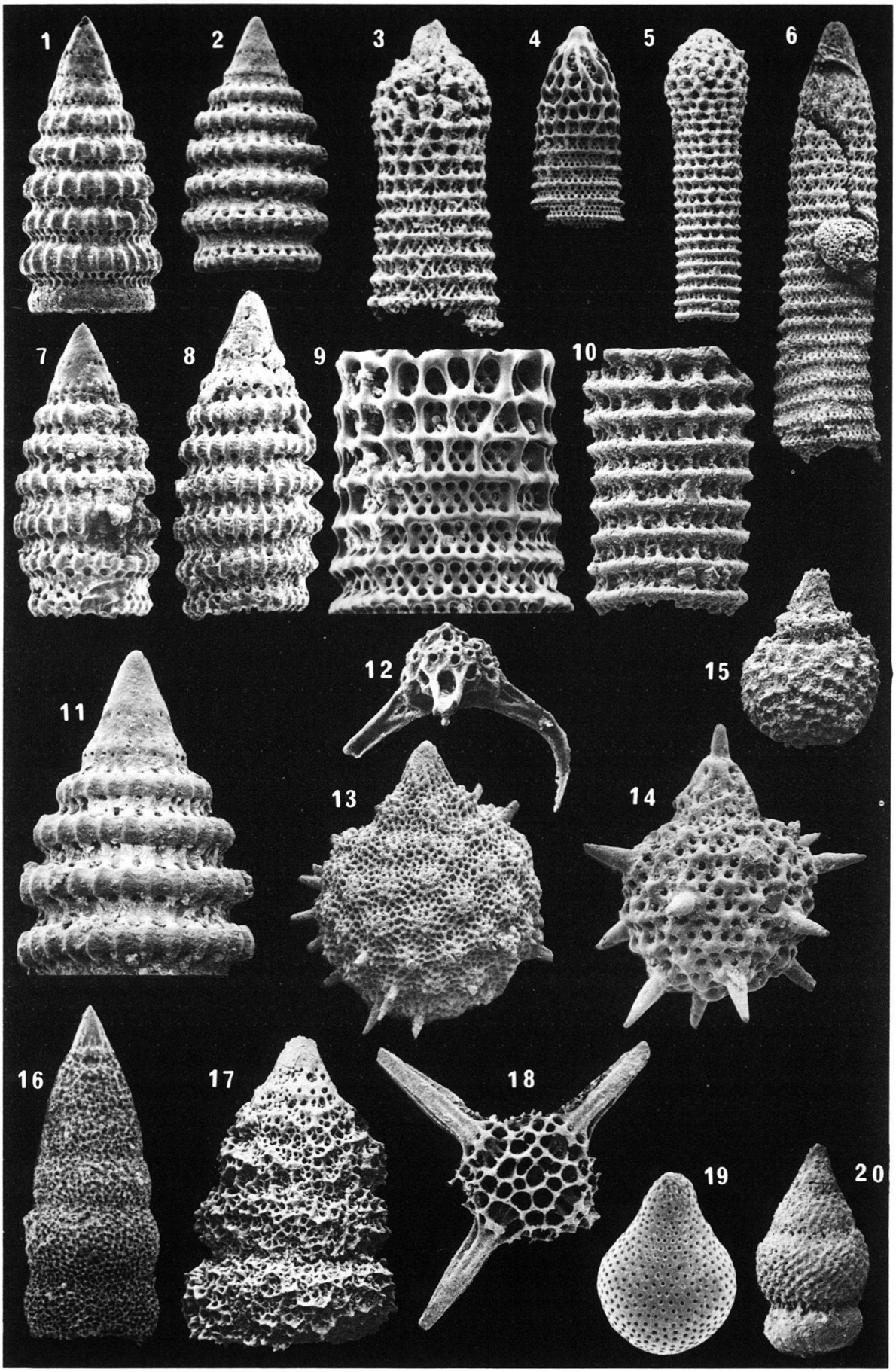
1
2
3
4
5
6
7
8
9
10
11
12
13
14
15
16
17
18
19
20

Plate 9

Scanning electron micrographs of Middle Jurassic to Early Cretaceous siliceous (si) and pyritized (py) Radiolaria from Blake-Bahama Basin (DSDP Site 534), Lombardy (POB 1205), Greece (POB 28, 899, 986), western Switzerland (POB 1134) and Japan (IN 7) (see locality descriptions).

Fig. 1–2 *Stylocapsa oblongula* KOCHER
(data 6, range 53, pob 59, rk 111), 1: 534A-125-3-29/81/2438, C 35864, py, ×250; 2: POB 325/80/3802, C 35865, si, ×250.

Fig. 3–4 *Syringocapsa agolarium* FOREMAN
(data 105, range 104, pob 291, rk –), 3: MO 22/79/3706, C 35866, py, ×150; 3: 534A-81-2-64/81/9108, C 35867, py, ×150.

Fig. 5 *Syringocapsa lucifer* BAUMGARTNER n. sp.
(data 96, range 91, pob 283, rk –), holotype POB 1205/79/5033, C 35858, si, ×75.

Fig. 6–7 *Tetraditryma corralitosensis* (PESSAGNO)
(data 20, range 17, pob 124, rk 58), 534A-126-2-125/81/9188, C 35869, py, 6: ×100; 7: lateral view of same specimen as Figure 6, showing internal ray structure with three primary canals and cortical space, ×250.

Fig. 8–9, 13, 13a *Tetraditryma praeplena* BAUMGARTNER n. sp.
(data 5, range 6, pob 125, rk –), 8: paratype IN 7/81/3027, C 35870, si, ×75; 9, 13–13a: holotype IN 7/79/4404, C 35871, si, 9, 13: ×75, 13a: note delicate porous cortical wall (arrow), ×250.

Fig. 10 *Tetratrabs zealis* (OZVOLDOVA)
(data 36, range 24, pob 121, rk 61), POB 1341/81/2955, C 35872, si, small specimen! ×75.

Fig. 11 *Tetratrabs bulbosa* BAUMGARTNER
(data 62, range 74, pob 122, rk 60), S 4/79/4700, C 35873, si, ×75.

Fig. 12, 14 *Tetraditryma pseudoplena* BAUMGARTNER
(data 57, range 36, pob 123, rk 59), 12: POB 28/78/3400, C 35874, si, ×75; 14: holotype POB 899/79/1500, C 34760, si, ×75.

Fig. 15 *Thanarla pulchra* (SQUINABOL)
(data 109, range 107, pob 296, rk –), MO 46a'/81/0948, C 35875, py, ×150.

Fig. 16–17 *Theocapsomma cordis* KOCHER
(data 15, range 30, pob 277, rk 99), 534A-126-2-125/82/9094, C 35876, py, Figure 17 shows basal aperture, ×250.

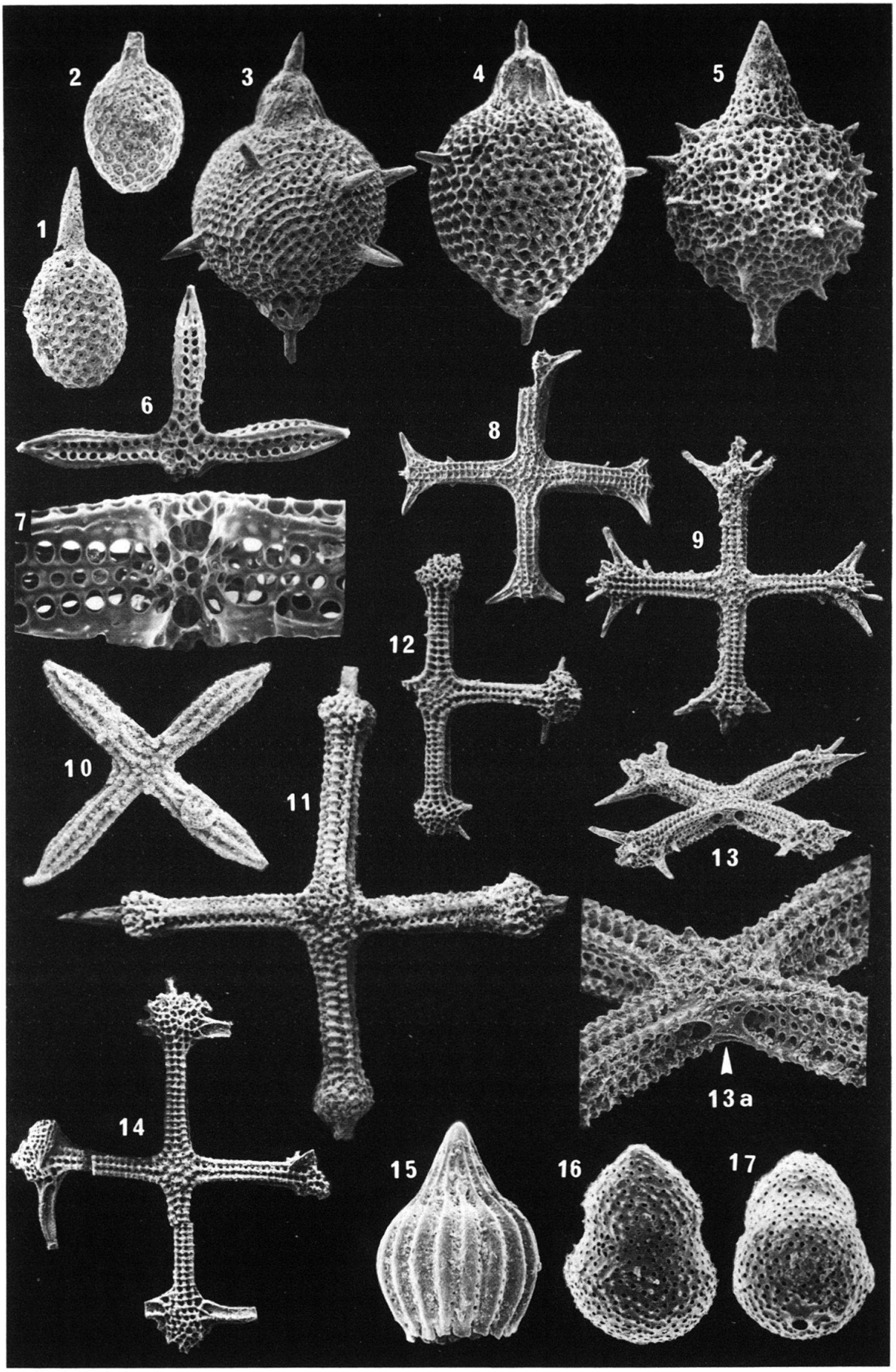
1
2
3
4
5
6
7
8
9
10
11
12
13
13a
14
15
16
17

Plate 10

Scanning electron micrographs of Middle Jurassic to Early Cretaceous siliceous (si) and pyritized (py) Radiolaria from Blake-Bahama Basin (DSDP Site 534), Greece (POB 28, 899, 986, 1262), Romania (MO) and Sicily (S 4) (see locality descriptions).

Fig. 1 *Triactoma cornuta* BAUMGARTNER
(data 89, range 65, pob 166, rk 78), topotype POB 899/78/6085, C 35877, si, ×75.

Fig. 2 *Triactoma echiodes* FOREMAN
(data 81, range 89, pob 94, rk 19), MO 46a'/81/0986, C 35878, si, ×100.

Fig. 3 *Triactoma blakei* (PESSAGNO)
(data 25, range 46, pob 95, rk 64), 534A-126-2-125/81/9133, C 35879, py, ×75.

Fig. 4 *Triactoma jonesi* (PESSAGNO)
(data 29, range 25, pob 96, rk 33), 534A-126-2-125/81/9131, C 35880, py, ×100.

Fig. 5 *Triactoma tithonianum* RÜST
(data 30, range 52, pob 97, rk 40), POB 899/78/6173, C 35881, si, ×100.

Fig. 6–7 *Tricolocapsa plicarum* YAO
(data 9, range 8, pob 51, rk –), 6: POB 1262/80/3954, C 35882, si, ×250; 7: 534A-122-1-43/81/2242, C 35883, py, ×250.

Fig. 8 *Trillus* sp. cf. *T. seidersi* PESSAGNO & BLOME
(data 1, range 1, pob 39, rk –), POB 1262/80/3957, C 35884, si, ×250.

Fig. 9 *Tritrabs casmaliaensis* (PESSAGNO)
(data 26, range 45, pob 117, rk 81), POB 28/78/3777, C 35885, si, ×75.

Fig. 10 *Tritrabs ewingi* (PESSAGNO)
(data 54, range 70, pob 113, rk 34), S 4/79/4689, C 35886, si, ×75.

Fig. 11 *Tritrabs exotica* (PESSAGNO)
(data 27, range 37, pob 118, rk 35), POB 899/78/6222, C 35887, si, ×75.

Fig. 12 *Tritrabs hayi* (PESSAGNO)
(data 28, range 20, pob 116, rk 101), POB 899/78/6292, C 35888, si, ×75.

Fig. 13 *Tritrabs rhododactylus* BAUMGARTNER
(data 27, range 26, pob 118, rk 35), POB 986/79/1631, C 35889, si, ×75.

Fig. 14–15 *Unuma echinatus* ICHIKAWA & YAO
(data 2, range 4, pob 231, rk –), 14: POB 1262/80/2144, C 35890, si, ×150; 15: POB 1262/80/2857, C 35891, si, ×150.

Fig. 16–17 *Xitus* sp. cf *X. spicularius* ALIEV
(data 106, range 98, pob 295, rk –), 16: MO 22/79/0177, C 35892, py, ×150; 17: 534A-81-2-64/81/9104, C 35893, py, ×150.

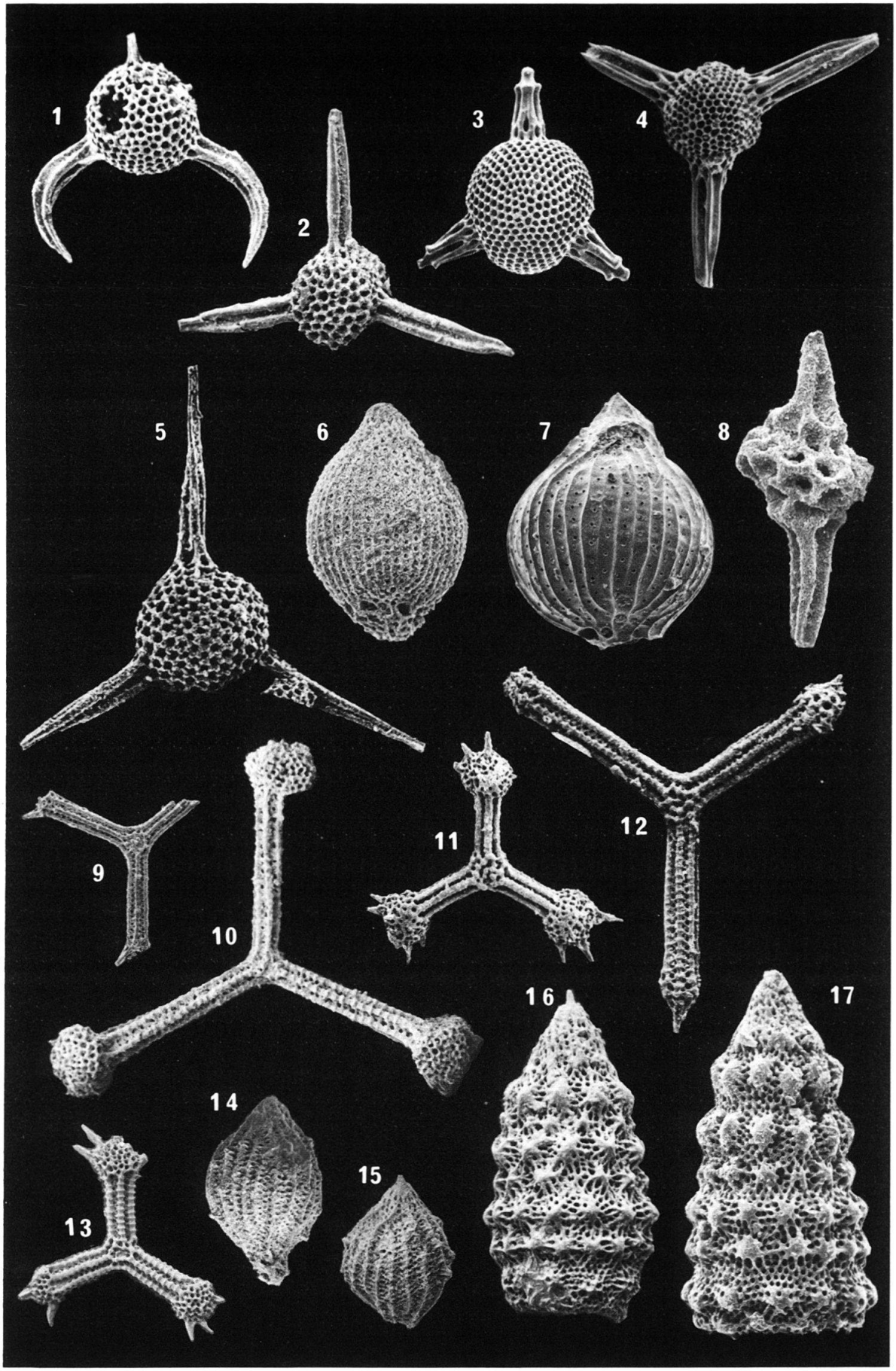
1
2
3
4
5
6
7
8
9
10
11
12
13
14
15
16
17

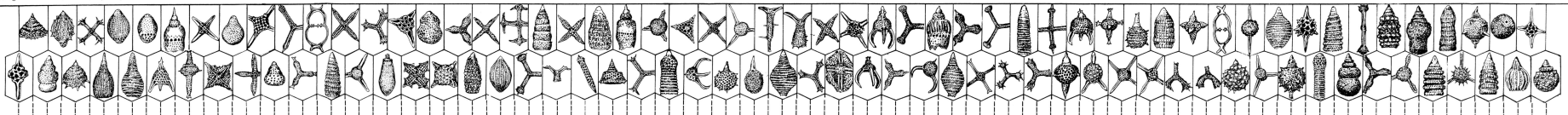

MIDDLE JURASSIC TO EARLY CRETACEOUS RADIOLARIAN RANGE CHART AND ZONAL DEFINITIONS BASED ON UNITARY ASSOCIATIONS

(computed after GUEX & DAVAUD 1982,1984)

ZONES	UNITARY ASSOCIATIONS	
E2	14	
E1	13	
D	12	
	11	
C2	10	
C1	9	
B	8	
	7	
A2	6	
	5	
A1	4	
	3	
	2	
A0	1	
	0	

(1)	Trillus sp. cf. T. seidersi
(3)	Andromeda praepodsolensis
(4)	Stichocapsa sp. aff. S. japonica
(2)	Unuma echinatus
(10)	Andromeda praecrassa
(5)	Tetraditryma praeplena
(63)	Eucyrtid gen. et sp. indet.
(9)	Tricolocapsa plicarum
(14)	Mirifusus fragilis
(34)	Diacanthocapsa normalis
(12)	Napora pyramidalis
(17)	Eucyrtidiellum unumaensis
(18)	Podobursa helvetica
(19)	Emiluvia premvogii
(66)	Higumastra sp. aff. H. inflata
(61)	Stichocapsa convexa
(20)	Tetraditryma corralitosensis
(40)	Emiluvia sedecimporata elegans
(22)	Stichocapsa japonica
(28)	Triterabs hayi
(58)	Paronaella bandyi
(24)	Acanthocircus suboblongus
(23)	Hsuum brevicostatum
(36)	Tetrahedrabs zealis
(29)	Triactoma jonesi
(27)	Triterabs rhododactylus
(7)	Guexella nudata
(11)	Gorgansium pulchrum
(13)	Higumastra imbricata
(15)	Theocapsomma cordis
(87)	Praeconocaryomma (?) hexacubica
(38)	Paronaella mulleri
(90)	Parvicingula dhimenensis
(52)	Pseudocrucella adriani
(21)	Protunuma costata
(57)	Tetraditryma pseudoplena
(43)	Homoeoparonaella argolidensis
(50)	Spongocapsula palmerae
(39)	Bernoullius cristatus
(92)	Archaeohagiastrum munitum
(8)	Hagiastrid sp. A
(47)	Hsuum maxwelli group
(16)	Andromeda podbielensis
(91)	Eucyrtidiellum pustulatum
(26)	Tritrabs casmaliaensis
(25)	Triactoma blakei
(32)	Ristola altissima
(31)	Perispyridium ordinarium
(88)	Saitoum pagei
(33)	Emiluvia sedecimporata salensis
(84)	Sethocapsa leicostraca
(30)	Triactoma tithoniana
(6)	Stylocapsa oblongula
(42)	Monotrabs plenoides
(37)	Mirifusus guadalupensis
(35)	Bernoullius dicera
(67)	Angulobracchia purisinaensis
(51)	Pseudocrucella sanfilippoae
(41)	Emiluvia (?) sp. P.
(49)	Staurosphaera antiqua
(73)	Napora bukryi
(46)	Napora deweveri
(65)	Homoeoparonaella elegans
(48)	Paronaella kotura
(89)	Triactoma cornuta
(56)	Eucyrtidiellum ptyctum
(76)	Mirifusus mediodilatatus s.l.
(70)	Homoeoparonaella gigantheа
(74)	Emiluvia hopsoni
(54)	Triterabs ewingi
(44)	Triterabs exotica
(45)	Ristola procera
(53)	Paronaella brennimanni
(62)	Tetratrabs bulbosa
(55)	Dibolachras chandrika
(72)	Napora iospensis
(59)	Acaeniotyle diaphorogona s.l.
(64)	Podobursa spinosa
(71)	Emiluvia pessagnoi
(77)	Mirifusus chenodes
(60)	Emiluvia orea
(75)	Archaeodictyomitra apiara
(78)	Formanella hipposidericus
(69)	Podocapsa amphitreptera
(79)	Formanella diamphidia
(82)	Acanthocircus dicranacanthos
(68)	Sethocapsa cetia
(80)	Acaeniotyle umbilicata
(81)	Triacoma echiodes
(99)	Mirifusus mediodilatatus minor
(96)	Syringocapsa lucifer
(93)	Pantanellium (?) berriasianum
(101)	Ristola cretacea
(102)	Parvicingula cosmoconica
(83)	Obesacapsula rotunda
(103)	Ditrabs sansalvadorensis
(98)	Angulobracchia (?) portmanni
(106)	Xitus sp. cf. X. spicularius
(94)	Acaeniotyle diaphorogona dentata
(95)	Obesacapsula rusconensis
(97)	Pseudodictyomitra depressa
(100)	Archaeodictyomitra excellens
(104)	Alievum helenae
(105)	Syringocapsa agolarium
(107)	Pseudodictyomitra carpatica
(108)	Holocryptocanium barbui
(109)	Thanarla pulchra
(110)	Cecrops septemporatus
(111)	Sethocapsa uterculus

UNITARY ASSOCIATIONS	ZONES
14	E2
13	E1
12	D
11	
10	C2
9	C1
8	B
7	
6	A2
5	
4	A1
3	
2	
1	
0	A0

CORRELATION TO CHRONOSTRATIGRAPHY

(VAN HINTE 1976)

STAGES			M.a.
HAUTERIVIAN			125
VALANGINIAN			130
BERRIASIAN			135
TITHONIAN	late	PORTLANDIAN	140
	mid		
	eo.	VOLGIAN	
KIMMERIDGIAN			145
OXFORDIAN			150
CALLOVIAN			155
BATHONIAN			160

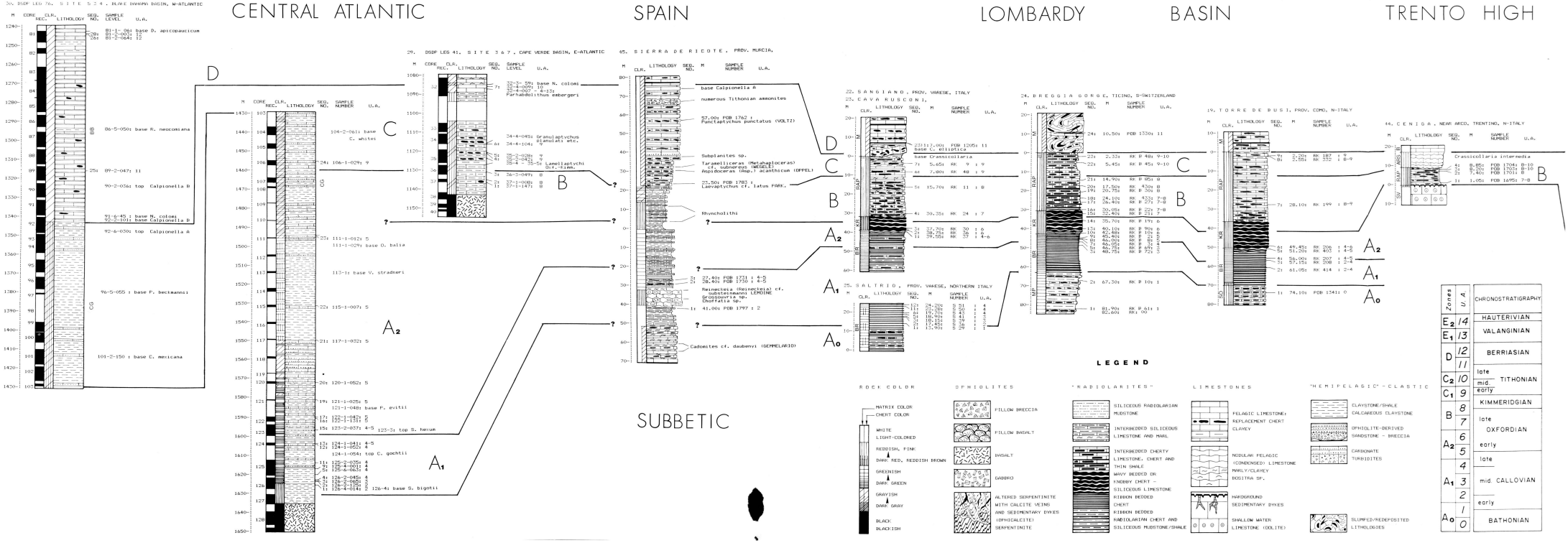
CENTRAL ATLANTIC
SPAIN
LOMBARDY BASIN
TRENTO HIGH
SUBBETIC
30. DSDP LEG 76, SITE 534, BLAKE BAHAMA BASIN, W-ATLANTIC
29. DSDP LEG 41, SITE 367, CAPE VERDE BASIN, E-ATLANTIC
45. SIERRA DE RICOTE, PROV. MURCIA,
22. SANGIANO, PROV. VARESE, ITALY
23. CAVA KUSCONI,
24. BREGGIA GORGE, TICINO, S-SWITZERLAND
25. SALTRIO, PROV. VARESE, NORTHERN ITALY
19. TORRE DE BUSI, PROV. COMO, N-ITALY
44. CENIGA, NEAR ARCO, TRENTINO, N-ITALY
LEGEND
ROCK COLOR
OPHIOLITES
"RADIOLARITES"
LIMESTONES
"HEMIPELAGIC"-CLASTIC
Zones
CHRONOSTRATIGRAPHY
HAUTERIVIAN
VALANGINIAN
BERRIASIAN
TITHONIAN
KIMMERIDGIAN
OXFORDIAN
CALLOVIAN
BATHONIAN

ELBA

LIGURIA

UMBRIA

GREECE

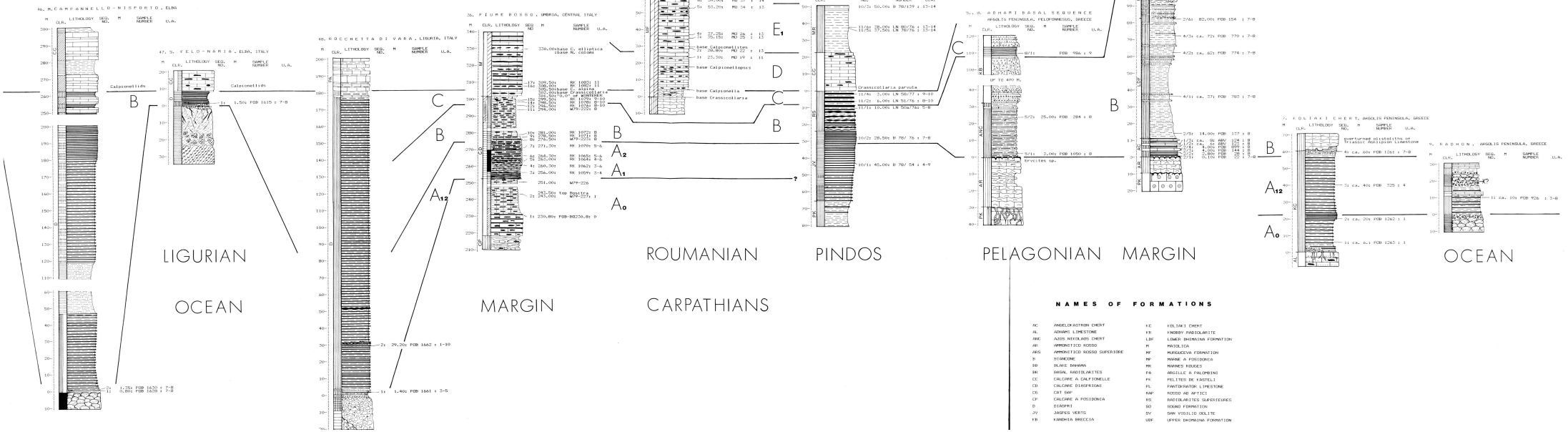

NAMES OF FORMATIONS

AC	ANGELOKASTRON CHERT	KE	KOLIAKI CHERT
AL	ADHAMI LIMESTONE	KR	KNOBBY RADIOLARITE
ANC	AJOS NIKOLAOS CHERT	LDF	LOWER DHIMAINA FORMATION
AR	AMMONITICO ROSSO	M	MAIOLICA
ARS	AMMONITICO ROSSO SUPERIORE	MF	MARGGEVA FORMATION
B	BIANCONE	MP	MARNE A POSIDONIA
BB	BLAKE BAHAMA	MR	MARNES ROUGES
BR	BASAL RADIOLARITES	PA	ARGILLE A PALOMBINI
CC	CALCAIRE A CALPIONELLE	PK	PELITES DE KASTELI
CD	CALCAIRE DIASPRIGNI	PL	PANTOKRATOR LIMESTONE
CS	CAT GAP	RAP	ROSSO AD APTICI
CP	CALCAIRE A POSIDONIA	RS	RADIOLARITES SUPERIEURES
D	DIASPRI	SO	SOGNO FORMATION
JV	JASPES VERTS	SV	SAN VIGILIO OOLITE
KB	KANDHIA BRECCIA	UDF	UPPER DHIMAINA FORMATION